GPO PRICE $ _____

CFSTI PRICE(S) $ _____

Hard copy (HC) 3.00

Microfiche (MF) 1.00

ff 653 July 65

JET PROPULSION LABORATORY
CALIFORNIA INSTITUTE OF TECHNOLOGY
PASADENA, CALIFORNIA

THERMAL SCALE MODELING TECHNIQUES FOR VOYAGER-TYPE SPACECRAFT

prepared for:

Jet Propulsion Laboratory
Pasadena, California
(Contract 951417)

by

Frank Gabron
Arthur D. Little, Inc.
Cambridge, Massachusetts

June 15, 1966

C-66326-02

This work was performed for the Jet Propulsion Laboratory, California Institute of Technology, sponsored by the National Aeronautics and Space Administration under Contract NAS7-100.

Table of Contents

List of Tables

List of Figures

List of Figures (continued)

Summary and Conclusions

Techniques for designing one-half and one-fifth scale thermal models of a Voyager-type spacecraft and entry capsule have been studied. The objective of the study was to determine the feasibility of testing reduced-scale thermal models in a simulated space environment and, from the test results, predicting the equilibrium temperatures of a full-scale prototype.

Two techniques for predicting prototype temperatures from scale-models were studied. One is a technique in which the temperatures are made identical at homologous locations in model and prototype. The other is a technique in which the temperatures are made different in model and prototype. The temperatures in model and prototype in this case are related by a fixed, predictable ratio. Theoretical considerations show that either technique provides considerable freedom in the selection of model materials, and temperature scaling ratios when temperature fields are not three-dimensional in the prototype.

The results of this study indicate that the use of a 1/2 scale model, designed in accordance with the temperature preservation technique, is the best choice for predicting the temperatures of a Voyager-type spacecraft. Significant practical problems exist in modeling the thermal characteristics of temperature control louvers, multi-layer insulations and bolted joints when temperatures are not preserved in model and prototype. If temperatures are preserved in model and prototype, the conductances of thermal paths must also be preserved. Suitable choices of model materials and geometric distortions of the minor

dimensions (thickness of plates, shells, etc.) can be effectively used to satisfy this requirement. From studies of the modeling problems associated with each of the two techniques, it is concluded that a model designed in accordance with the temperature preservation technique cannot be easily modified for use in predicting prototype temperatures when temperatures are not preserved. Major modifications in the temperature control louver assemblies, bolted joints, insulations, and critical conductive heat flow paths would be required. It is also shown that modeling a Voyager-type spacecraft at 1/5 scale may not be practical because of difficulties in fabricating small, actively-operated, temperature control louvers. The feasibility of modeling at 1/5 scale will depend on the size of the louver assemblies selected for the final prototype design.

Several heat flow problems are presented to illustrate the relative importance of radiative and conductive effects in determining temperature distributions. The results are used to show that simplifications can be made in the design of a model when temperature distributions are controlled by radiative effects. A considerable portion of the report is directed to the important problems of modeling bolted joints, multilayer insulations and spacecraft appendages.

A brief study was made to determine the feasibility of scaling-up small spacecraft appendages with low power dissipation typical of those used on Mariner IV. It is concluded that temperatures measured in thermal tests of full-scale appendages will be more accurate than data obtained from increased-scale models.

An analysis was completed to determine the need for cooling the internal shroud of a cold-wall, thermal-vacuum chamber to below liquid

nitrogen temperature in order to adequately simulate outer space conditions. Emphasis was placed on determining the error in heat leak through multi-layer insulations. The results show that the errors in heat flow are negligible compared to the internal power dissipation in the Voyager capsule when the shroud is maintained at liquid nitrogen temperature (77.5K).

Introduction

Currently, the thermal designer of a spacecraft has at his disposal two tools for predicting the thermal performance of a spacecraft in orbit. One is a computer model of the spacecraft's thermal characteristics. Another is a simulation facility, usually having some type of solar simulation together with cooled walls and a high-vacuum capability.

Some spacecraft, or components thereof, are flown without any tests, others are flown on the basis of limited analytical calculations and yet others are launched after extensive thermal analyses and tests. It appears that the method or methods used to predict performance depend heavily on the characteristics and requirements of the spacecraft, and, in certain cases, on the experience and facilities of the company or agency responsible for the development. The reasons why the characteristics of the spacecraft affect the choice of methods used to predict thermal performance may be illustrated by considering two examples. The performance of many optical instruments is relatively unaffected by average temperature level but is critically dependent on temperature gradients which may be less than a hundredth of a degree over a rather large dimension. Computer techniques are used to accurately and reliably predict gradients but experimental predictions would be hopeless. Conversely, some spacecraft, containing mainly electronic packages, are performance dependent on temperature level. In cases where the geometry, surface radiation properties, and heat flow paths are difficult to describe analytically, or physical properties are not well known, test techniques are more useful in predicting thermal behavior than computational techniques.

With the development of large booster rockets, spacecraft payloads have become increasingly large and the facilities required to test large satellites in a simulated space environment have become large, complex and costly to operate. The time required to set up and complete a thermal test may limit the number of tests that can be made during the development of a large spacecraft. Furthermore, the ground handling of large spacecraft with delicate appendages and critical thermal control surfaces is a significant problem.

For these reasons it appears that the use of a thermal model tested in a simulated space environment to predict temperatures of a full-scale prototype will provide the thermal designer with another tool. The use of thermal scale models may significantly reduce the testing time and costs, and the ground handling problems. The modeling technique will prolong the useful life of present solar simulation facilities, and may reduce the needs for developing larger test facilities. In general, it would appear that the use of reduced-scale models, geometrically similar to prototypes, will be most useful. However, increased-scale models of very small components and perhaps even geometrically dissimilar models may also be applied to temperature prediction.

In order to have thermal scale modeling be attractive as a tool for predicting temperatures in complicated spacecraft, it is essential that the design of the model be based on a reasonably simple set of similarity criteria derived from basic heat flow equations. If detailed thermal studies, made with computer techniques, were required to design the model, the usefulness of the modeling technique would be lost. Similarly, the usefulness of the technique would be lost if a major test

program were required to design the model. In theory, it is possible to design a thermal model from existing sets of simple thermal similitude relationships using a set of drawings describing the prototype. However, previous experience in designing a small-scale thermal model of the Mariner IV spacecraft has shown that limited amounts of analysis and some ancillary testing may generally be required for model design purposes.

All spacecraft structures are designed to meet certain structural and thermal requirements, therefore, in many cases the thermal model which need not meet flight structural requirements can be made less complex than the prototype. Simplified analyses for determining whether, for example, conductive or radiative heat flow effects are dominant, can be effectively used to reduce the complexity and, therefore, the costs and time required to fabricate the model. Testing may be required to determine the thermal behavior and scaling procedures for a particular bolted joint whose characteristics are not analytically tractable. Such procedures are often required to obtain data for use in computer simulations of thermal behavior. Thus, it is seen that limited theoretical analyses and testing will be useful in reducing the complexity of thermal models and may be required to obtain information for design purposes.

This report is concerned with the problem of modeling the thermal behavior of a prototype Voyager spacecraft which may be 20 feet in diameter and have a mass greater than 5 tons. Plans for the Voyager mission to Mars are presently being developed and it is anticipated that flights will occur during the early 1970's. The time schedule for launching the Voyager spacecraft would appear to be sufficiently long to

permit the use of thermal-vacuum testing of reduced-scale models during development. The Voyager spacecraft will be equipped with scientific experiments and communication equipment whose performance will be critically dependent on maintaining temperatures within certain prescribed limits. Clearly, it would be desirable to minimize the amount of full-scale testing of such a large spacecraft in a solar simulator.

The main purpose of this report is to determine the feasibility of using reduced-scale thermal models in the Voyager program as an aid in the preliminary design and development of the spacecraft. Since the spacecraft has not yet been designed, a detailed design of a thermal scale model cannot be presented. This feasibility study is thus restricted to a somewhat general discussion of various approaches to the design of a thermal scale model. Most of the technical discussion of appropriate scaling techniques for a Voyager-type spacecraft is based on experience previously gained in designing and testing a one-half (approximately) scale thermal model of the Mariner IV spacecraft. The results of this work showed that a reduced-scale model tested in a solar simulated facility can be used to predict equilibrium flight temperatures with an accuracy sufficient for development of a spacecraft. With few exceptions, the flight temperature predictions made by use of the model were nearly as accurate as predictions made in pre-flight tests of the Mariner IV in the JPL solar simulator.

The entire discussion presented in this report is based on establishing the feasibility of "steady-state" thermal modeling for a Voyager-type spacecraft, and there are several cogent reasons for so restricting the study. First, in typical transfer orbits between Earth and Mars,

the rate of change of solar intensity is so small that spacecraft temperatures change by only fractions of a degree per day. Therefore, interplanetary cruise temperatures can be predicted from "steady-state" test measurements at a series of different solar intensities ranging from 1 to 0.43 solar constants at Earth and Mars, respectively. Second, much of the background work in thermal scale modeling of complex spacecraft has been completed using "steady-state" models. Transient modeling is judged to be more complicated in practical applications and will introduce uncertainties in the model temperature predictions which are, at present, not well understood.

The first part of this report contains a brief review of the literature pertaining to thermal similitude in spacecraft, a discussion of the theory of thermal similitude, and practical applications of the technique. The discussion of the practical applications is purposely restricted to two techniques of "steady-state" thermal scale modeling. The first being the temperature preservation technique where the temperatures of model and prototype are made identical at homologous locations by use of different materials in model and prototype. The second being the "materials preservation" technique where identical materials are used in model and prototype. In this case the temperatures in model and prototype are in fixed ratio at homologous locations. The selection of these techniques (among others which are available) was based, in part, on previous studies of different methods for designing a thermal model of a typical JPL spacecraft, and on the results of experiments carried out with half and fifth scale models using both the temperature and materials preservation techniques.

The second part of this report deals with the feasibility of thermally modeling a Voyager spacecraft at approximately one-half and one-fifth scale using both materials and temperature preservation techniques. Consideration is given to modeling the spacecraft and its principal components as separate configurations. Finally, a short discussion of testing techniques to simulate the environment is presented.

I. Literature Review

Theoretical Studies

The following review of the literature is intended to provide the reader with background material on the subject of thermal similitude in spacecraft. Vickers (1965) has presented a survey of thermal scale modeling which included discussions of the problem, available scaling techniques and the "state of art." This review is intended to supplement Vickers' survey in light of recent developments. For reference, an Annotated Bibliography of published papers on thermal scale modeling is presented in Appendix A.

An early discussion of the technique of thermal scale modeling was presented by O'Sullivan (1957). Dimensional analysis was used to formulate the conditions of thermal similitude where identical materials are used in model and prototype. A rigorous treatment of modeling of structural deformations resulting from thermal and external loading stresses was presented.

Katz (1962) briefly presented the dimensionless groups pertinent to thermal modeling and later Katzoff (1963) presented similar dimensionless groups and discussed, in some detail, the applications of scaling techniques from the practical viewpoint. Vickers (1963) also presented the dimensionless groups and examined the feasibility of using different scaling techniques with geometrically similar models and prototypes. It was concluded that only two methods of thermal scaling appear to be practical. They are the materials and temperature preservation techniques. The similitude relations were derived for three-

dimensional, non-steady temperature fields for opaque surfaces whose radiative properties can be characterized by the total hemispherical emittance and absorptance. Theoretical analyses were made to determine the magnitude of temperature prediction errors introduced by variations of thermal properties.

Jones (1964) has rederived the dimensionless groups in different nomenclature by considering a set of "n" differential equations that describe the temperature of "n" isothermal bodies that are at different temperatures. It is suggested that the use of geometric distortions in conducting paths will be useful in applying the scaling technique in practical situations. Chao and Wedekind (1965) have extended Vickers' (1963) analysis by deriving the scaling criteria for both temperature and materials preservation techniques with consideration of temperature variations of bulk thermal properties and the non-diffuse, non-grey properties of opaque surfaces. The similitude relations are presented for two- and three-dimensional, non-steady temperature fields. The effects of inter-reflections are considered and the radiant fluxes are defined in terms of directional, monochromatic emittances, reflectances, and absorptances. The generalization of the problem introduces some complexity in the scaling relationships. It is pointed out that the use of materials which exhibit similar temperature dependency can improve accuracy in modeling with the temperature preservation technique. Analyses show that modeling of two-dimensional heat flow patterns can be made easier by employing models of distorted thickness.

Experimental Investigations

The first known attempts to predict prototype temperatures (as measured in test) from tests of reduced-scale models were undertaken at approximately the same time by Fowle, et al. (1964) and Wainwright, et al. (1964). Tests of thermal models had been undertaken previously by other investigators, but tests of the prototype were not made, thus, a direct analysis of errors in the modeling technique was not available. Fowle, et al. (1964) compared equilibrium temperature measurements within a prototype, which was a simplified version of a typical JPL spacecraft, with measurements of the temperatures of three, thermally-scaled models. Two models (one-half and one-fifth scale) were designed in accordance with the temperature preservation technique. A one-half scale model was also designed in accordance with the materials preservation technique. The results showed that the temperatures of both half-scale models agreed with the measured prototype temperatures within 3C (5.4F). The accuracy of the one-fifth scale model was accurate to within 10C (18F). All tests were performed in a cold-wall vacuum chamber without solar simulation.

Wainwright, et al. (1964) constructed three sets of models of different geometry and compared temperature measurements at equilibrium in a cold-wall vacuum chamber with solar simulation. The models were all fabricated from different materials than their corresponding prototypes. The errors in predicting temperatures of a full-scale aluminum cylinder with a lead cylinder (55% scale) and a steel cylinder (35% scale) were of the order of 5-10C (9-18F). Part of the error was attributed to the experimental procedure.

Experiments in thermal scale modeling where transient effects were important have been reported by Adkins (1965), Rolling (1965), Jones and Harrison (1965), and Shanklin (1965). Similar experiments by Adkins, and Jones and Harrison, were conducted with a cylinder-sphere-plate configuration modeled at half-scale. Geometric distortion of the minor dimensions was used to satisfy the scaling requirements. The prototype was designed so that the cylinder, sphere and plate were nearly isothermal but different in temperature from one another, thereby eliminating the need for scaling conductive effects. Tests in a cold-wall vacuum chamber without solar simulation showed that the half-scale model could be used to predict the temperatures of the cylinder and plate to within 8K (14.4F). The accuracy of results for the sphere was worse because it was not isothermal. Rolling (1965) tested half and quarter-scale models in steady-state and transient conditions. The test objects were heated radiatively (in a vacuum) with tungsten lamps whose intensity was modulated sinusoidally to provide a periodic temperature-time behavior in the test objects. The half-scale model was fabricated from the same materials as the prototype and the one-fourth-scale model of different materials. Geometrical distortions in minor dimensions were utilized in both models to satisfy the transient scaling criteria. Predictions using either model were generally within 8C (15F) of the measured prototype temperatures.

Perhaps, the most extensive test of the feasibility of thermal scale modeling was described by Gabron, et al. (1965, 1966). A 0.43 scale thermal model of the Mariner IV spacecraft, designed in accordance with the temperature preservation technique, was tested (at thermal

equilibrium) in a simulated solar environment. The temperature predictions made by use of the scale-model were compared with Mariner IV flight temperature data. The prototype and model contained bolted joints critical to the temperature distributions and included active temperature control louvers. Approximately 50% of the model measurements corresponded within 10F of the flight data and 85% were within 25F. The accuracy of temperature predictions made with the reduced-scale model was, with only several exceptions, equivalent to the accuracy of predictions made in pre-flight thermal tests of Mariner IV in a large solar simulator.

Discussion

The basic dimensionless groups which define the similarity between model and prototype are well understood for both steady and non-steady conditions. Most of the theoretical work has been devoted to studies of the practical application and errors associated with the materials and temperature preservation techniques. However, as Rolling (1965) has correctly pointed out "Considerable reference has been made in the literature to utilization of 'Temperature Preservation' or 'Material Preservation' techniques." "While practical considerations may often dictate material or temperature preservation, it is important to note that the model criteria are entirely general and do not in themselves lead to either of these accepted approaches." Apparently, the use of the terms "materials" or "temperature" preservation has led to a certain amount of confusion in the literature. In fact, there are only two methods for predicting prototype temperatures from model

tests. Either the temperatures are preserved at homologous locations in model and prototype or the temperatures are in fixed but predictable ratio.

When the temperature fields within spacecraft are three-dimensional, the temperature or materials preservation techniques appear to be the only practical methods for modeling when the surface optical properties are preserved. Preserving the surface optical properties may, at first glance, appear overly restrictive, but in typical spacecraft configurations the problems of inter-reflections make this restriction a practical necessity.

Typically, many spacecraft components are fabricated from thin plates, shells, tubing, rods, etc., where the temperature fields are one, or two-dimensional. When the temperature fields are not three-dimensional, it is possible, by distorting the minor geometrical dimensions of the model, to use identical materials in model and prototype and make the temperatures identical at homologous locations. Conversely, it is possible to use different materials in model and prototype and have the temperatures differ in fixed, predictable ratio. The use of geometrical distortions in the thicknesses of plates, shells, etc., provides the model designer with a wide variety of possible scaling techniques, and it eliminates many of the practical problems associated with perfectly scaling all dimensions and choosing materials to have specified thermal properties.

Thermal tests of full-scale prototypes and thermal scale models have demonstrated the feasibility of the technique in both steady-state and transient conditions. The errors associated with modeling by either

preserving or scaling temperatures in model and prototype have been determined for models as small as one-fifth scale, for widely different geometries, and prototype complexity. Equilibrium temperature data have been obtained in solar simulation tests with a detailed scale-model of an actual spacecraft and the results compared favorably with telemetered flight data. Actively-operated temperature control louvers and thermal contact resistances across bolted joints were successfully modeled at steady-state conditions in this case.

Further experimental work is required in scaling bolted joints, "super-insulations" and in the whole area of transient modeling with active temperature control elements for complicated prototypes. Additional experience will improve the accuracy and reliability of the technique of thermal modeling, and could possibly change the thermal modeling technique from a "development tool" to a usable technique for thermal qualification testing--particularly for very large spacecraft.

II. Theory of Thermal Scale Modeling

Three-dimensional Temperature Fields

The heat flow equation for a homogeneous, isotropic solid with internal power generation whose thermal properties are independent of temperature or position is given by the equation

$$\frac{\partial^2 T}{\partial x^2} + \frac{\partial^2 T}{\partial y^2} + \frac{\partial^2 T}{\partial^2 z} - \frac{1}{\kappa}\frac{\partial T}{\partial t} = -\frac{q'''}{k} \qquad (1)$$

where $\kappa = \frac{k}{\rho c}$

and
- T - temperature
- x,y,z - coordinate dimensions
- k - conductivity (w/cmK)
- κ - diffusivity (cm^2/sec)
- t - time (sec)
- q''' - rate of heat flow per unit volume (w/cm^3)
- c - specific heat (w sec/gr K)
- ρ - density (gr/cm^3)

The initial conditions are

$$T = f(x, y, z, t) \qquad (2)$$

The surface conditions for an opaque solid may be of three types:

1. Radiation from the surface;

$$k\frac{\partial T}{\partial n} + \varepsilon \sigma T^4 = 0 \qquad (3)$$

where $\frac{\partial T}{\partial n}$ denotes differentiation in the direction of the outward normal to the surface, and

- ε - total hemispherical surface emittance
- σ - Stefan-Boltzmann constant

2. Prescribed radiative flux into the surface;

$$-k\frac{\partial T}{\partial n} + \alpha S(t) = 0 \tag{4}$$

where $S(t)$ - incident radiative flux (w/cm^2)

α - absorptance of the surface for the incident flux

3. Surface in contact with another body

$$-k\frac{\partial T}{\partial n} + C\,T_o(t) = 0 \tag{5}$$

where $T_o(t)$ - temperature of contacting body

C - thermal resistance between surfaces (w/cm^2K)

Five basic dimensionless groups are obtained by inspection from Equations (1-5) using characteristic lengths L_m and L_p for model and prototype, respectively. It will be assumed throughout this discussion that the radiation configuration factors between elements will be made identical in model and prototype by geometrically scaling all major dimensions of radiating surfaces.

$$\left(\frac{\rho c L^2}{kt}\right)_m = \left(\frac{\rho c L^2}{kt}\right)_p \tag{6}$$

$$\left(\frac{q''' L^2}{kT}\right)_m = \left(\frac{q''' L^2}{kT}\right)_p \tag{7}$$

$$\left(\frac{\varepsilon\sigma T^3 L}{k}\right)_m = \left(\frac{\varepsilon\sigma T^3 L}{k}\right)_p \tag{8}$$

$$\left(\frac{\alpha SL}{kT} \right)_m = \left(\frac{\alpha SL}{kT} \right)_p \tag{9}$$

$$\left(\frac{CL}{k} \right)_m = \left(\frac{CL}{k} \right)_p \tag{10}$$

These five equations can now be used to obtain various modeling techniques. Vickers (1963) has shown that among several choices two techniques appear to offer advantages in situations where the heat flow fields are three-dimensional. They are: (1) setting the temperatures equal at homologous locations in model and prototype, and (2) using identical materials in model and prototype. In both cases the emittances and radiation configuration factors are made equal in model and prototype.

The controlling equations are presented in Table 1. From Table 1, we see that the temperature preservation technique requires that the thermal conductivities and power generation be scaled. The time dimension may be different in model and prototype. Thermal resistances across surfaces in contact and heat fluxes absorbed on surfaces must be identical in model and prototype. With the materials preservation technique the temperatures of model and prototype are in fixed ratio, and all other variables except material properties must be scaled. The significant limitation in both techniques is the scaling ratio attainable. Using the temperature preservation technique the size of the model may be limited by available materials. A one-tenth scale model requires a material with a conductivity one-tenth that of the prototype. Using

Table 1

Comparison of Controlling Equations for Model and Prototype (three-dimensional temperature fields)

Technique 1 Temperature & Surface Emittances the Same in Model and Prototype.		Technique 2 Materials & Surface Emittances the Same in Model and Prototype.	
$\frac{k_m}{k_p} = \frac{L_m}{L_p} = R$	(11a)	$\frac{T_m}{T_p} = \left(\frac{L_p}{L_m}\right)^{1/3} = \left(\frac{1}{R}\right)^{1/3}$	(11b)
$\frac{C_m}{C_p} = 1$	(12a)	$\frac{C_m}{C_p} = \frac{L_p}{L_m} = \frac{1}{R}$	(12b)
$\frac{t_m}{t_p} = \frac{(\rho c)_m L_m}{(\rho c)_p L_p} = \frac{(\rho c)_m}{(\rho c)_p}(R)$	(13a)	$\frac{t_m}{t_p} = \left(\frac{L_m}{L_p}\right)^2 = R^2$	(13b)
$\frac{q'''_m}{q'''_p} = \frac{L_p}{L_m} = \frac{1}{R}$	(14a)	$\frac{q'''_m}{q'''_p} = \left(\frac{L_p}{L_m}\right)^{7/3} = \left(\frac{1}{R}\right)^{7/3}$	(14b)
$\frac{\alpha_m S_m}{\alpha_p S_p} = 1$	(15a)	$\frac{\alpha_m S_m}{\alpha_p S_p} = \left(\frac{L_p}{L_m}\right)^{4/3} = \left(\frac{1}{R}\right)^{4/3}$	(15b)

the materials preservation technique, the absolute temperature of the model is higher than the prototype (a one-tenth scale model of a prototype operating at 300K (80F) would operate at 645K (700F)) and this requirement poses practical problems because of temperature-dependent thermal properties.

Two-dimensional Temperature Fields

Fortunately, most spacecraft are fabricated from plates, shells, bars, rods, etc., where the temperature fields are not three-dimensional. In cases other than those with three-dimensional fields, the requirements for thermal scale modeling are simplified because of the fact that geometric distortions of the minor dimensions (i.e., the thicknesses of plates, etc.) are permitted providing that the over-all geometry is retained for purposes of making radiation configuration factors identical in model and prototype.

The similarity criteria for two-dimensional fields may be conveniently obtained by considering the heat flow in a thin plate of thickness δ with an internal power generation per unit surface area of q". The thermal properties are assumed independent of temperature or position. The plate emits radiation on one side to a non-reflecting medium at absolute zero, is in contact through a thermal contact resistance C with a body also at absolute zero on the other side, and absorbs radiation from a source of intensity S(t).

The differential equation for the temperature in the plate is

$$-k\delta\left(\frac{\partial^2 T}{\partial x^2} + \frac{\partial^2 T}{\partial y^2}\right) + \varepsilon\sigma T^4 + CT + q'' + \alpha S(t) = \rho c\delta\frac{\partial T}{\partial t} \qquad (16)$$

From this equation, we obtain the following dimensionless groups

$$\left(\frac{\rho c L^2}{kt} \right)_m = \left(\frac{\rho c L^2}{kt} \right)_p \tag{17}$$

$$\left(\frac{q'' L^2}{k\delta T} \right)_m = \left(\frac{q'' L^2}{k\delta T} \right)_p \tag{18}$$

$$\left(\frac{\varepsilon \sigma T^3 L^2}{k\delta} \right)_m = \left(\frac{\varepsilon \sigma T^3 L^2}{k\delta} \right)_p \tag{19}$$

$$\left(\frac{\alpha S L^2}{k\delta T} \right)_m = \left(\frac{\alpha S L^2}{k\delta T} \right)_p \tag{20}$$

$$\left(\frac{CL^2}{k\delta} \right)_m = \left(\frac{CL^2}{k\delta} \right)_p \tag{21}$$

Again, we have chosen to illustrate the controlling equations for two techniques, viz., one in which the temperatures are made identical in model in prototype at homologous locations, and the other in which the temperatures are made different. In both cases, the emittances of model and prototype are made identical. The controlling equations are presented in Table 2. It can be seen that the temperatures may be preserved using Technique 1 by scaling the product $k\delta$ where conductive effects are important. This provides considerable freedom in choosing materials and thicknesses for fabricating the prototype, and eliminates the need for obtaining a perfectly scaled conductivity which is required

Table 2

Comparison of Controlling Equations for Model and Prototype (two-dimensional temperature fields)

Technique 1 Temperature & Surface Emittances the Same in Model and Prototype.		Technique 2 Temperatures Different but Surface Emittances the Same in Model & Prototype.	
$\frac{(\kappa t)_m}{(\kappa t)_p} = \frac{L_m^2}{L_p^2} = R^2$	(22a)	$\frac{(\kappa t)_m}{(\kappa t)_p} = R^2$	(22b)
$\frac{(k\delta)_m}{(k\delta)_p} = R^2$	(23a)	$\frac{(k\delta)_m}{(k\delta)_p} = R^2 \frac{T_m^3}{T_p^3}$	(23b)
$\frac{q''_m}{q''_p} = 1$	(24a)	$\frac{q''_m}{q''_p} = \frac{T_m^4}{T_p^4}$	(24b)
$\frac{(\alpha S)_m}{(\alpha S)_p} = 1$	(25a)	$\frac{(\alpha S)_m}{(\alpha S)_p} = \frac{T_m^4}{T_p^4}$	(25b)
$\frac{C_m}{C_p} = 1$	(26a)	$\frac{C_m}{C_p} = \frac{T_m^3}{T_p^3}$	(26b)

when the temperature fields are three-dimensional. Note that Equation (23a) allows the temperatures to be made identical using identical materials if the thickness is scaled by the square of the ratio used to scale the major dimensions. The characteristic times in model and prototype are related to the scaling ratio and thermal diffusivities. Naturally, the diffusivity ratios of all elements within the configuration must be made identical. The internally generated heat fluxes, absorbed fluxes and joint conductances must be made identical in model and prototype.

Technique 2 offers many interesting possibilities since both the geometric scaling ratio and temperature ratio between model and prototype may be chosen somewhat arbitrarily. Practical limitations are imposed by Equation (23b) if the scale ratio is small and it is desired to operate the model at higher temperatures than the prototype. At high temperature ratios the total emittances and absorptances in the model and prototype may differ even though the same coatings are used because of spectral shifts. Limitations in the temperature ratio may also be imposed by Equation (26b) which requires that the joint conductances scale by the cube of the temperature ratio. For example, if a joint in the prototype has a very high conductance, it would be difficult to build a model joint with a higher conductance. Note that if materials are preserved the time scale is proportional to the square of the geometric scale ratio; however, the selection of a temperature scaling factor (Equation 23b) is flexible since the thickness ratio may be varied.

Chao and Wedekind (1965) have investigated the similarity relationships when the thermal conductivity and specific heat are temperature

dependent and expressible as power functions according to

$$k = \bar{k}T^a \qquad c = \bar{c}T^b$$

The similarity relations show that for perfect scaling in steady-state

$$a_m = a_p \tag{27}$$

and for transient modeling

$$b_m - a_m = b_p - a_p \tag{28}$$

To illustrate these results for two-dimensional modeling using Technique 1, we find that the corresponding equation to Equation (22a) is

$$\frac{t_m}{t_p} = \frac{\delta_m}{\delta_p}\,\frac{\bar{c}_m}{\bar{c}_p}\,\frac{\rho_m}{\rho_p} \tag{29}$$

The corresponding equation to Equation (23a) is

$$\frac{\bar{k}_m\,\delta_m}{\bar{k}_p\,\delta_p} = R^2 \tag{30}$$

Similarly, for Technique 2 where the temperatures are made different, Equation (22b) becomes

$$\frac{(\rho\bar{c})_p\,\bar{k}_m\,t_m}{(\rho\bar{c})_m\,\bar{k}_p\,t_p} = R^2\,\frac{T_m^{\,b_m-a_m}}{T_p^{\,b_p-a_p}} \tag{31}$$

and Equation (23b) becomes

$$\frac{(\bar{k}\delta)_m}{(\bar{k}\delta)_p} = R^2\,\frac{T_m^{\,3-a_m}}{T_p^{\,3-a_p}} \tag{32}$$

The conclusions presented by Chao and Wedekind show that difficulties exist in choosing materials with proper temperature exponents particularly for transient modeling of systems where more than one material is used. They also conclude that accurate modeling of systems with large temperature gradients may be difficult because of temperature dependent properties. (The temperature errors associated with modeling when temperature dependent properties are considered will be calculated for typical applications in a following section of this report. It will be shown that the magnitude of the errors is small. This observation has also been confirmed by Vickers (1963) for the case of steady-state modeling of conductive systems with temperature-dependent conductivity.)

Discussion

The similitude relations for thermal modeling in two and three-dimensional temperature fields have been presented. The requirements for modeling three-dimensional fields are somewhat restrictive, and the only practical techniques available are the temperature or materials preservation techniques. Modeling of two-dimensional temperature fields may be accomplished by either temperature preservations or temperature scaling. In either case, allowable geometric distortions in the minor dimensions increase the flexibility of applying the similitude relations. Eliminating the need for scaling temperature transients considerably reduces the practical problems of thermal modeling.

It must be emphasized that the similitude relations have been presented for the general case in which radiation and conductive effects

are both important in determining temperature distributions. In many practical applications, the temperature distributions may be dominated by conduction or radiation. If the temperature fields are dominated by radiative effects, it is unnecessary to exactly scale the thermal conductivity of model materials, and conversely, if conductive effects are dominant it is unnecessary to exactly scale the surface optical properties. Such situations, which are commonly found in complex spacecraft, eliminate the need for precisely modeling all parts of the prototype. In general, the model may contain elements which are: 1) modeled precisely in accordance with all similitude relations for either two or three-dimensional temperature fields, 2) modeled for only conductive or radiative effects, and 3) "mocked-up" to provide structural integrity, but are not thermally modeled when the temperatures or heat flow patterns in such elements are unimportant.

A final word of caution should be noted with respect to the oversimplification of modeling by use of geometric distortions in applying the two-dimensional modeling techniques. While it is true that the temperature fields in plates, shells, etc., may generally be two-dimensional, the heat flow patterns around bolted joints or edges of the plates may produce three-dimensional temperature fields. Gross distortions of the thicknesses in such areas may lead to temperature prediction errors which are difficult to evaluate.

III. Special Topics

Temperature Errors Associated with Temperature-dependent Properties

Since the basis for all modeling is to predict prototype temperatures as closely as possible from a model, it is of interest to examine the magnitude of the temperature prediction errors due to the fact that practically all materials used in spacecraft have temperature-dependent properties. The discussion here will be restricted to steady-state modeling, and in particular to the effects of changes in thermal conductivity due to temperature.

Vickers (1963) examined the temperature errors in 1/10 scale models designed in accordance with temperature and materials preservation using a prototype configuration which would result in large errors by comparison to most elements in a typical spacecraft. The results showed that the maximum errors in temperature were 0.3% (1K) for the temperature preservation technique and 1.7% (6K) for the materials preservation technique. These computations are perhaps overly conservative since 1/10 scale is judged to be a very low scale ratio. (One-half or 1/4 scale models of the largest planned spacecraft could now be tested in available solar simulation facilities.)

In order to estimate the temperature and heat flow errors in more typical situations, we consider the steady flow of heat in an infinitely long bar losing heat by Newton's Law of Cooling. One end of the bar is maintained at a constant temperature T_1, and the bar is exchanging heat with a medium held at a constant temperature T_o. For moderate tempera-

ture ranges, typical of spacecraft elements, the conductivity of metals can be represented by an equation of the form

$$k(T) = k_1 + \alpha\ (T - T_1) \tag{33}$$

where α - temperature coefficient of thermal conductivity.

k - thermal conductivity

k_1 - thermal conductivity at temperature T_1

To obtain an estimate of the errors produced by neglecting the temperature variations of thermal conductivity, we have calculated both the maximum temperature error and the error in heat flow into the bar at the end where the temperature is fixed at T_1. The results are presented in Table 3 for five materials which might be typical of spacecraft and model materials. The materials chosen have widely different characteristics. Materials with high and low conductivities having either large positive or large negative temperature coefficients were purposely selected. The temperature errors, i.e., the maximum difference between the temperature along a bar with constant conductivity and the temperature along a bar with variable conductivity, are less than 0.3K (.5F) for a temperature span of 50K (90F). The temperature errors are proportional to the square of the temperature span, so if the span were made 100K (180F) the maximum error would be about 1.2K (2F). The errors in heat flow at the end of the bar are less than 2% in all cases.

It is now of interest to compute the error in prototype temperature prediction made with a model when temperature-dependent properties are considered. Again we have chosen the rod example discussed in the previous paragraphs to illustrate the effects. To examine errors in the

Table 3

Temperature and Heat Flow Errors in Neglecting Temperature Variation of Thermal Conductivity

Material	Beryllium*	Iron	304 S.S.	Magnesium Mg-An-M-29	Aluminum 7075-T6
$k_1 \left(\frac{\text{watts}}{\text{cmK}}\right)$	1.8	.803	.157	0.79	1.26
$\alpha \times 10^4 \left(\frac{\text{watts}}{\text{cmK}^2}\right)$	-13.9	-8.0	2.76	16.6	22.0
Maximum temperature error (K) **	-0.111	-0.143	+0.252	+0.302	+0.251
Error in rate of heat flow (%)	-0.64	-0.82	1.49	1.78	1.48

* Sintered beryllium.
** T_1 = 300K, T_o = 250K.

temperature preservation scaling technique, we have purposely chosen a magnesium prototype with a high positive temperature coefficient of conductivity, and a beryllium model with a high negative coefficient to amplify the errors. (As shown previously, the coefficient should have the same sign and magnitude for perfect scaling.) The errors in predicting the prototype temperature are shown in Figure 1 as a function of the non-dimensional length of the bar. The model in this case is 0.44 scale, and the length is non-dimensionalized by the factor

$$\lambda^2 = \frac{k_1 A}{ph} \tag{34}$$

where

A - cross sectional area of the bar
p - perimeter
h - heat transfer coefficient

From Figure 1 it is seen that the maximum temperature error is 0.4K (.7F), and the average error along the entire length is much less. Note that if temperature measurements were made at $\frac{x}{\lambda} = 0.606$ in model and prototype, the temperatures would be identical. Also note that if the distances along the bar where temperatures are measured are large with respect to λ, the errors again become very small. At large values of x/λ conductive effects are negligible.

The temperature prediction errors for a half-scale model designed in accordance with the materials preservation technique are shown in Figure 2. Beryllium was chosen for the illustration as it has a reasonably high temperature coefficient. The results show that the maximum error is less than 0.6K (1F).

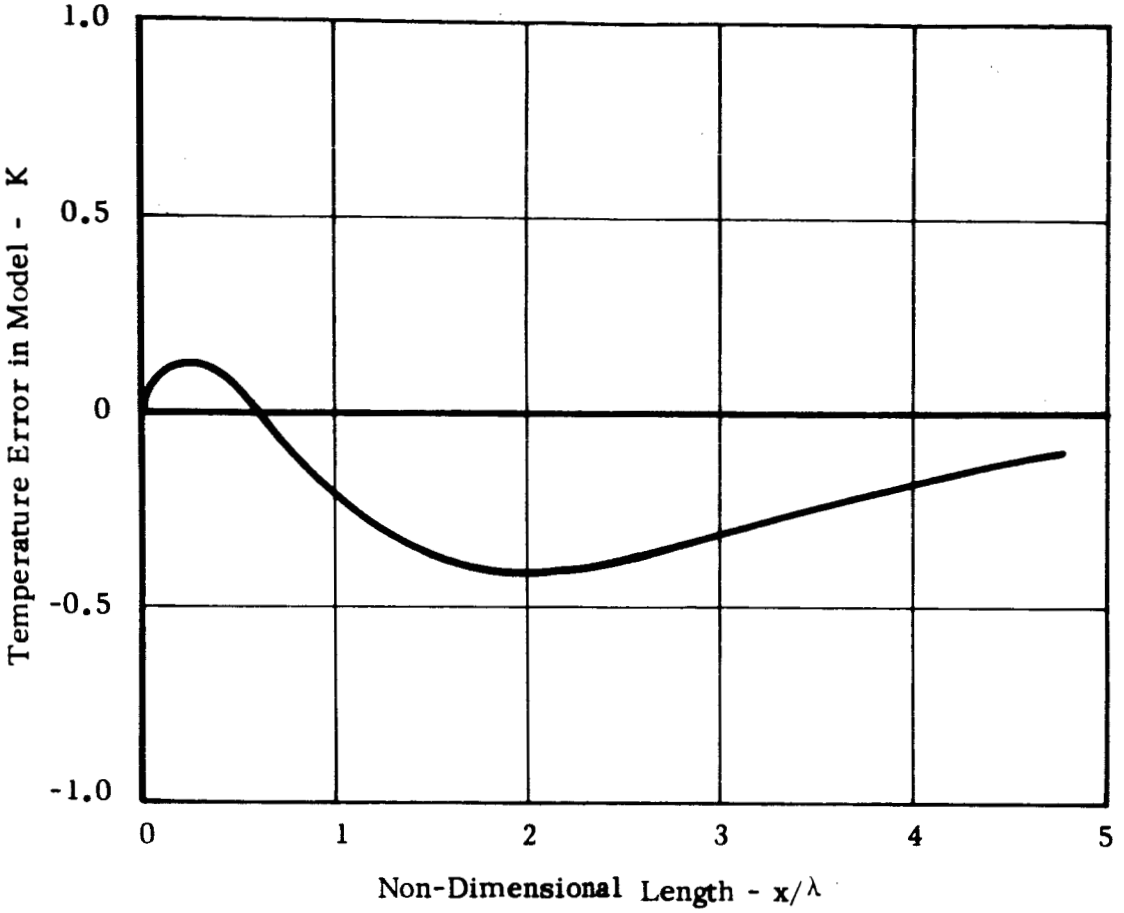

Model Material - Magnesium ($\alpha = 16.6 \times 10^{-4}$ w/cm K^2)
Prototype Material - Beryllium ($\alpha = 13.9 \times 10^{-4}$)

FIGURE 1 TEMPERATURE ERROR FROM PROPERTY VARIATIONS IN A 0.44 SCALE MODEL USING THE TEMPERATURE PRESERVATION TECHNIQUE

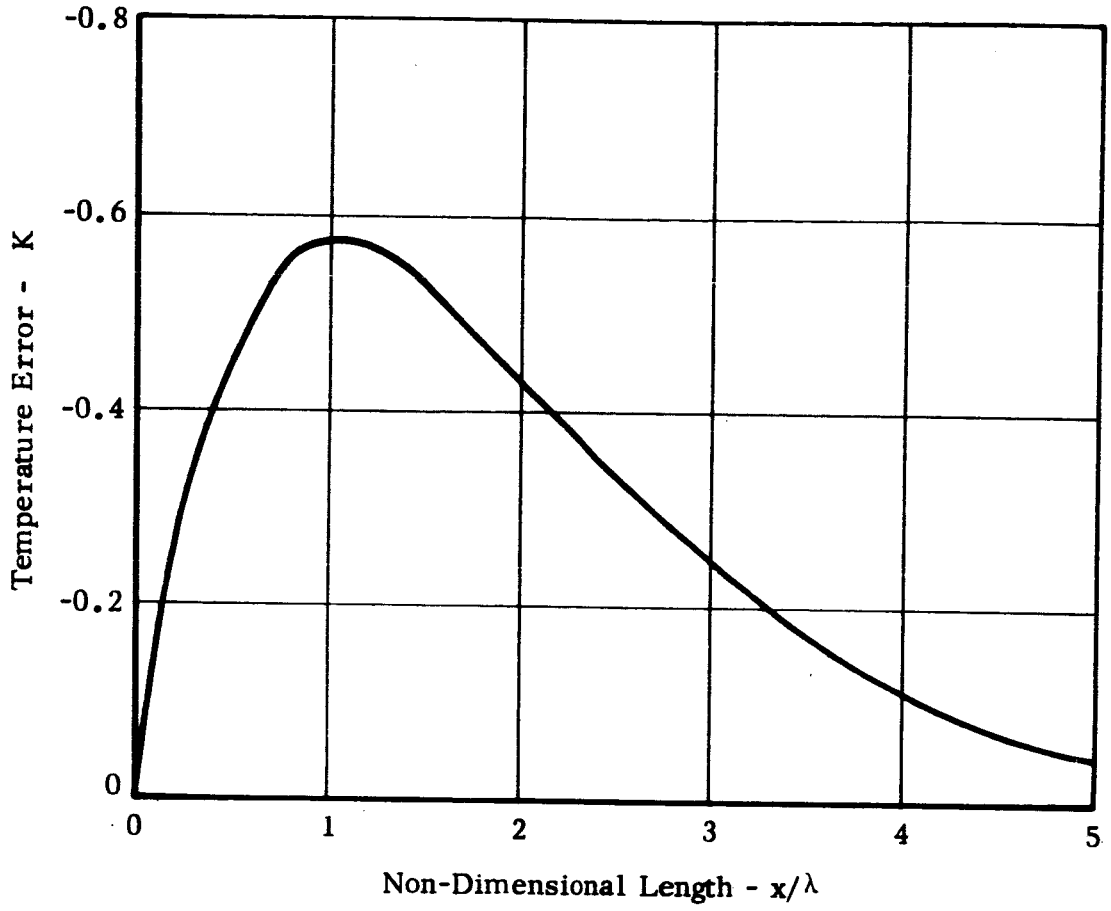

Material - Sintered Beryllium ($\alpha = -13.9 \times 10^{-4}$ w/cm K^2)

FIGURE 2 TEMPERATURE ERROR FROM PROPERTY VARIATIONS IN A HALF-SCALE MODEL USING THE MATERIALS PRESERVATION TECHNIQUE

Based on these results, we conclude that the effects of temperature dependent properties can be neglected in typical modeling situations since the errors are small. If temperatures are preserved in model and prototype by selecting different materials for the model, the errors can be made vanishingly small by proper choice of the temperature coefficient of conductivity. If materials are preserved in model and prototype and the temperatures of model and prototype differ by large ratios, the errors in temperature prediction could become significant. It is important to note that the magnitude of the temperature errors introduced by temperature-dependent properties depend, in general, on the location of temperature measurements.

Role of Radiation Skin Depth in Model Design

To illustrate the relative effects of radiation and conduction in determining the temperature fields in an object, we will again consider the simple problem of an infinite bar whose temperature at one end is fixed at T_1. The bar is exchanging heat by radiation with a "black" environment at a constant temperature T_o.

The differential equation for the bar temperature is

$$-kA \frac{d^2T}{dx^2} + \epsilon p \sigma T^4 = \epsilon p \sigma T_o^4 \qquad (35)$$

where

A - cross sectional area

ϵ - bar emittance

p perimeter

If T_1 is not greatly different than T_o, this equation may be solved by linearizing the temperature around T_o. With the boundary conditions

$T = T_1$ at $x = 0$, and $T = T_o$ at $x = \infty$, the temperature distribution is given by

$$T(x) = T_o + (T_1 - T_o)\, e^{-x/\lambda} \tag{36}$$

where

$$\lambda^2 = \frac{kA}{4\varepsilon p \sigma T_o^3} \tag{37}$$

The term λ may be referred to as a "radiation skin depth" and it is a measure of the length required for the bar to reach radiative equilibrium with its environment. The temperature distributions in a bar are plotted in Figure 3 for end temperatures of 300 and 270K. At lengths along the bar equal to or greater than about 3 "skin depths" the bar is in radiative equilibrium and a 30K change in the end temperature changes the temperature at $\frac{x}{\lambda} \to 3$ by approximately 1K. If the distance along the bar where the temperature is measured is small with respect to the skin depth, conductive effects predominate. From the definition of skin depth we see that the temperatures in members having a high thermal conductance or low emittance tend to be dominated by conductive effects and the temperatures in members with high emittance and low conductance are dominated by radiative effects.

The effects of uncertainties in conductivities of a bar are shown in Figure 4 for the same problem. The results show that errors of 10 or 25 percent do not produce large errors at lengths greater than 3 or 4 skin depths. This also illustrates the fact that perfect modeling of conductances is unessential where radiative effects predominate.

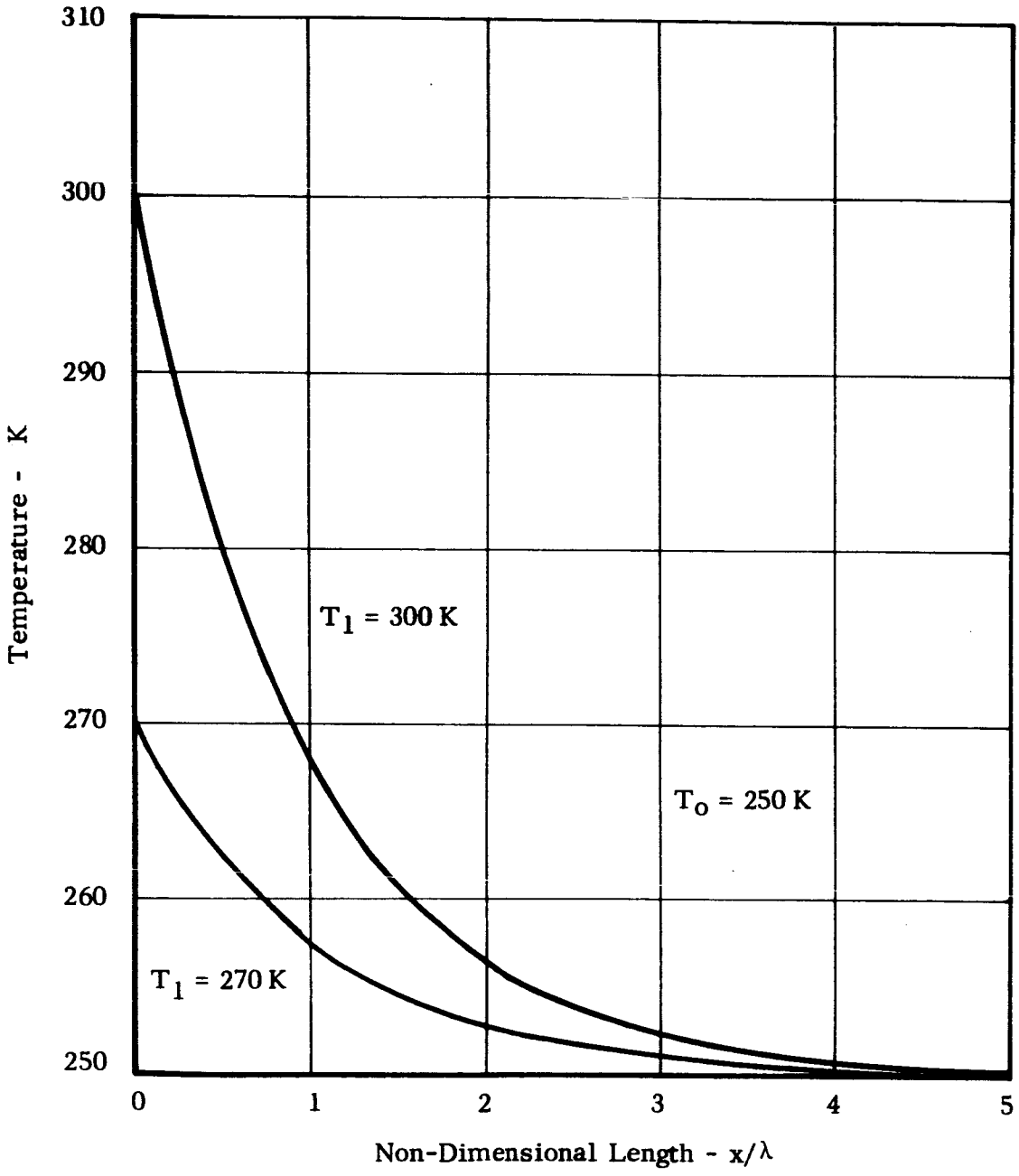

FIGURE 3 TEMPERATURE DISTRIBUTION IN A RADIATING BAR

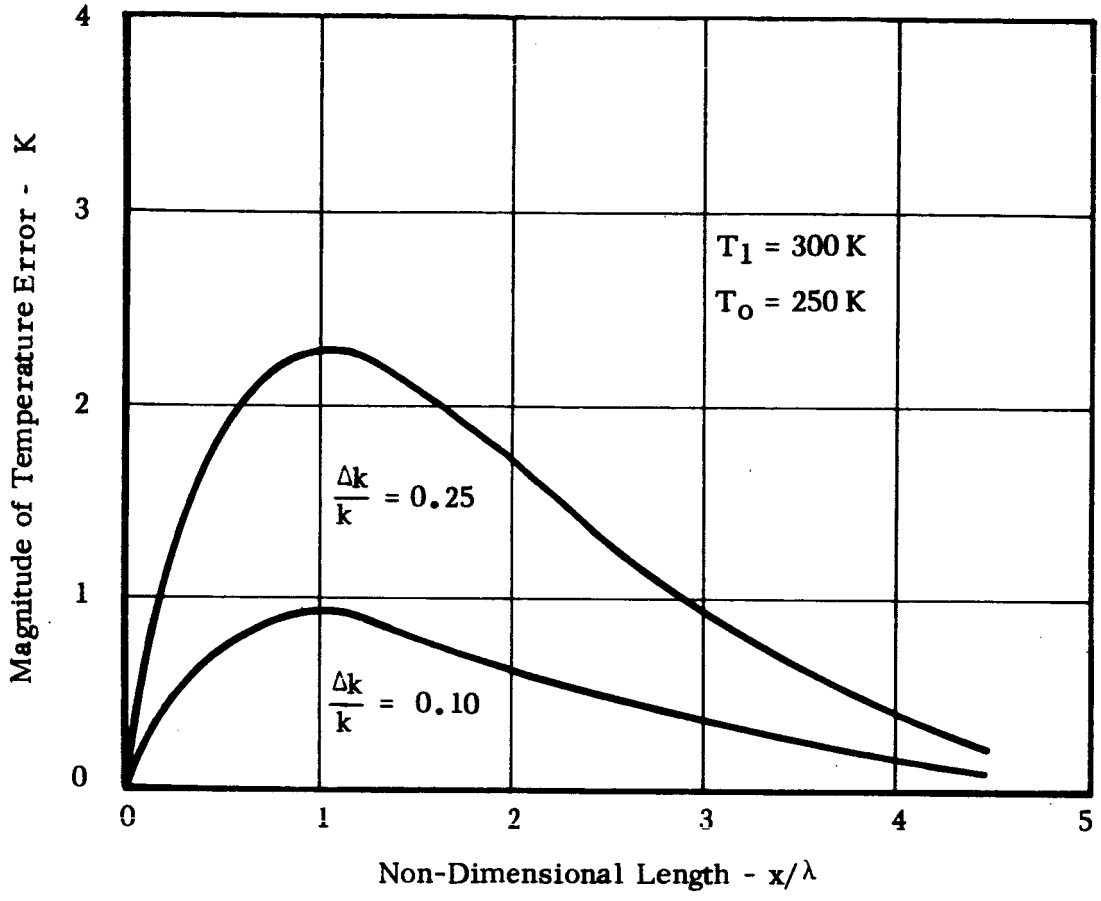

FIGURE 4 TEMPERATURE ERROR IN A BAR DUE TO UNCERTAINTIES IN CONDUCTIVITY

In order to further demonstrate the importance of the radiation skin depth in the design of thermal models, we will next consider another simple problem of determining the temperature distribution in a circular disc whose edge is maintained at a fixed temperature T_i. One side of the disc receives radiation from a source at T_i, and the other side receives a uniform flux S from a source at much different temperature (e.g., sunlight) and radiates to an environment at absolute zero. The infrared emittance of the disc is assumed equal to its absorptance for radiation received from the source at T_i and the absorptance for the flux S is α.

The differential equation for the heat flow in the disc is

$$-\frac{k\delta}{r}\frac{d}{dr}\left(r\frac{dT}{dr}\right) = \varepsilon\sigma T_i^4 + \alpha S - 2\varepsilon\sigma T^4 \qquad (38)$$

where

k - thermal conductivity

δ - disc thickness

r - disc radius

If the disc temperature does not appreciably differ from the edge temperature, this equation may be linearized about T_i. The solution, subject to the boundary condition that $T = T_i$ at $r = R$, is given by

$$T(r) - T_i = \frac{\alpha S - \varepsilon\sigma T_i^4}{8\varepsilon\sigma T_i^3}\left[1 - \frac{I_o\left(\frac{r}{\lambda}\right)}{I_o\left(\frac{R}{\lambda}\right)}\right] \qquad (39)$$

where $I_o\left(\frac{r}{\lambda}\right)$ is the zero order Bessel function with imaginary argument, and the radiation skin depth λ is given by

$$\lambda^2 = \frac{k\delta}{8\varepsilon\sigma T_i^3} \tag{40}$$

The normalized temperature distribution in the disc is plotted in Figure 5 for various values of $\frac{R}{\lambda}$. The normalized temperature is given by

$$1 - \frac{I_o\left(\frac{r}{\lambda}\right)}{I_o\left(\frac{R}{\lambda}\right)} \tag{41}$$

and may be thought of as the ratio of the temperature at any point to the temperature of a non-conducting disc. When the disc radius is large compared to the skin depth the temperature at the center is determined by radiative effects, and conversely when $\frac{R}{\lambda}$ is small the temperatures will be controlled by conductive heat flow from the edges of the disc.

To relate these observations to thermally modeling a disc in a radiation environment, Figure 6 shows the percent error in the difference between the center and edge of the disc as a function of the percent error in thermal conductivity of a reduced-scale temperature preservation model of the disc. From Figure 6 it is seen that when the disc radius is large compared to the skin depth, the conductivity of the model material is unimportant. With a radius six times the skin depth, a 50% error in conductivity would produce an error of only 3% of the temperature difference between the center and edge of the disc. Note that a 50% error in conductivity is equivalent to using identical materials in a prototype and half-scale model designed in accordance with the temperature preservation technique.

Further discussions of methods for determining whether radiative

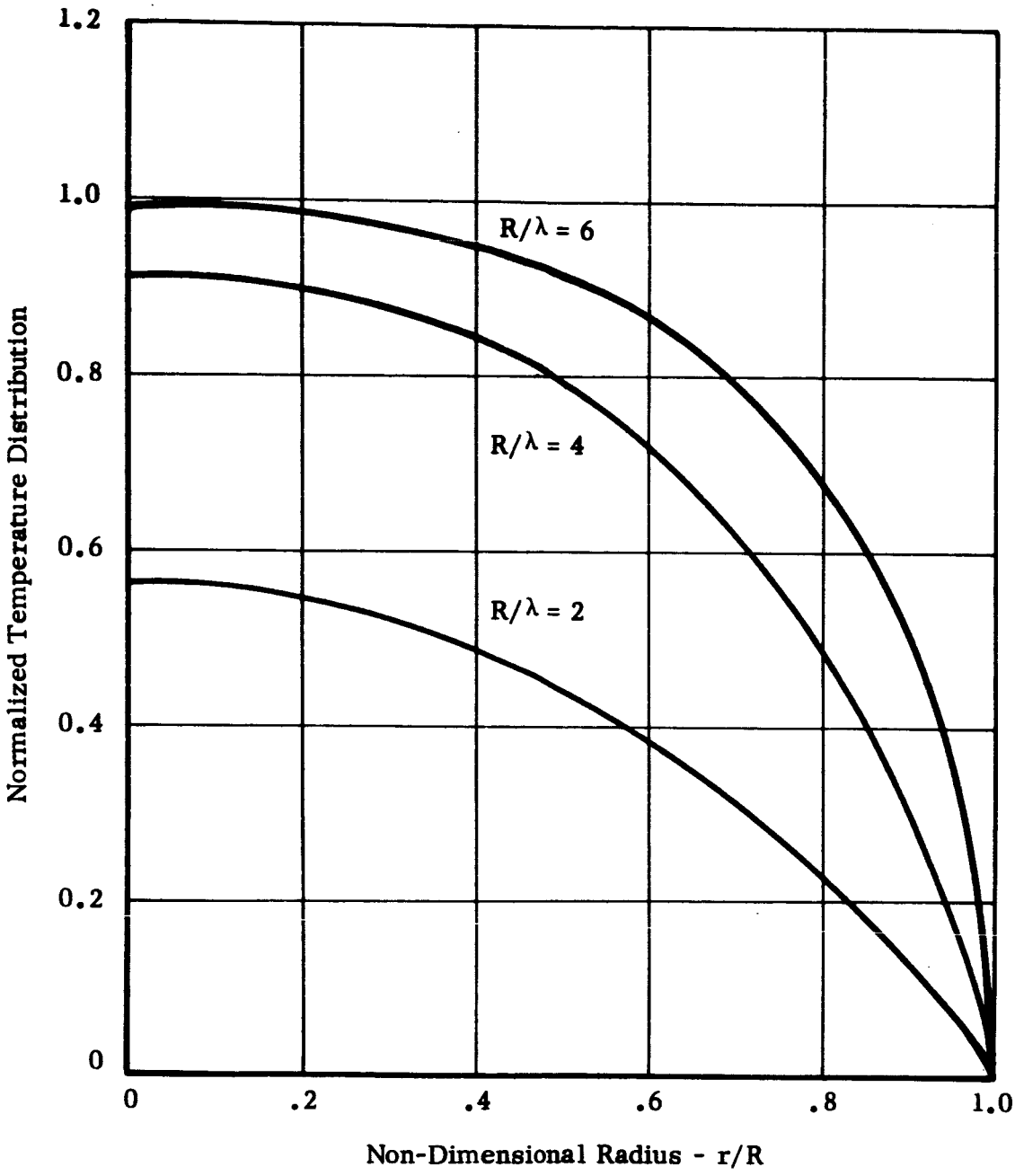

FIGURE 5 TEMPERATURE DISTRIBUTION IN A CIRCULAR DISC IN A RADIATION ENVIRONMENT

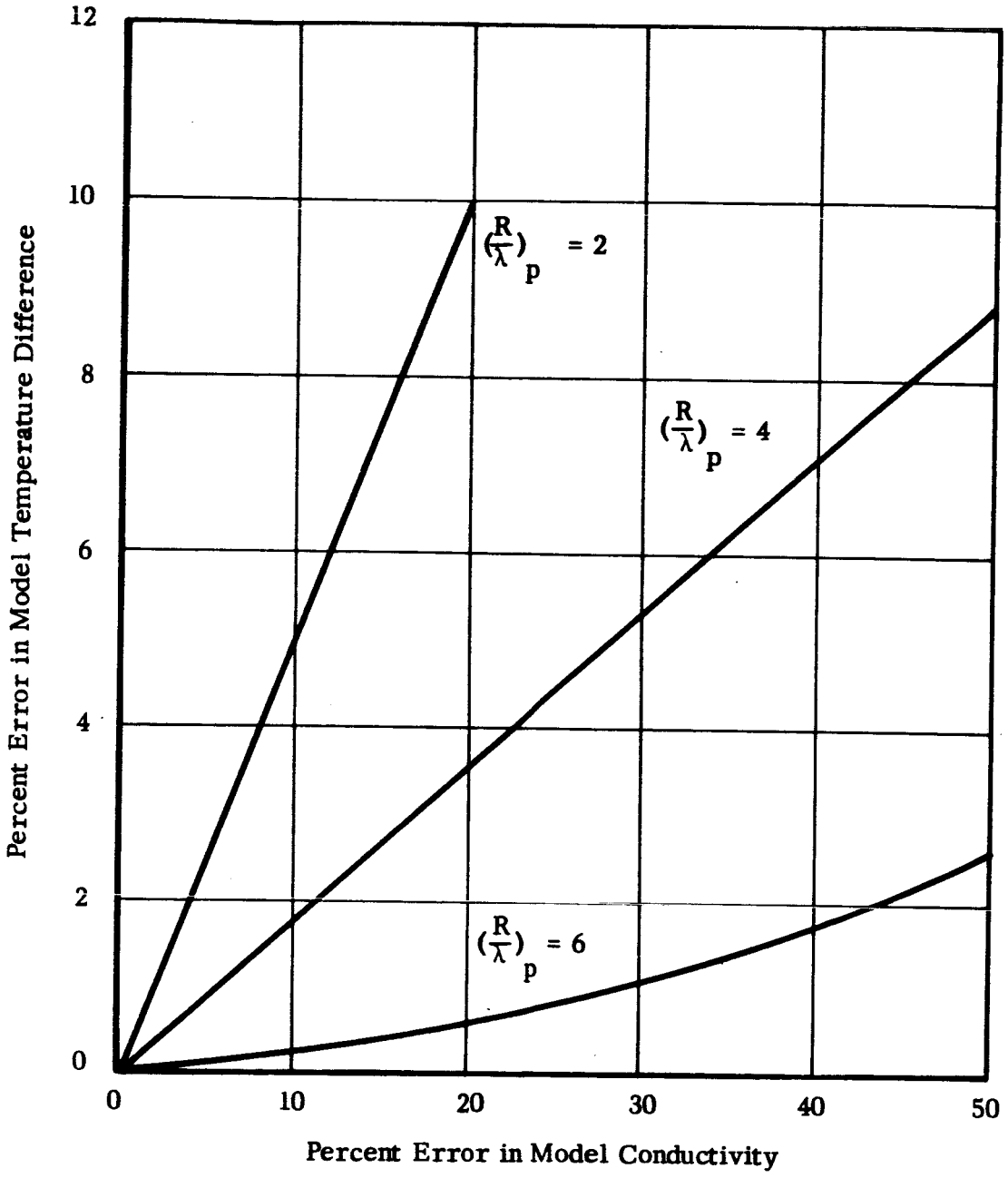

FIGURE 6 TEMPERATURE ERRORS IN A DISC MODELED WITH NON-SCALED THERMAL CONDUCTIVITY

or conductive effects are important in a spacecraft will be presented in Section IV.

Modeling of Temperature Control Louvers

Variable-emittance temperature control louvers have been effectively used to regulate the internal temperatures of interplanetary spacecraft and it is expected that such devices may be utilized on the Voyager spacecraft. Six temperature control louver assemblies, each comprising 11 pairs of bimetallically actuated louver blades, were used on the Mariner IV spacecraft to regulate the temperatures of critical electronic bays. The assemblies are designed to have a reasonably low emittance with the blades closed, and a high emittance when the blades are fully opened. Typical thermal data for a single assembly are listed below:

Effective emittance closed	0.12
Effective emittance open	0.76
Total area of assembly	1.62 ft^2
Fully open temperature	80F
Fully closed temperature	55F
Radiating power closed (55F)	6.9 watts
Radiating power open (80F)	52.6 watts

The performance of the Mariner IV louvers has been successfully modeled at 0.43 scale (Gabron, F., et al., 1965) using the temperature preservation technique. Certain difficulties were encountered in the fabrication of these scale model louvers and the following discussion of the problems of scaling louvers is partially based on this experience.

It appears that the feasibility of scaling temperature control louvers, or thermal switches operated by bimetal elements, may be

determined by the following considerations. First, the scale ratio may be limited by the size of the parts used in the prototype, which in typical full-scale prototypes is small. Second, the scale ratio of a louver assembly may be limited by the gaps required at the end of the blades for operating clearance. The clearances cannot, in general, be reduced in proportion to the over-all scale ratio and create an un-scaled heat leakage path. Third, if the temperatures are not made identical in model and prototype, the characteristics of the bimetal coils used for actuations will have to be altered.

Figures 7 and 8 show a 0.43 scale model of the Mariner IV louver and illustrate the basic problem of reducing the size of the actuating coils, axles, etc. It is doubtful if an assembly much smaller than 0.43 scale of a typical JPL louver assembly could be fabricated without excessive costs.

The second problem of size reduction involves the heat leakage via the gaps at the ends of each blade when the louvers are completely closed. The area created by the gaps radiates with an effective emittance near unity because of the cavity effect. The clearances cannot, in general, be scaled down in reduced-size models and create a non-scaled radiating area. To illustrate the importance of this effect, Figure 9 shows the percent error in the over-all emittance of a typical JPL louver assembly with the blades closed for various scale ratios. The gap dimensions of 1/32 and 1/64" were chosen as being typical of the range of tolerances attainable in fabricating sheet metal parts of such dimensions. It can be seen that the errors in the effective emittance of an assembly can be greater than 20 percent for a 1/5 scale model. This is, of course,

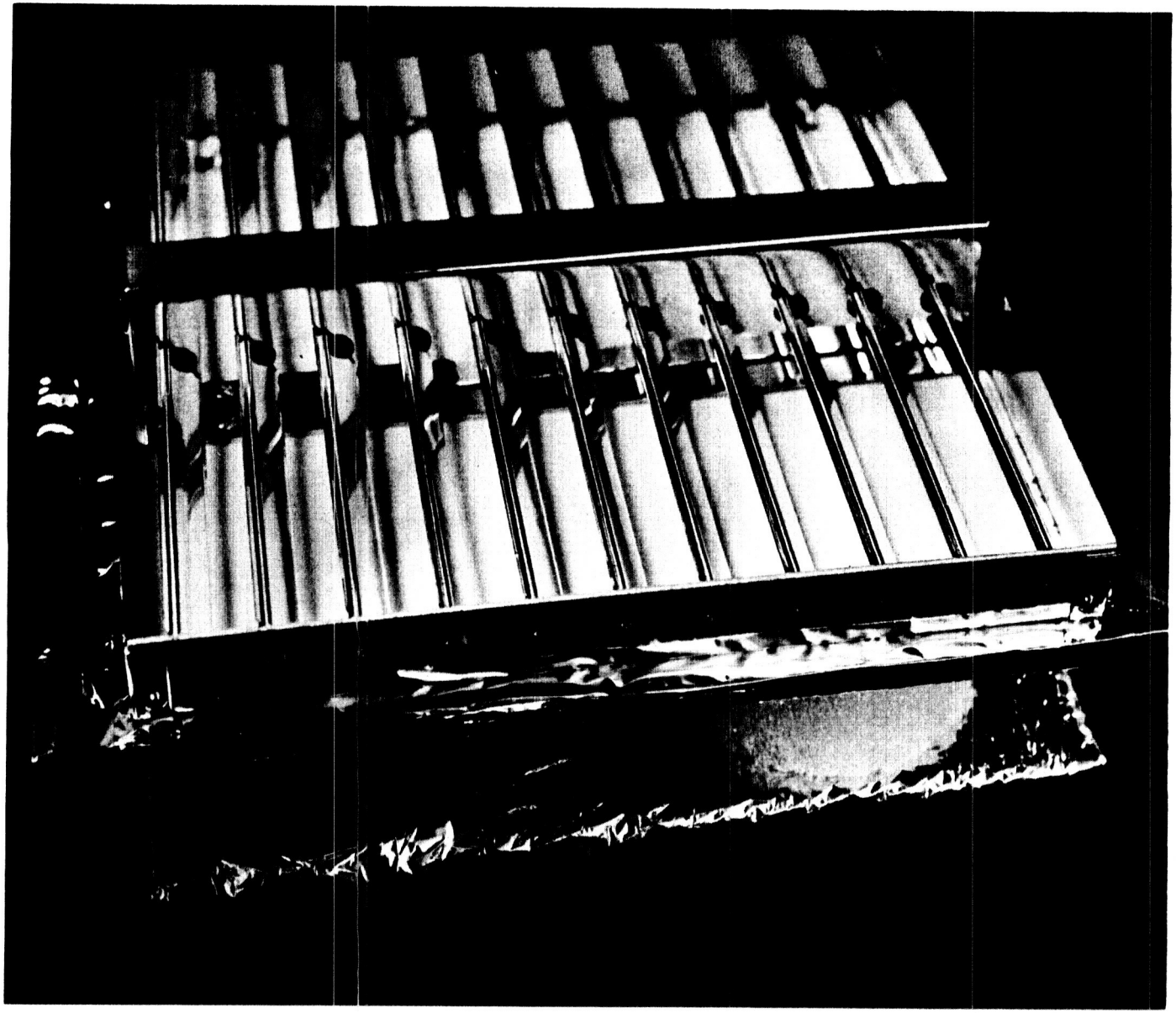

FIGURE 7 0.43 SCALE LOUVER ASSEMBLY

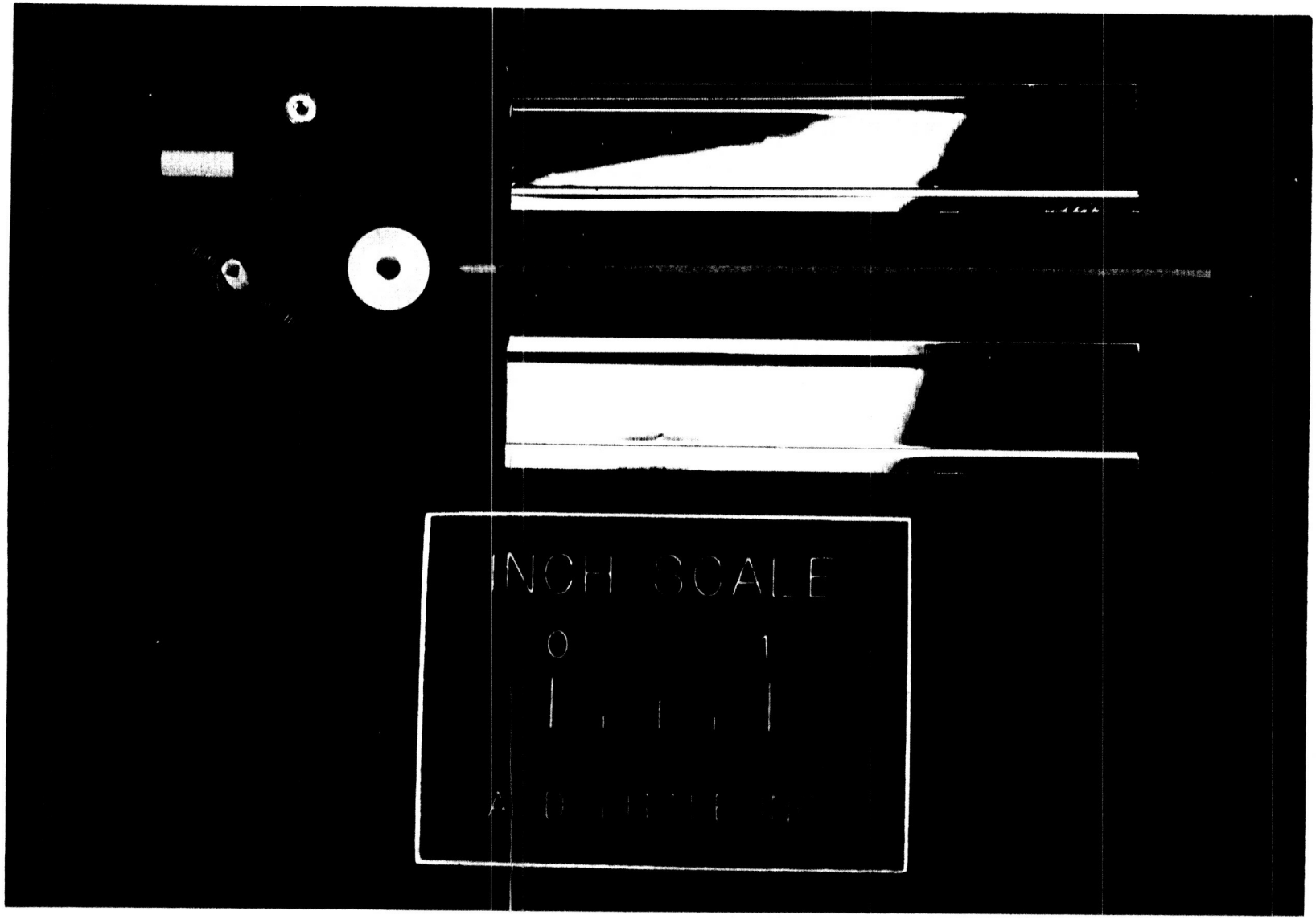

FIGURE 8 THERMAL CONTROL LOUVER BLADE ASSEMBLY

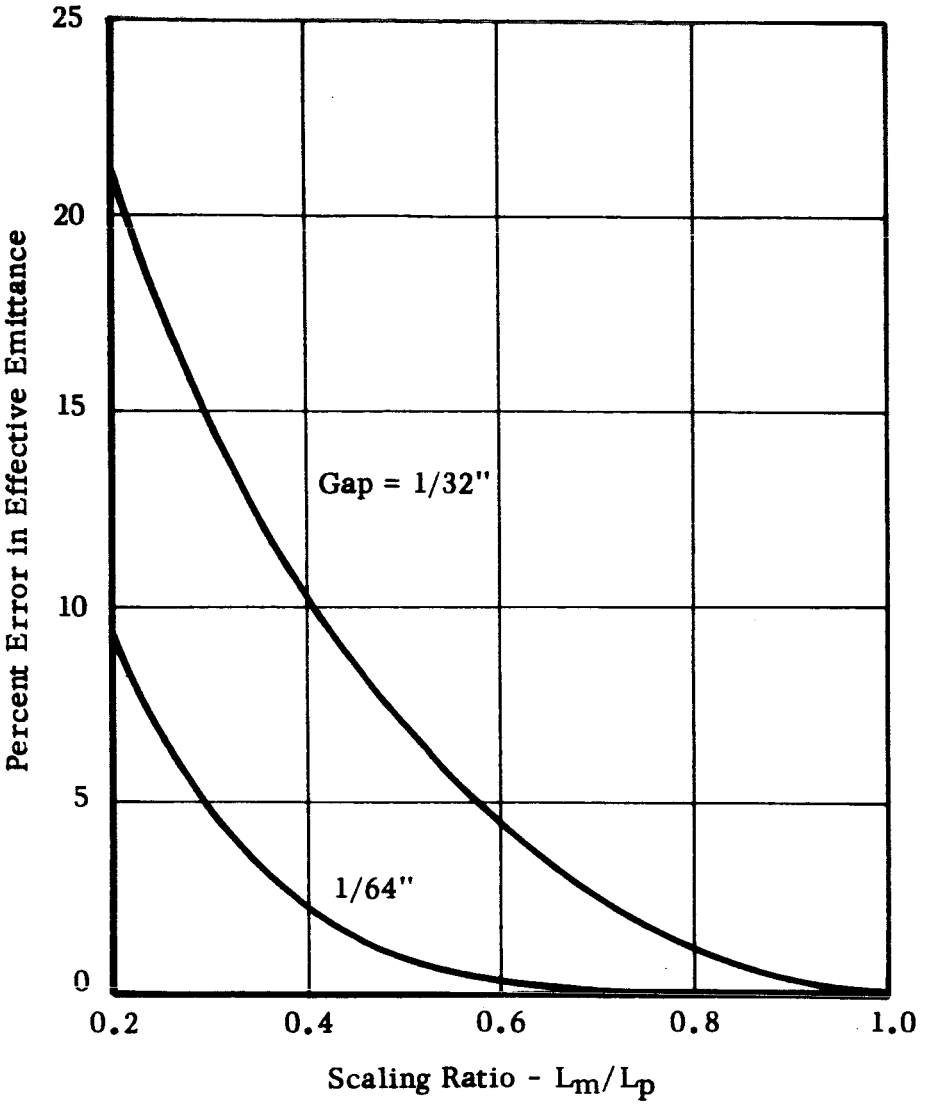

FIGURE 9 ERROR IN LOUVER EMITTANCE DUE TO NON-SCALED GAPS--BLADES CLOSED

equivalent to a 20% error in radiated power. In a spacecraft similar to Mariner IV, the error in internal temperature (at a condition where all louvers were closed) would be approximately 15C (27F).

If a scale-model louver assembly is designed in accordance with a modeling technique which requires that the emittances be made identical in model and prototype, but the temperatures be different, the difference in range of actuation temperatures will require that different bimetal springs be used in model and prototype. In the following table are listed the "fully closed" and "fully opened" temperatures for a 1/2 and 1/5 scale model of a Mariner IV louver assembly.

	Actuation Temperatures (F)		
	Closed	Open	ΔT
Full scale (Mariner IV)	55	80	25
1/2 scale $\frac{T_m}{T_p} = 1.26$	189	221	32
1/5 scale $\frac{T_m}{T_p} = 1.71$	420	463	43

From this tabulation it can be seen that the ΔT available to rotate the blades 90° from their closed to open position for a 1/5 scale model is nearly twice that of the prototype. This can be accomplished by use of active bimetal elements in the model which have 1) lower deflection constants, 2) shorter lengths of the active elements, or 3) an increased thickness. These design variables can be used by the manufacturer to obtain the desired rotation rate.

It should be noted that if the same basic model can be used for temperature and materials preservation techniques (by modifying the basic structure) the louver actuating element must be changed.

In conclusion, we have attempted to point out some practical limitations on the modeling of temperature control louvers. If the prototype louver assemblies are similar in size to Mariner IV assemblies, it is doubtful that a model smaller than 40% scale could be fabricated with active control elements. Modeling of louver assemblies using a technique where the model temperatures are greater than the prototype is possible by using special bimetal elements.

If it is necessary to model the thermal characteristics of a prototype spacecraft, with louvers similar in size to those used on Mariner IV, using a very small model, say 1/5 scale, it would be possible to replace the louvers with surfaces having certain effective emittances. For example, a test could be made with all louvers replaced with thermal shields having effective emittances equal to the effective emittance of a "closed" prototype assembly, and another test could be made with different thermal shields having emittances equal to the effective emittance of an "open" prototype assembly. This procedure could be used to obtain the temperature limits of the spacecraft, but the smoothing effect of having certain louvers open and others closed would be lost. Perhaps, in very preliminary development testing such information would be useful in determining the limits in average temperature of the internal structure.

Modeling of Multi-layer Insulations (MLI)

In typical spacecraft the use of multi-layer insulations (MLI)--commonly referred to as "super-insulation"--to reduce the heat transfer to or from certain areas is widespread. It is of interest, therefore, to consider methods for thermally modeling these insulation packages.

There are several applications which may require the use of MLI in spacecraft. A common application is to use MLI over a certain portion of the spacecraft to reduce the heat flow to a small value with respect to the heat flow from other areas. A typical application was the use of a MLI blanket on the shaded portion of the Mariner IV. In this case, it was desired to control the internal temperature by use of thermal control louvers and to minimize the heat flow from the shaded portion. As long as the effective emittance of the MLI blanket was small with respect to the effective emittance of the louvers, most of the internal power dissipation was emitted by the louvers. The absolute value of the shielding factor or effective emittance of the MLI was unimportant provided that the heat flow was small with respect to that dissipated by the louvers. Such applications are relatively simple to model. The Mariner IV MLI blanket was modeled in a 0.43 scale model with the same material, and, in fact, fewer layers without altering the heat balance on the interior of the model spacecraft.

However, other cases exist where the magnitude of the small heat flux through a MLI blanket is important in determining the internal temperatures of a component. As we will discuss in a following section, one concept for the thermal control of the Voyager capsule during the flight

from Earth to Mars is to completely insulate the capsule and to supply power within the capsule to maintain internal temperatures within tolerable limits. Here, the heat loss through the MLI must be minimized to reduce the heater power requirements. We will consider this as an important case in modeling of MLI blankets.

The one-dimensional, steady heat flow through a MLI system consists of two parallel paths, viz., radiation between the foils or layers which have a low emittance and conduction between the foils or layers. The conduction between layers is controlled by a contact resistance when no spacer or separator is used between the low emittance foils or by a combination of contact resistance and a resistance of the spacer when the foils are separated. The combination of a radiation and conduction path can be characterized by an equation of the form

$$n\,q'' = \frac{\sigma T_o^4 - \sigma T_n^4}{\frac{2}{\varepsilon} - 1} + C\,(T_o - T_n) \qquad (42)$$

where

- n - number of foils of MLI
- q'' - heat flux (watts/cm^2)
- T_o - temperature of the inner layer of insulation
- T_n - temperature of the n^{th} layer
- ε - emittance of the foil
- C - over-all thermal conductance between foils (watts/cm^2 K)

Equation (42) may be used to obtain two dimensionless groups which relate the similitude in model and prototype. They are

$$\left(\frac{CT}{nq''}\right)_m = \left(\frac{CT}{nq''}\right)_p \tag{43}$$

$$\left(\frac{\varepsilon T^4}{nq''}\right)_m = \left(\frac{\varepsilon T^4}{nq''}\right)_p \tag{44}$$

We will now consider two cases in which these similitude relations can be applied, one in which the temperatures are preserved in model and prototype, and the other in which the temperatures are not preserved in model and prototype (c.f. Table 2). The appropriate relations are presented in Table 3. Here we have assumed that distortions in the thickness of the MLI blanket would be permissible. Before drawing conclusions about the feasibility of either technique, we should point out that the behavior of the inter-layer conductance C in typical MLI is not well understood or easily evaluated. Typically, the conductance is strongly influenced by the compression of the MLI that occurs during installation and the characteristics of the spacer material. However, the emittance of the foils is relatively easy to evaluate by direct measurement. Therefore, in considering scaling of MLI, we believe that the only approach suitable is to attempt to retain the same inter-layer conductance in model and prototype by using essentially the same number of layers per unit thickness and keeping the characteristics of the spacer material, if used, identical in model and prototype.

Examination of the controlling equations using Technique 1, where temperatures are preserved, shows that the number of foils and the emittances must be made identical in model and prototype if the conductance

Table 3

Comparison of Controlling Equations for One-dimensional, Steady Heat Flow Modeling of MLI

Technique 1 Temperature & Emittances the Same in Model and Prototype.		Technique 2 Temperatures Different in Model & Prototype	
$\frac{q''_m}{q''_p} = 1$	(45a)	$\frac{q''_m}{q''_p} = \frac{T_m^4}{T_p^4}$	(45b)
$\frac{n_p}{n_m}\frac{C_m}{C_p} = 1$	(46a)	$\frac{n_p}{n_m}\frac{C_m}{C_p} = \frac{T_m^3}{T_p^3}$	(46b)
$\frac{\varepsilon_m}{\varepsilon_p}\frac{n_p}{n_m} = 1$	(47a)	$\frac{\varepsilon_m}{\varepsilon_p}\frac{n_p}{n_m} = 1$	(47b)

is made identical. Thus, the thickness of the MLI blanket would be approximately the same in model and prototype. This technique would, therefore, require that identical materials be used in model and prototype with a distorted thickness.

If we again choose to make the conductances between layers equal in model and prototype and make the temperatures different, Technique 2 requires that the number of layers and foil emittances be different in model and prototype. For a model operating at a higher temperature than a prototype, the number of layers used in the model would be less than the number in the prototype, and the emittances of each foil in the model would have to be decreased. In most cases, decreasing the emittance of the model foils would be a practical impossibility because the prototype insulation would most likely have the lowest attainable emittance. Only two alternatives exist. One is to scale only the radiative effects by using the same number of layers and foil emittances in model and prototype, the other is to scale the conductive effects by reducing the number of layers in accordance with Equation (46b). In either case, errors in the heat flux through the MLI on the model will exist. The errors in heat flux associated with modeling a typical MLI consisting of 34 layers, each with an emittance of 0.02, with the prototype source temperature set at 300K and the model temperature at 450K $\left(\frac{T_m}{T_p} = 1.5\right)$ are plotted in Figure 10. It can be seen that retaining the same number of layers in model and prototype reduces the errors in heat flux for insulations dominated by radiative effects, and that reducing the number of layers reduces the errors for conductively dominated insulations.

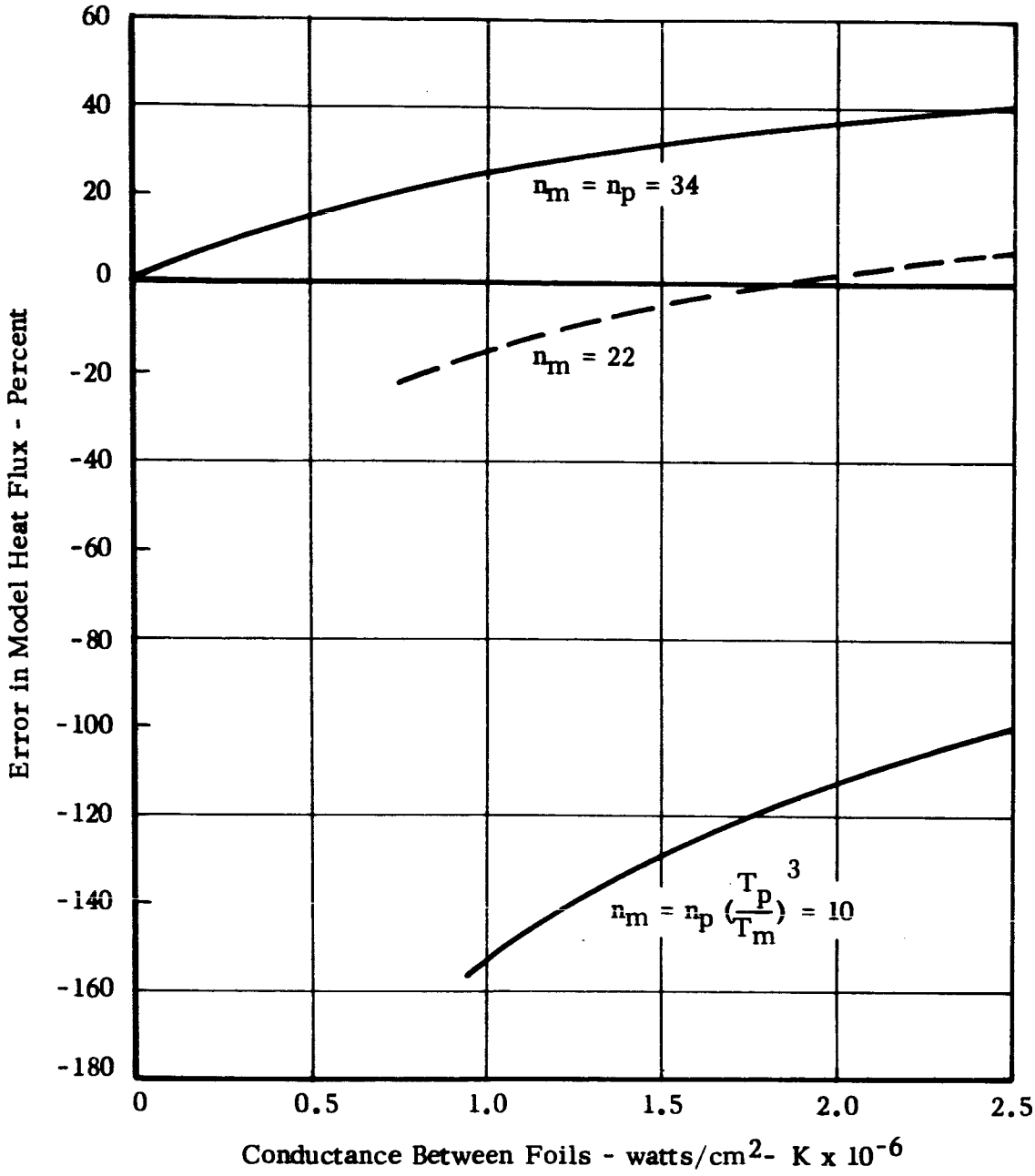

FIGURE 10 ERROR IN HEAT FLUX IN A MODEL MULTILAYER INSULATION BLANKET

From this discussion, it appears that thermal similitude can be retained in model and prototype if the model is designed in accordance with the temperature preservation technique. If model and prototype temperatures are different, it will be difficult to exactly scale a multi-layer insulation except in special cases where, 1) the temperature of the model is lower than the prototype, 2) the conductance between foils is known, or 3) the heat flow is principally through conductive elements. Figure 10 shows that the procedure of making the number of foils identical in model and prototype, ($n_m = n_p = 34$), i.e., scaling the radiative effects, leads to greater accuracy because typical MLI blankets are radiatively dominated. However, because one procedure produces positive errors and the other negative errors, it is possible to further reduce the errors by arbitrarily choosing the number of foils as the arithmetic average. The dashed line shows that 22 foils, for example, makes the error in modeling the heat flux zero at one particular conductance and reasonably small over the range of conductances expected in typical multi-layer insulations.

These conclusions are based on the assumption that the heat flow through the insulation blanket is one-dimensional, and such conditions do exist in practice for large surfaces covered with an unpenetrated blanket of MLI. However, in other areas the MLI blanket may be penetrated by supports, struts, wires, etc., and may have seams and gaps where edges of adjacent sections meet. In these cases, the heat flow is not one-dimensional and heat flows in directions both perpendicular and parallel to the foils of MLI.

If we assume that penetrations, where the heat flow is conductively controlled, are scaled by the techniques presented in Section II, some local heat flux errors will be introduced when the thickness of the MLI on the model is equal to the prototype thickness (Technique 1). If the number of foils are reduced, the local heat flux errors will tend to be smaller. The same conclusions may be applied to edges and seams in a MLI blanket.

Unfortunately, little information exists on the nature of the heat flow around seams and penetrations. The three-dimensional heat flow patterns in these regions are complicated by the anisotropic behavior of MLI and by the non-linearities due to radiation between and along the foils. In fact, it is practically impossible to make accurate estimates of the heat flow in such regions for penetrations of simple geometry. Until such information is developed, methods for scaling heat flows in penetrations will be subject to error.

If penetrations appear to be important in controlling the heat flow in a MLI blanket of a prototype, one method for determining a suitable procedure for scaling the heat fluxes in a model would be to make a thermal test of a single full-scale penetration, and then design and test various scale models until one arrived at a model design with the appropriate scaled heat flux. This is a rather unattractive procedure because of the iterative process involved, and the inherent difficulty in making measurements of small heat fluxes.

Bolted Joints

The theory of thermal scale modeling requires that the thermal conductances between surfaces in contact be scaled in accordance with Equations (12a, b). When the temperatures are preserved the thermal conductances, measured in watts/cm^{2}K (Btu/hr-ft^{2}R), must be equal in model and prototype. When temperatures are not preserved, the joint conductance in the model must be made greater than the corresponding joint conductance in the prototype. To avoid confusion, it may be well to restate the modeling requirements in terms of the rate of heat flow per unit temperature difference. For temperature preservation scaling:

$$\left(\frac{q_j}{\Delta T_j}\right)_m = \left(\frac{q_j}{\Delta T_j}\right)_p \left(\frac{L_m}{L_p}\right)^2 \qquad (48)$$

where q_j - heat flow through joint (watts)

ΔT_j - temperature difference across joint

L - characteristic length

Since the temperature differences in model and prototype must be equal, the heat flow through the model joint must equal the heat flow in the prototype multiplied by the square of the scaling ratio.

If temperatures are not preserved in model and prototype:

$$\left(\frac{q_j}{\Delta T_j}\right)_m = \left(\frac{q_j}{\Delta T_j}\right)_p \left(\frac{L_m}{L_p}\right)^2 \left(\frac{T_m}{T_p}\right)^3 \qquad (49)$$

From this equation, it can be seen that the heat flow in the model joint per unit temperature difference depends on both the geometric

scaling ratio and the temperature ratio.

In order to present methods for scaling the heat flows through bolted joints, it is necessary to discuss the thermal characteristics of bolted joints typically found in spacecraft. A schematic diagram of a bolted joint where it is desired to obtain a highly conductive path is shown in Figure 11. Heat flows from a source, e.g., an electronics packaging module, to a portion of the spacecraft where the heat is radiated and conducted away from the joint. In the relatively thin sections typical of spacecraft, the source and sink are in contact over a local area where the contact pressures are high. (The diameter at which the interfacial pressure falls to zero may be of the order of 1-1/2 to 3 bolt head diameters.) As shown, there is a drop in temperature due to the interfacial contact resistance in the contact area, and a drop in temperature due to constriction of the heat flow lines introduced by the thermal resistance of the sink. High bolt torques are used to decrease the interfacial contact resistance and increase the area of contact and thereby provide a good heat flow path. In many cases, typical of those found in the Mariner IV design, the over-all temperature drop in the joint is controlled by the constriction resistance rather than the interfacial contact resistance.

Another type of joint is shown in Figure 12. This joint is typical of those used where it desired to minimize the heat flow and provide thermal isolation. In this case, the over-all resistance of the joint is controlled by several interfacial contact resistances in series, and by the thermal resistance of insulating bushings. The constriction resistances of the source and sink are usually small because the rate of

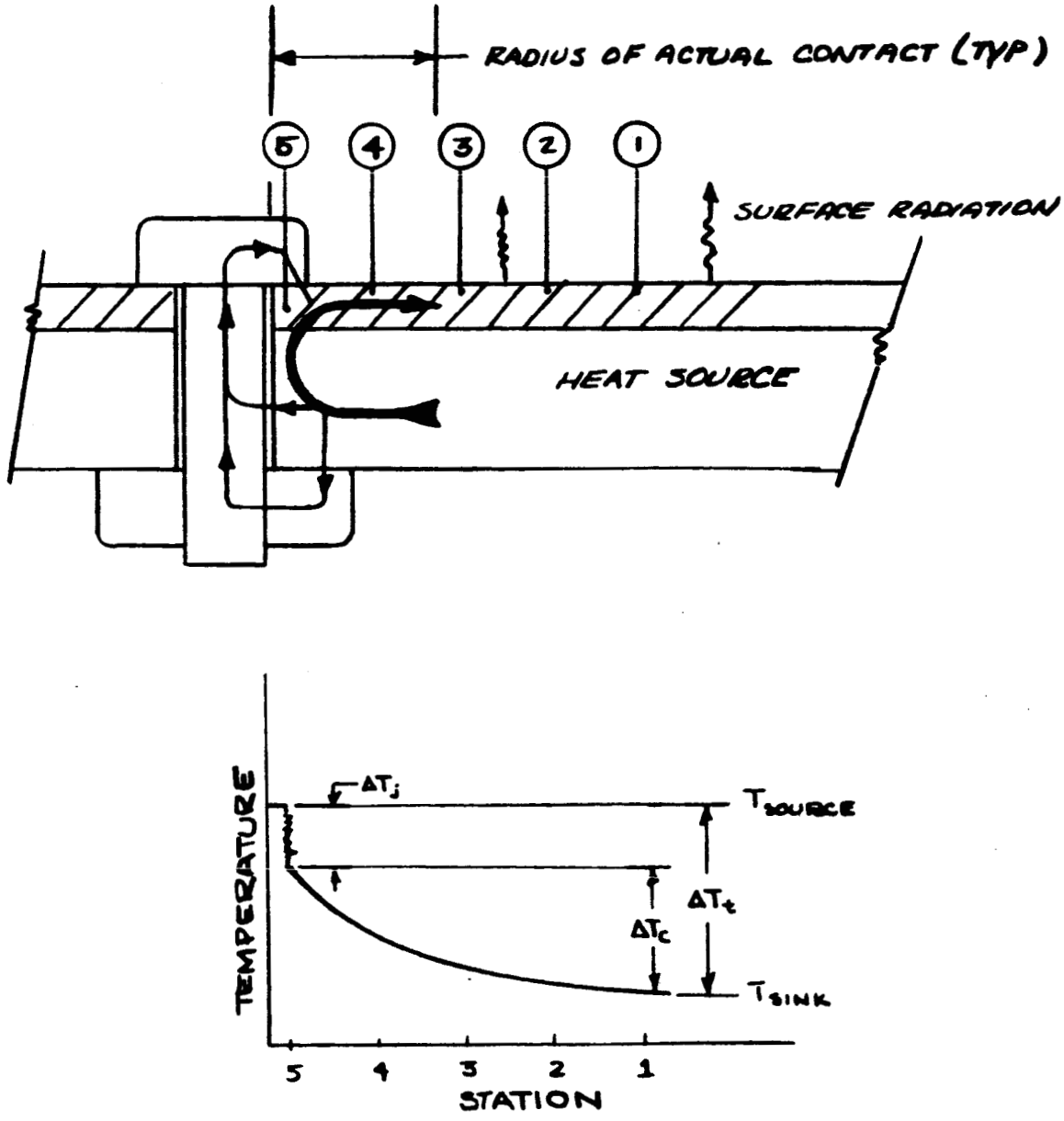

ΔT_j - contact resistance temp. drop
ΔT_c - constriction resistance temp. drop
ΔT_t - temp. difference across joint.

FIGURE 11 SCHEMATIC OF CONDUCTIVE BOLTED JOINT

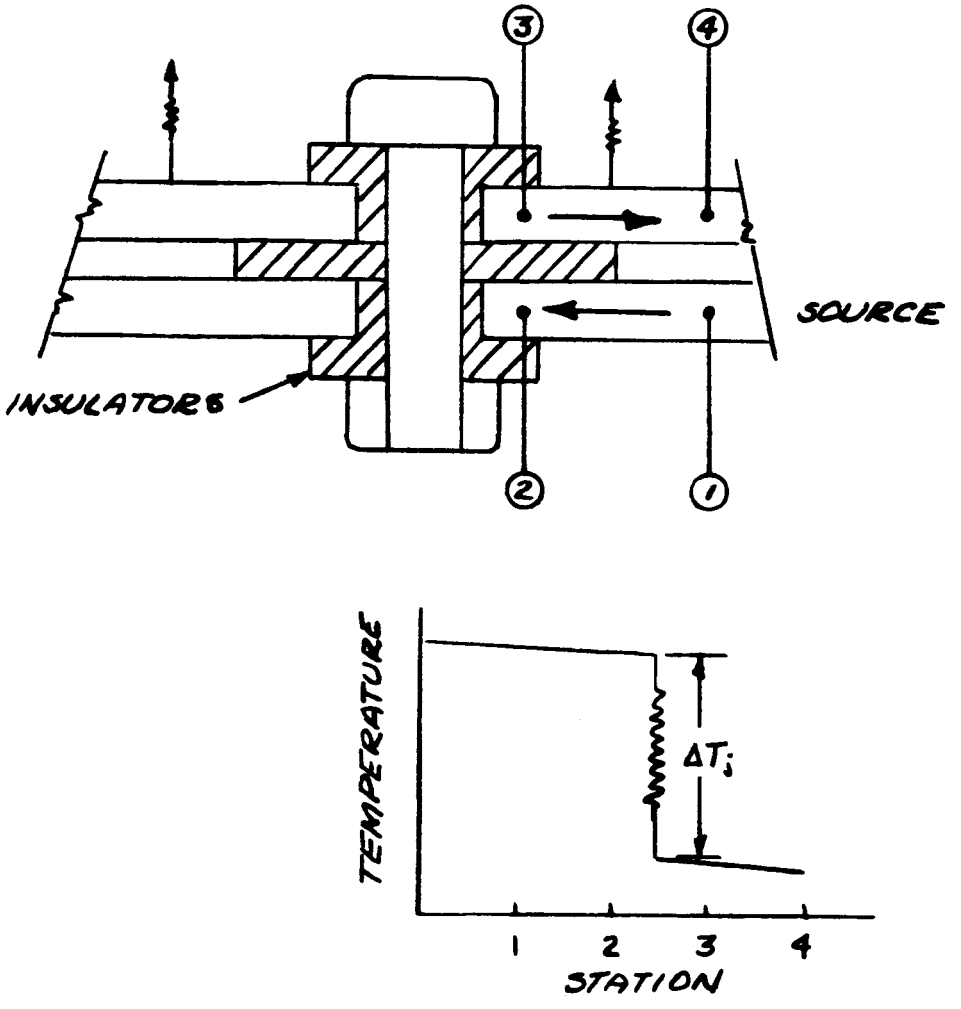

FIGURE 12 SCHEMATIC OF INSULATING BOLTED JOINT

heat flow is small.

Unfortunately, sufficient information is not now available for a thermal design engineer to design a typical bolted joint which will have a certain prescribed conductance. The problem is formidable because the heat flow patterns around the bolt are complicated, and in order to compute the heat flow across the contact area it is necessary to first solve for the stress distribution in the region of contact. The structural problem is complicated by the fact that, often, the high-strength bolts are stressed to the point where stresses and deformations of the mating surfaces cannot be described by elastic theory. However, the work which has been completed in the field of contact resistance can be used to identify the variables and their functional relationship. The following discussion of the modeling of bolted joints is based on using a simplified analytical approach to merely indicate the direction in which certain important variables should be changed in the model in order to preserve thermal similitude in model and prototype. In areas where the behavior of a joint is critical to the thermal balance of a prototype component, it will be necessary to determine the conductance of the prototype joint by test and then test a modeled joint to insure that thermal similitude is retained. This technique was used successfully in modeling the thermal behavior of a number of critical joints on the Mariner IV spacecraft.

First, we will discuss the important problem of modeling the interfacial contact resistance for the cases in which temperatures are preserved or distorted in model and prototype. For two plane surfaces in contact it is possible to approximately represent the heat flow by an

equation* of the form

$$\frac{q}{\Delta T} = C_1 \frac{kF}{Hb} \tag{50}$$

where

C_1 - proportionality constant

k - mean thermal conductivity of the mating surfaces

F - force over the contact area

H - as perity hardness of the softer of the two materials

b - surface roughness factor

If the temperatures are to be preserved

$$\left(\frac{kF}{Hb}\right)_m = \left(\frac{kF}{Hb}\right)_p \left(\frac{L_m}{L_p}\right)^2 \tag{51}$$

Also, for temperature preservation

$$\frac{k_m}{k_p} = \left(\frac{L_m}{L_p}\right) \qquad \text{c.f. Equation (11a)}$$

Now, if materials can be chosen for the model which have approximately the same surface finish and hardness as those in the prototype

$$\frac{F_m}{F_p} = \frac{L_m}{L_p} \tag{52}$$

---

* It is recognized that the equation presented here may not exactly account for the functional relationships between variables; however, some insight to the methods available for scaling can be obtained without introducing considerable complexity in the analysis.

Thus, we can approximately scale the interfacial resistance by scaling the bolt loads. The bolt loads can be varied by changing bolt diameter and torque, since

$$F = \frac{T}{D\phi} \tag{53}$$

where T - bolt torque

D - bolt diameter

ϕ - torque friction coefficient

It must be emphasized that it is important to maintain, as closely as possible, geometric similarity of the bolt and hole pattern in model and prototype to properly scale the constriction resistance. Thus, smaller bolts should be used on the model with the proper torque to scale the bolt loads. Choosing exactly scaled bolts would, in general, be impractical and the torque must be adjusted to produce the correct scaled load in the model.

If identical materials are used in model and prototype, and the temperatures are not preserved

$$\frac{F_m}{F_p} = \frac{L_m^2}{L_p^2} \quad \frac{T_m^3}{T_p^3} \tag{54}$$

The interfacial resistance may be properly scaled by adjusting the dimensions of the bolt and bolt torque.

The above procedures, while relatively simple in concept, lead to certain practical difficulties. For example, in "isolating" joints where the thermal resistance of the insulating bushings is important, materials with lower conductivities may not be available for the model,

or the size of the prototype bolt configuration may be sufficiently small to preclude the use of smaller bolts in a reduced scale model. Such practical difficulties can often be overcome, for example, by adding more interfacial contacts, reducing the bolt torques, increasing the constriction resistance by altering the geometry around the bolt, etc. Each situation of this type must be individually evaluated, and ancillary tests should be made on both a model and prototype configuration to verify the model design concept.

The temperature distribution resulting from a constriction resistance around a bolted joint, with a configuration as shown in Figure 11, can be approximated by considering the heat flow in an infinite plate with a circular source of heat of radius r_s. If the plate dimensions are large with respect to the source radius, and the plate radiates on both sides, the difference between the source temperature and the plate temperature at distances far removed from the source is given by the equation

$$\Delta T = \frac{\lambda q}{2\pi r_s k\delta} \frac{K_o\left(\frac{r_s}{\lambda}\right)}{K_1\left(\frac{r_s}{\lambda}\right)} \qquad (55)$$

where $$\lambda^2 = \frac{k\delta}{8\varepsilon\sigma\bar{T}^3}$$

and

q - heat flow

r_s - source radius

k - conductivity of the plate

δ - plate thickness

K_o, K_1 - modified Bessel functions

ε - emittance of the plate

The behavior of the constriction resistance as a function of the source radius and the conductance of the plate is shown in Figure 13 for several typical cases. The upper curve is for a 0.040 inch thick magnesium (AZ31) plate which corresponds to the conductance of a 0.020 inch thick aluminum (6061) plate. An emittance of unity was used in the calculations. The dimensions of the head diameters of several typical bolt sizes are noted on the abscissa for reference. From the curves it can be seen that the thermal constriction resistance can be large when the source radius is small. The importance of the constriction resistance for a typical bolted joint can be demonstrated by comparing the calculated constriction resistance to a measured over-all resistance for a bolted joint used in bolting an electronic subchassis in the Mariner IV spacecraft. The configuration was similar to that shown in Figure 11. Details of the test configuration and the calculated constriction resistance are presented below.

Plate material	AZ 31 B magnesium
Thickness	0.040 in.
Clearance hole diameter	0.166 in.
Bolt	#6-32 (0.138 in. dia.)
Bolt head diameter	0.270
Bolt material	Titanium
Torque	18 inch pounds
Stress in bolt	Approximately 100,000 psi
Heat flow	8.3 watts
Measured temperature difference	46K
Measured joint resistance	5.5 K/watt

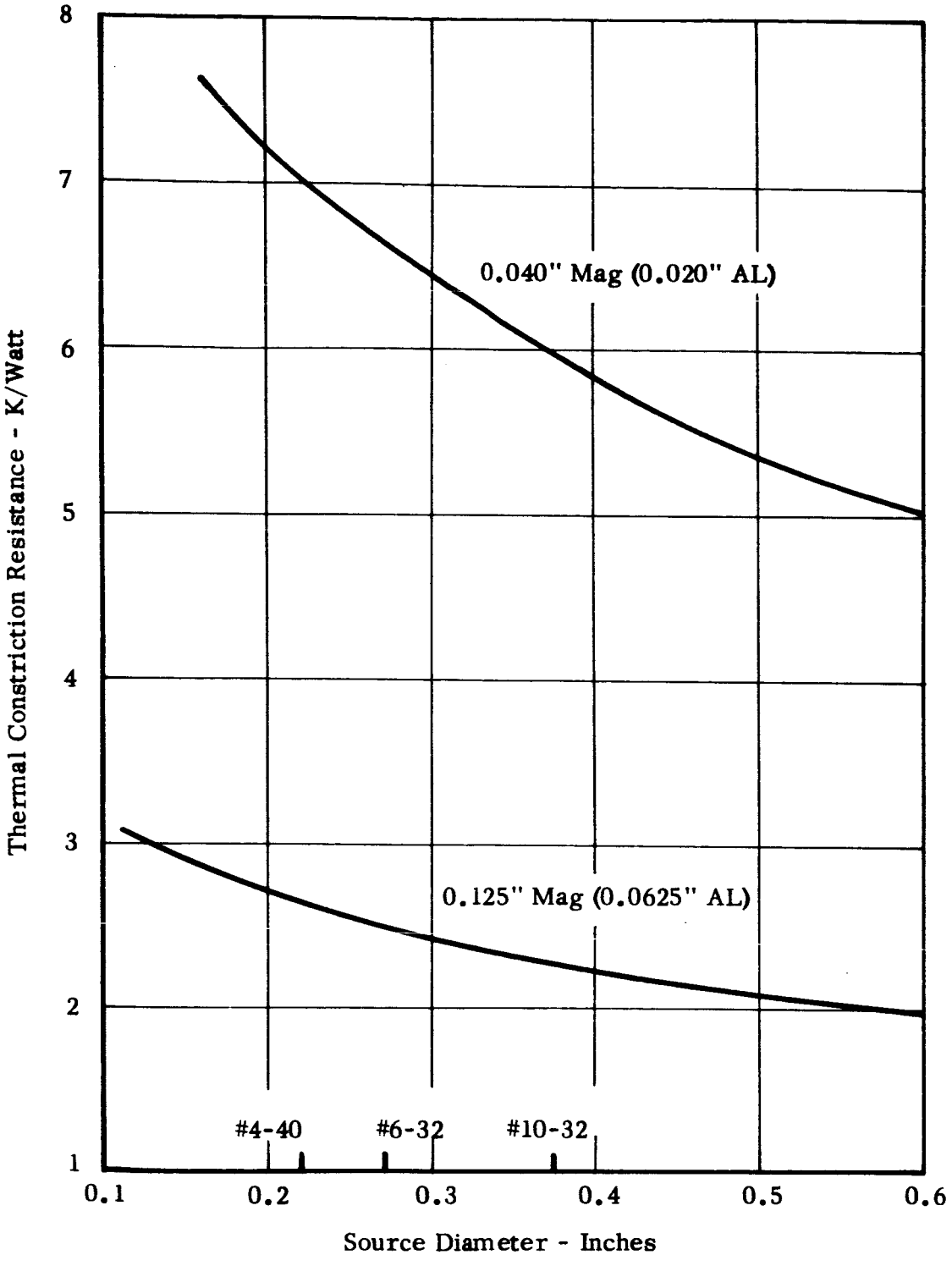

FIGURE 13 THERMAL CONSTRICTION RESISTANCE IN A RADIATING HEAT SINK

Calculated constriction resistance*	5.67 K/watt

This approximate calculation shows that the constriction resistance is of the same order as the total resistance of the joint.

The constriction resistance is a function of the thermal properties of the plate, the thickness of the plate and, importantly, the radius of contact. The thermal conductance of the plate can be modeled using the equations presented in Table 1 of Section II for cases where temperatures or materials are preserved. However, the source radius or radius at which the interfacial contact pressures approach zero is a function of the bolt load, geometry of the bolt, the clearance hole diameters in the mating plates and the modulus of elasticity and thickness of the contacting plates. For thermal similitude in model and prototype, the following equation applies

$$\left(\frac{r_s k\delta T}{qL}\right)_m = \left(\frac{r_s k\delta T}{qL}\right)_p \tag{56}$$

If temperatures are preserved in model and prototype and all dimensions are scaled, or if the materials are made identical in model and prototype but the temperatures differ

$$\frac{r_{sm}}{r_{sp}} = \frac{L_m}{L_p} \tag{57}$$

---

* The source radius was based on the approximation that the radius equals the bolt head radius plus 1.5 times the total thickness of the mating plates.

Thus, it may be seen that the source radius must be geometrically scaled in the model. We note that some difficulties exist if the thicknesses of the plates are not scaled in model and prototype because of the influence of plate thickness on the contact radius. Fortunately, the influence of an error in modeling the source radius in an example such as that shown in Figure 13 has less effect than an error in modeling the conductance of the plates (i.e., the product of conductivity and thickness). This is, of course, only true when the source radius is fairly large. For typical ranges of source diameters and plate conductances, as shown in Figure 13, a threefold change in plate conductance changes the constriction resistance by approximately 150%. We conclude that the modeling of bolted joints, whose thermal resistance is controlled by constriction to heat flow in the mating surfaces, is strongly influenced by the conductances in the plates. The area of contact should be scaled in model and prototype by use of smaller bolts in a reduced-scale model. If the thermal behavior of the joint is critical, tests of a prototype and model joint should be made to select a modeled joint which will satisfy the similitude relations.

Following the previous discussion of methods for scaling the behavior of bolted joints, it is appropriate to briefly review the results of the first known attempt to model bolted joints in a spacecraft. The temperature preservation technique was used to model, at 0.43 scale, a number of bolted joints in the Mariner spacecraft.* Within the space-

* "Thermal Scale Modeling of the Mariner IV Spacecraft," Final Report to JPL, Contract 950789, by A.D. Little, Inc., 20 August 1965.

craft, a number of high power dissipation electronic sub-chassis were bolted to a relatively thin magnesium shear web which radiated the dissipated power to outer space through a set of louvers. The procedure for modeling the bolted joints consisting of thermally scaling the shear webs by using a lower conductivity material in the model and a geometrically scaled thickness. Smaller bolts were used in the model and the bolt loads were scaled by adjusting the torques on the model bolt assembly. The thermal behavior of a typical prototype joint and a 0.43-scale joint was investigated in a separate experiment to verify the model design approach. It was found that the bolt torque, clearance hole diameter and the conductivity of the shear web significantly influenced the overall joint conductance. The conductivity of the bolt was found to be unimportant. The temperature differences measured in tests of the complete spacecraft and model are presented below:

	Prototype	Model
Temperature difference (F)	28.5	25.9
Power dissipation (watts)	20.1	3.7
Resistance of joint (F/watt)	1.42	6.9
Bolt size	#6-32 Ti	#4-40 S.S.
Torque	18 in.lb	5.5 in.lb
Clearance hole dia. (in)	0.169 $^{+005}_{-001}$	.136 $^{+005}_{-001}$
Shear web material	ZK 60 A Mag.	1015 Steel
Shear web thickness (in)		
max.	0.100	0.047
min.	0.040	0.017

The above data shows that the error measured temperature differences between model and prototype were extremely small, and we conclude that

for this type of joint, modeling techniques can be successfully applied in practice.

Unfortunately, no direct comparison of data for "thermally isolating" bolts can be obtained from the results of the previously mentioned program. Several joints of this type were modeled, but the conductances of the joints were relatively unimportant to the temperatures of the components.

Isolated Appendages

In certain cases, a spacecraft may contain one or more appendages such as scientific instruments, optical sensors, antennae, etc., which are, to a degree, thermally isolated from the main structure. The thermal control of such appendages is often a problem in prototype spacecraft because the design may, for example, be dictated by electrical isolation requirements, or the requirement for the instrument to be mounted remotely to eliminate stray magnetic fields, etc. The amount of internal power dissipation available for temperature control is usually small or it may be variable if the instrument is turned on and off, which makes the situation worse. Because these problems are typical in un-manned scientific spacecraft, it is beneficial to review such problems to determine their implication in thermal scale modeling.

First, consider an appendage which is conductively coupled to a spacecraft via support mounts, electrical lead wires, etc., and is shielded from other radiative sources. (An example of this general type is the Canopus star tracker on Mariner IV.) The instrument dissipates power internally and it is assumed that the thermal behavior can be

represented by a single average temperature T. The spacecraft is assumed to be a heat sink at a temperature T_s = 300K. The temperature of the appendage, neglecting transient effects, is given by the equation

$$\varepsilon A \sigma T^4 = P + C\ (T_s - T) \tag{58}$$

where

εA - effective radiating area of the appendage to outer space (cm^2)

C - total conductance between the appendage and spacecraft (watts/K)

P - internal power dissipation

To illustrate the thermal behavior of an appendage of this type, the temperature level is plotted in Figure 14 as a function of the conductance per unit of effective radiating area for two levels of internal power. The curves illustrate the sensitivity in temperature change due to changes in the conductance per unit of radiating area. If the appendage is de-coupled by having small conductances or large radiating areas with no internal power, a small error in the conductance can significantly change the temperature. If internal power is dissipated, the change in temperature due to an error in conductance is less. If the conductance is made large or the emittance very small, the change in temperature due to an error in conductance or emittance becomes smaller. Thus, the temperatures of thermally de-coupled appendages with small internal power dissipations are extremely sensitive to errors in the conductance or effective radiating area. When the conductance is zero, i.e., completely de-coupled, the error in temperature is

$$\frac{\Delta T}{T} = \frac{1}{4}\,\frac{\Delta p}{p} = -\frac{1}{4}\,\frac{\Delta \varepsilon A}{\varepsilon A} \tag{59}$$

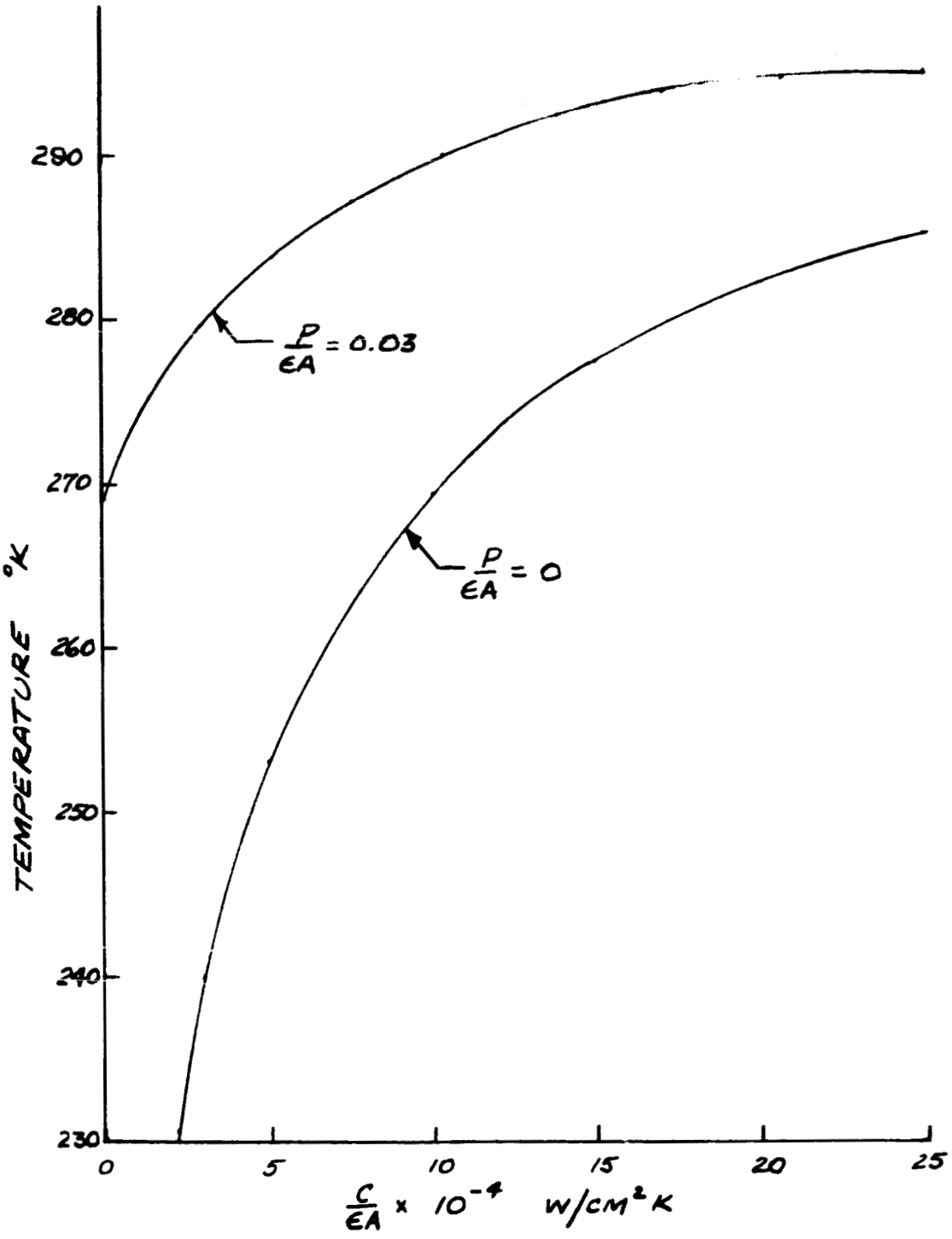

FIGURE 14 THERMAL BEHAVIOR OF AN ISOLATED APPENDAGE

These situations will, in general, be more difficult to model successfully than cases where the conductance is relatively high. In small model appendages, parasitic heat leaks from instrumentation wires become problems. The scaling of low conductance bolted joints becomes difficult because of the availability of low conductivity isolating materials. In addition, the emittances in model and prototype must be carefully reproduced. On the other hand, when the conductances are reasonably large or the effective radiating is very small, quite large errors can be tolerated in modeling either the conductance or area without significantly affecting the temperature. Each situation will have to be separately evaluated to determine which variables must be most closely controlled to insure similarity in model and prototype.

We will next consider a sunlit appendage, isolated conductively from the spacecraft, whose temperature is fixed by internal power dissipation and absorbed sunlight. The appendage is assumed to be illuminated by sunlight over a portion of its area A_1, which is covered with a multilayer insulation. The remaining area A_2 is assumed to be unshielded. (Typical examples of this type are the magnetometer and ion chamber experiments on Mariner IV.) Neglecting transient effects, a heat balance on the appendage yields the equation

$$\left[\left(\frac{A_1}{\mu}\right) + \epsilon_2 A_2\right] \sigma T^4 = \frac{\alpha S}{\epsilon \mu} + P \qquad (60)$$

where

ϵ_2 - emittance of the unshielded area A_2

α/ϵ - solar absorptance to emittance ratio of the outermost layer of insulation facing the Sun

P - internal power (watts)

S - sunlight incident on the outermost insulation layer (watts)

μ - shielding factor of the insulation

The temperatures are plotted in Figure 15 for a solar intensity corresponding to one solar constant with a solar absorptance to emittance ratio of unity as a function of the ratio of the effective areas of the shielded and unshielded portions of the appendage. When the shielding factor of the insulation (proportional to the number of layers) is large, the instrument is de-coupled from sunlight and the instrument temperature is sensitive to small uncertainties in the shielding factor or effective emittance of the unshielded portion. The effects are amplified when the internal power dissipation is extremely small. Similarly, when the shielding factor is large the difference in temperatures when the internal power is turned off becomes extremely sensitive to uncertainties in the effective emittance of the unshielded portion.

In modeling sunlit appendages with small internal power dissipation, the emittances of unshielded portions must be carefully controlled in the model if the appendage is poorly coupled to the Sun by use of insulation. This situation is typical of many interplanetary spacecraft appendages where it is desired to minimize the temperature excursion of the instrument due to the change in solar intensity encountered in the "cruise" portions of the flight.

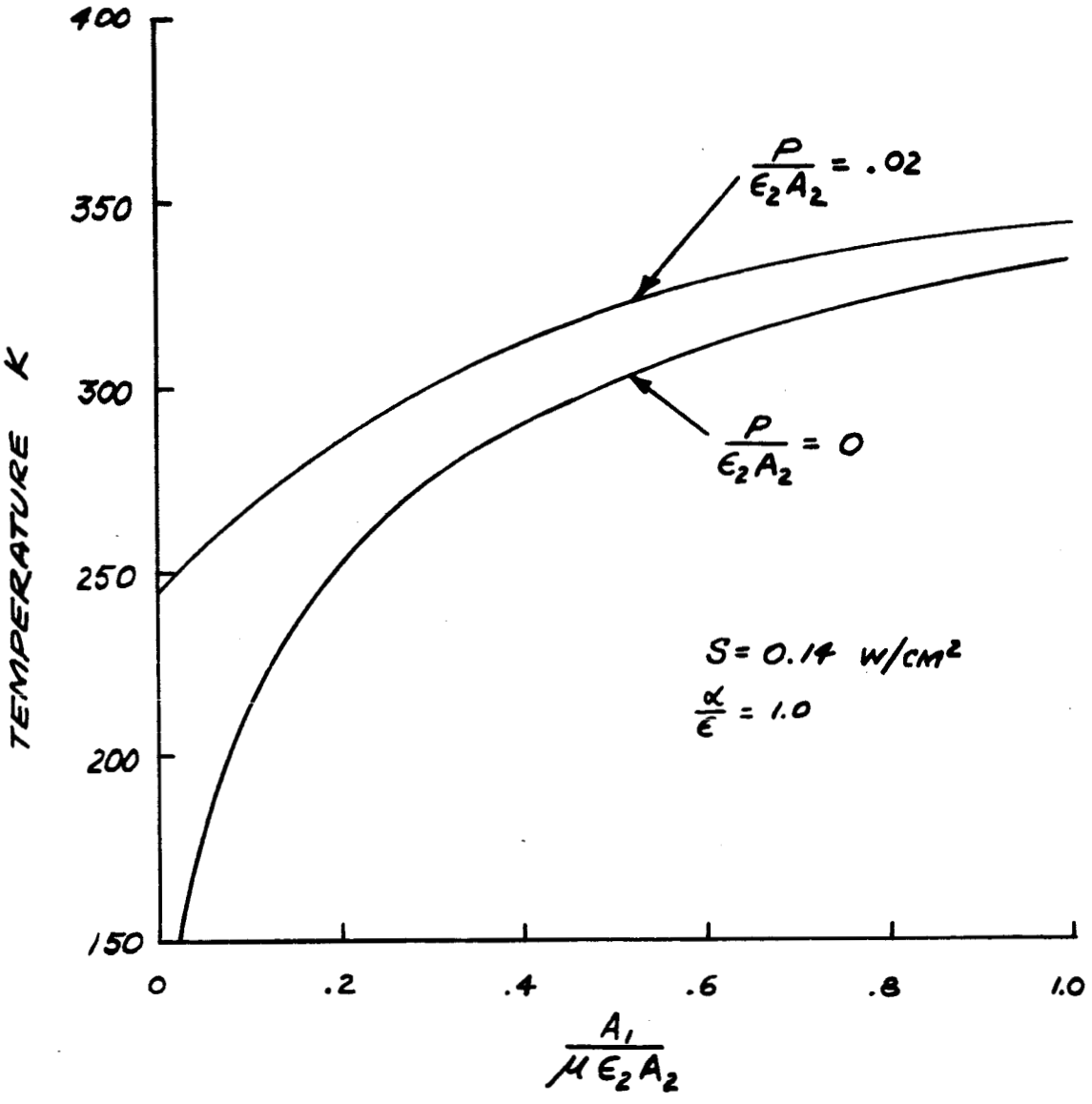

FIGURE 15 THERMAL BEHAVIOR OF A SUNLIT APPENDAGE

IV. Thermal Modeling of a Voyager-type Spacecraft

Description of Typical Prototype Configuration

An over-all view of a typical conceptual design for the Voyager spacecraft is shown in Figure 16. The spacecraft contains two main sections--the spacecraft "bus," which consists of all items below the flight capsule interface, and a separable sterilized capsule to be landed on the Martian surface. The proposed mission plans include an Earth parking orbit for approximately 1.5 hours, an injection and acquisition phase for approximately six hours. The entire spacecraft will then be Sun-oriented with the spacecraft-Sun vector colinear with the roll axis. The interplanetary cruise during transfer from Earth orbit to Mars will require approximately 230 days. The spacecraft will be Sun-oriented during this period except for perhaps brief periods of mid-course maneuvering. Approaching Mars, the retro-propulsion system will be fired to place the entire system in an orbit around Mars. During one of the orbits, the sterilization canister will be separated from the capsule, and the capsule will then be separated from the Voyager spacecraft. The capsule will be de-orbited, enter the Martian atmosphere, and land on the Martian surface by use of a separate propulsion system and a parachute system. An entry heat shield will be provided to protect the capsule payload of scientific instruments and the telemetry equipment used to transmit data to the orbiting Voyager spacecraft bus which will act as a relay link to Earth.

The over-all size of the Voyager spacecraft bus is approximately 3-4 times the size of the Mariner IV. The over-all mass will be approximately 15,000 lbs. of which 12,700 lbs. will be propulsion system mass.

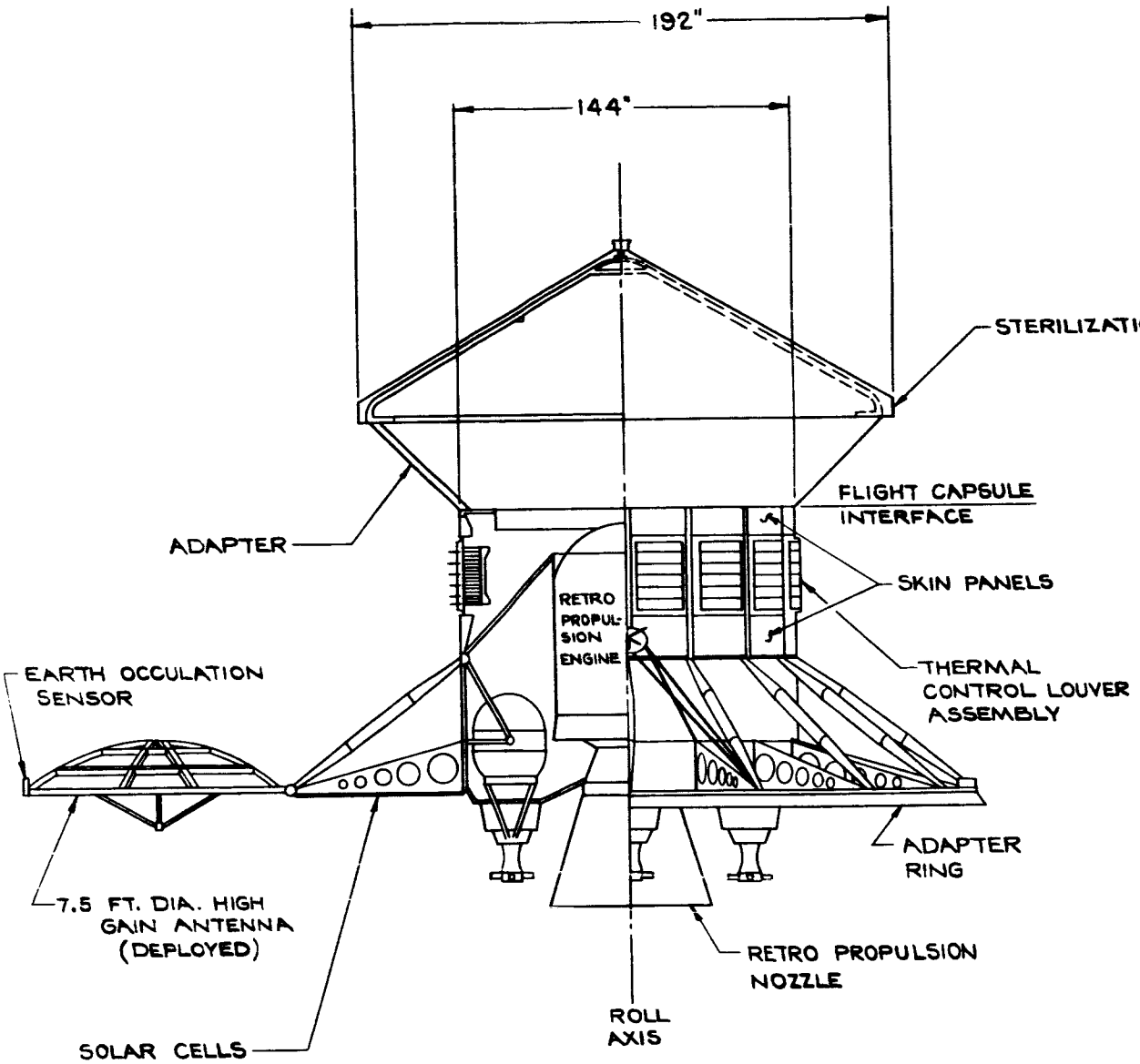

FIGURE 16 OVERALL SPA

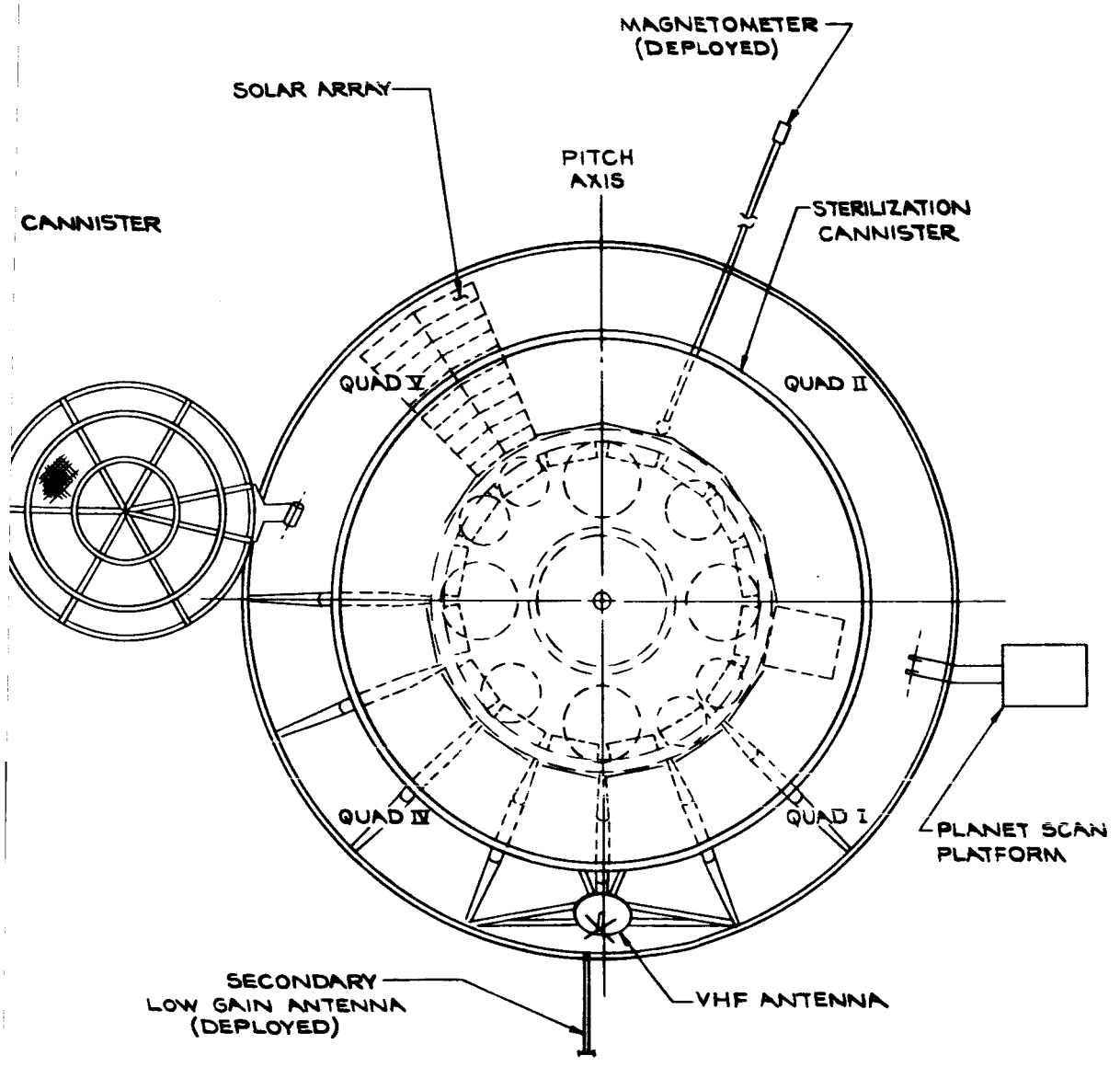

CECRAFT LAYOUT

The diameter of the bus is approximately 12 feet compared to 4-1/2 feet for Mariner IV. The bus consists of 16 bays (compared to 8 on Mariner IV) containing the electronics for science instruments, power conditioning, data storage, telemetry, guidance and control, etc. The bus also houses the large modified Minuteman solid propellant retro-propulsion engine, four thrust vector control bi-propellant engines, and associated propellant and pressurant tankage. The solar panel array has a diameter of approximately 20 feet and is fixed to the spacecraft bus. The internal power dissipated within the bus is expected to be of the order of 500 watts during cruise modes, compared to 150 watts for Mariner IV. As shown in Figure 16, variable emittance temperature control louver assemblies will be attached to some of the electronic bays. Also shown are a magnetometer and a planet scan platform in the deployed position.

It is expected that the thermal control philosophy used in designing Mariner IV will perhaps be employed in the design of the Voyager spacecraft bus. The electronic bays will be thermally isolated as much as possible from the solar arrays and rocket engines which are directly heated by incident sunlight to minimize the temperature excursions caused by the change in solar intensity from Earth to Mars orbit. The bottom of the spacecraft at the capsule interface will also be insulated to minimize heat losses to outer space after capsule separation. Thus, the internal power dissipated radially through the louvers and other shielded or unshielded bays will be used to set temperature levels within the bus. The louvers will be used to minimize internal temperature excursions caused by changing power dissipation or variable heat loads from the environment. Approximately 50 lbs. of insulation mass

have been allocated for thermal control.

A section view of the capsule is shown in Figure 17. The total mass is expected to be approximately 3000 pounds. It will be approximately 15 feet in diameter, and 5-1/2 feet high. The section view shows the separable sterilization canister, the attitude control gas storage vessels and the payload equipped with parachute canisters. The payload, including scientific instruments, TV cameras, penetrometer, and associated electronic equipment is shown mounted centrally with separate temperature control louvers. The heat shield for the payload would be located beneath the sterilization canister. Not shown in Figure 17 are two 45 inch diameter altimeter antennae which are located in the capsule separation plane. In the descent configuration the payload would not include the sterilization canister, adapter ring, heat shield and deflection engine.

It is presumed that during interplanetary cruise, the entire capsule will be highly insulated to minimize the internal power dissipation required to maintain adequate storage temperatures for the electronics and other instruments. Approximately 150 watts of internal power will be available for maintaining internal temperatures during this period. The weight of insulation is expected to be of the order of 80 pounds. The entry heat shield may be of the order of 1/4" in thickness with a conductivity of $10^{-5} \frac{\text{Btu-ft}}{\text{ft}^2\text{secR}}$.

The over-all desired temperature limits of internal electronic equipment, etc., are expected to lie between 0 and +40C.

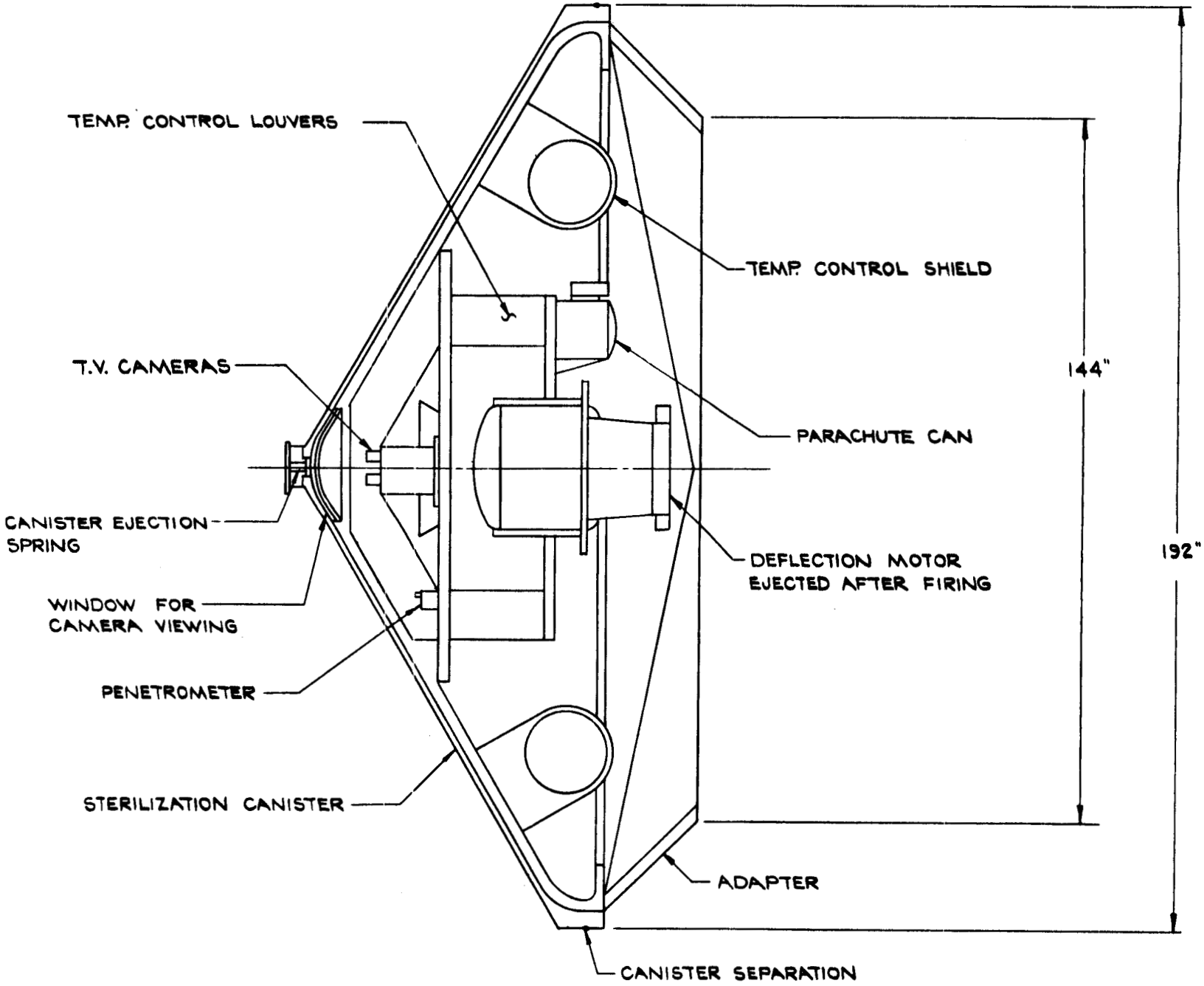

FIGURE 17 VOYAGER FLIGHT CAPSULE

The Modeling Problem--General Considerations

One purpose of this report is to present approaches to designing thermal scale models of the Voyager spacecraft at 1/2 and approximately 1/5 scale. Model design approaches will be presented for the "temperature preservation" technique, and the technique in which the model and prototype temperatures differ by a fixed but predictable ratio. The concept of preserving materials in model and prototype will be regarded as one of the latter approaches.

In discussing the various approaches to the modeling problem, the following spacecraft-capsule configurations will be considered:

1. The spacecraft with entry capsule attached--including the sterilization canister.
2. The entry capsule after separation from the spacecraft with sterilization canister attached.
3. The entry capsule without sterilization canister.

Previous discussions were devoted to the general advantages of using modeling techniques in spacecraft development. In order to fix ideas regarding the thermal modeling of a Voyager-type spacecraft at one-half and one-fifth scale, a number of pertinent dimensions, masses, and testing requirements are presented in Table 4. The estimates of the masses of prototype and model test configurations will only be approximate since the models and some test versions of the prototype may not contain all of the electronics and, therefore, will be lighter than the flight model. It is significant to note the differences in mass and the solar simulator testing time requirements of models and prototype since the differences

Table 4

Comparison of Voyager and Scale-Model Size, Weight, and Test Requirements

	Prototype	1/2-Scale Model	1/5 Scale Model
Over-all Dimensions (ft)			
Diameter (deployed configuration)	32	16	6.5
Diameter (solar panels)	20	10	4
Height (capsule attached)	20	10	4
Spacecraft bus mass (lbs)	2,300	290	18
Propulsion system mass	12,700	1600	100
Capsule mass	3,000	375	24
Thermal time constant of capsule[1] (typ.)	7.2 days	1.8 days	7 hours
Test time in simulation chamber required to test spacecraft bus[2] (typ.)	80 hours	20 hours	3 hours
Diameter of solar beam required			
Maximum (deployed)	32	16	6.5
Minimum[3]	10	5	2

1. Based on insulation requirements to maintain 0C internal temperature with 150 watts of power. Time constants of models based on "temperature preservation" techniques with distorted geometry in minor dimensions.

2. Extrapolated from test time of 20 hours for Mariner IV (MC-3) at a mass of 575 pounds. The time is computed from initiation of chamber shroud cooldown to thermal equilibrium at one solar constant.

3. Minimum solar beam diameter based on illuminating spacecraft bus with heater simulation of solar panel array.

are related to the ease of handling and the test costs. Of particular importance is the thermal time constant of the capsule. Since the capsule is expected to be highly insulated, the time constant of the prototype will be about seven days--it may take several time constants for the internal temperatures of the capsule to equilibrate. The savings in testing time using models are considerable. The dimensions of the solar beam required for testing are also important. It is noted that, at present, few, if any, operational simulation facilities have the capabilities for illuminating an entire Voyager-type spacecraft in a deployed configuration. To pictorially illustrate the relative difference in sizes of a prototype and half-scale model, photographs of a Mariner TCM and 0.43 scale model are shown in Figures 18 and 19.

Thermal Modeling of Spacecraft Bus

Structural Frame and Shear Webs

To present approaches for scaling the "bus" section, we will assume that the basic construction will be similar to that used in the Mariner IV design. Further, we will assume that the Voyager prototype will be approximately 2.5 times the diameter of the Mariner IV and the thickness of structural members will be increased by a factor of approximately 3.* The basic construction is assumed to consist of an upper and lower frame with longerons at each of the 16 bay corners, with shear webs (skin panels) bolted to the frame and longerons. A photograph of a typical

* The scaling of structural members depends on the type of loading, whether the structural problems are static or dynamic, etc. However, the thickness of plates and shells will scale-up by a factor considerably less than the square of the ratio of major dimensions.

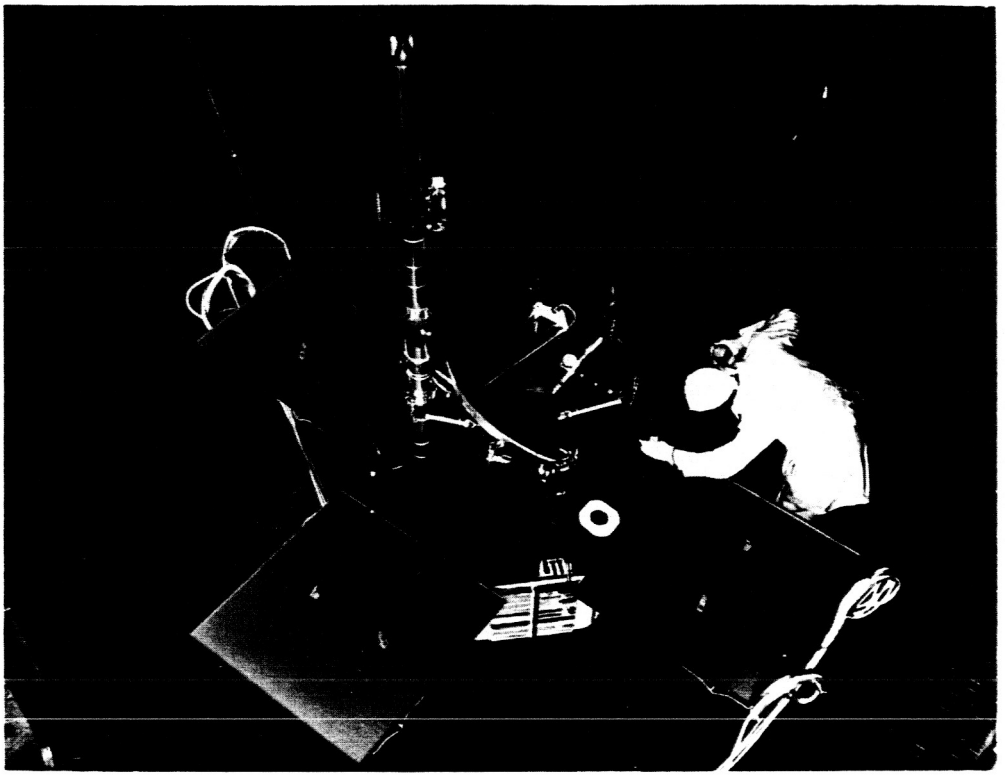

FIGURE 18 MARINER MARS 64 TEMPERATURE CONTROL MODEL

FIGURE 19 THERMAL SCALE MODEL - TOP VIEW

arrangement of longerons, shear webs and upper and lower frames is shown in Figure 20. This photograph is of a 0.43 scale model of the Mariner IV, however, it shows a typical design configuration. The shear webs, or skin panels are used to support electronic modules, and the thermal control louvers are bolted to the exterior surfaces. Views of the interior of the Mariner IV TCM illustrating the general packaging arrangement and structure are shown in Figures 21 and 22.

One concern in modeling the frames, longerons and shear webs is the determination of whether or not temperature gradients from bay-to-bay, which are introduced by non-uniform power dissipations, are controlled by conductive or radiative effects. Typically, the internal power generated varies from bay to bay. In Mariner IV, three of the bays dissipated 39%, 20% and 14% of the total power. The non-uniform power dissipations thus give rise to azimuthal temperature gradients, although the gradients may be smoothed somewhat by the action of variable-emittance temperature control louvers. Similarly, axial temperature gradients are introduced by the non-uniform power dissipation within a given bay. A second consideration in the scaling of the shear webs or skin panels to which electronic modules are bolted is the simulation of the thermal constriction resistance (c.f. Section III) around those bolted joints which transmit heat from modules with high internal power. If radiative effects control the azimuthal or axial temperature gradients, deviations from exact modeling of conductive paths may be made without introducing errors provided that the radiative properties (emittance and view factors) are properly scaled.

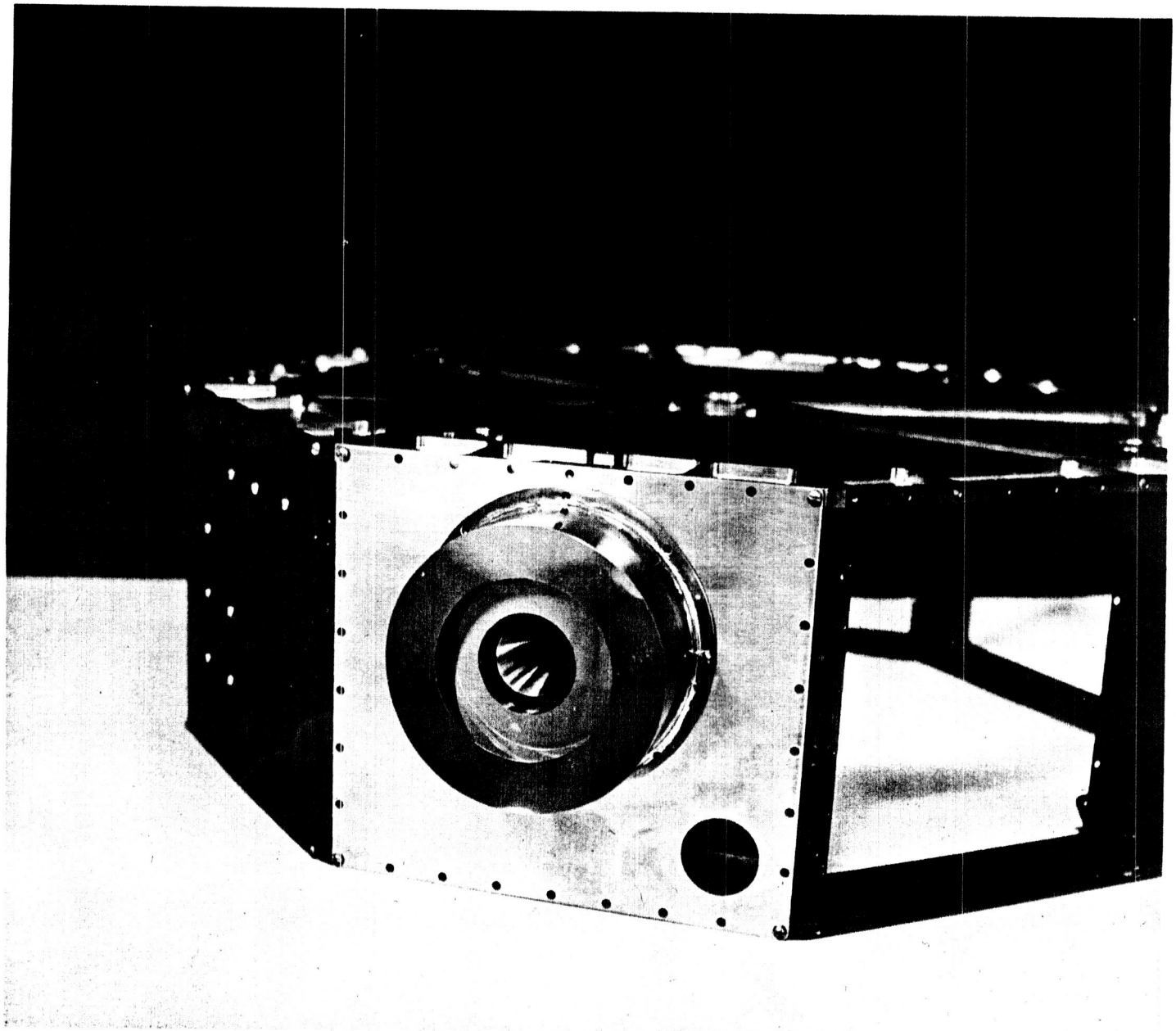

FIGURE 20 TYPICAL SPACECRAFT STRUCTURE

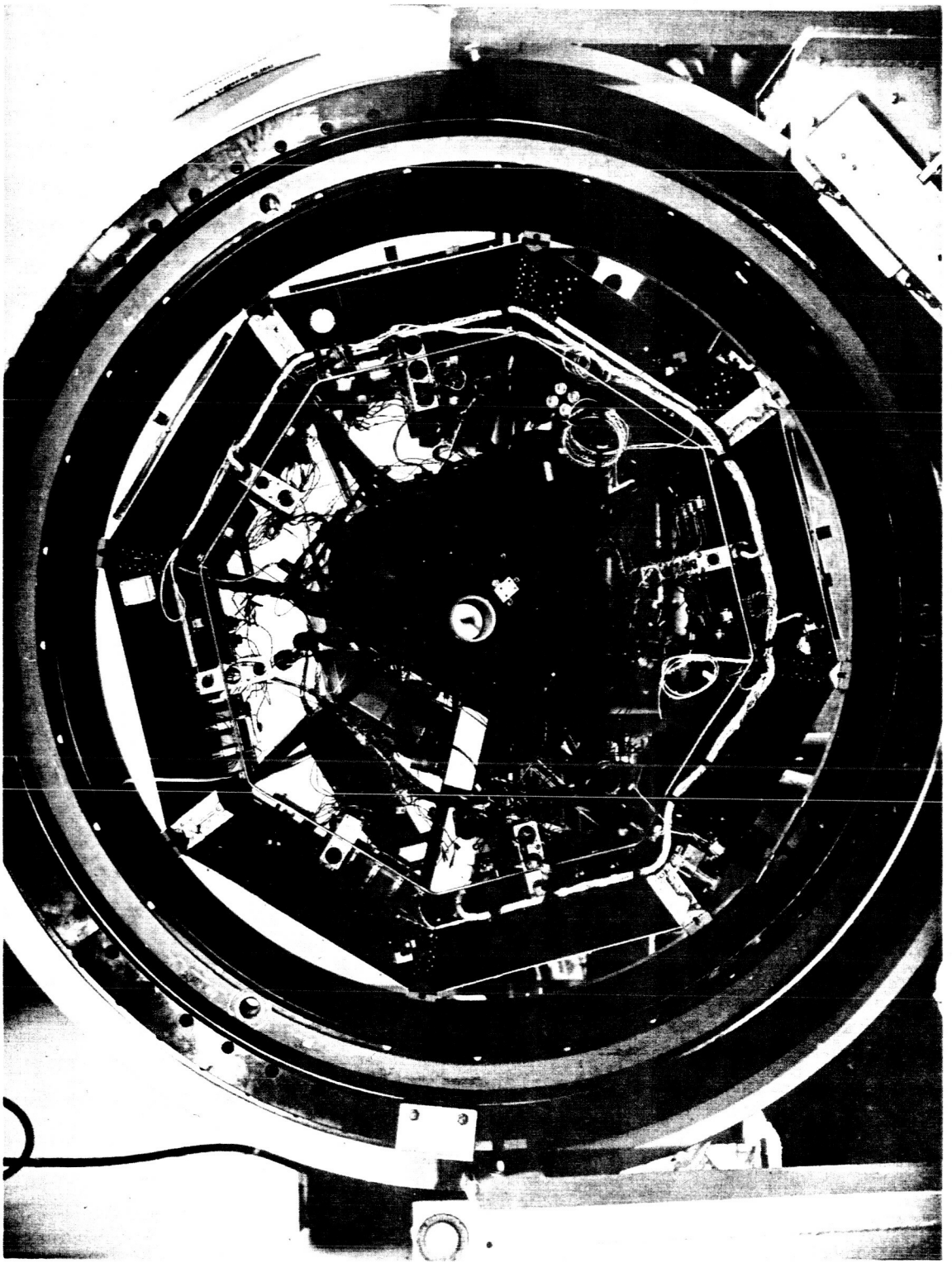

FIGURE 21 BOTTOM VIEW - TCM BUS

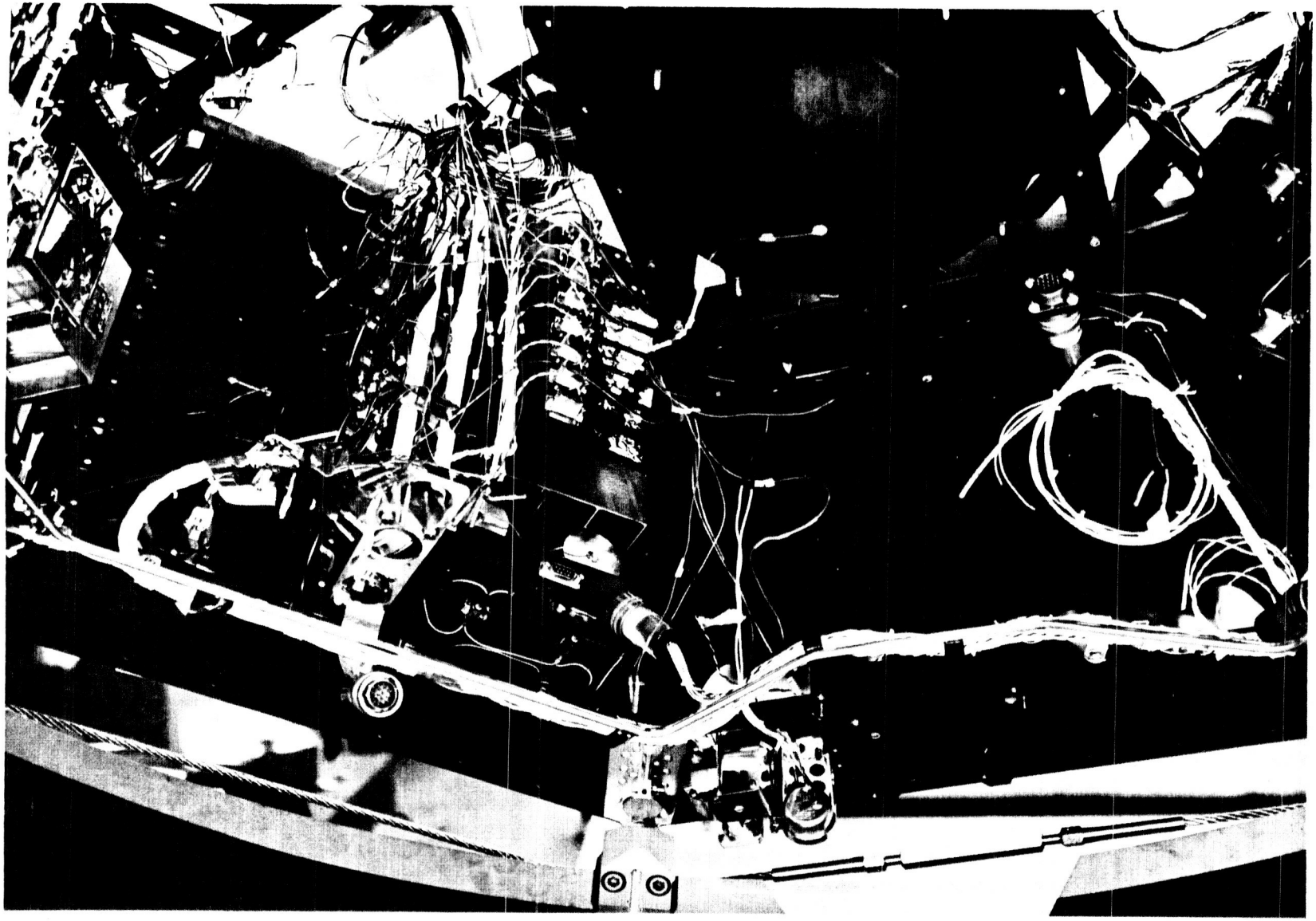

FIGURE 22 INTERIOR VIEW - TCM

To obtain an estimate of the relative effects of radiation and conduction in determining temperature gradients within the bus, we will consider a simplified model of the structure. We assume that the structure can be represented by a cylindrical shell of radius r, equivalent thickness t and length b, and that the average temperature of the interior can be represented by a single temperature $\bar{T}$. The interior surface of the shell is assumed to have an emittance of unity and the exterior to have an emittance ε_o. If the azimuthal distribution of power (per unit length) is of the form

$$P(x) = P_o + p_1 \cos \frac{x}{r} \tag{61}$$

where
- P_o - average internal power per unit length
- P_1 - amplitude of power variations
- x - distance along the circumference
- r - radius

the magnitude of the azimuthal temperature difference is given by the formula

$$|\Delta T| = \frac{P_1}{\frac{kt}{r^2} + 4(\varepsilon_o + 1)\sigma\bar{T}^3} \tag{62}$$

The first term in the denominator represents the smoothing effect due to conduction around the cylinder, the second term represents the radiative smoothing.

A similar formula for the magnitude of the axial temperature difference can be obtained for the case in which the axial distribution of power is of the form

$$P(x') = P_o' + P_1' \cos \frac{\pi x'}{b} \tag{63}$$

where x' - axial distance

b - height of cylinder

$P(x')$ - axial distribution of power

If the top and bottom are well-insulated, the formula is

$$|\Delta T| = \frac{P_1'}{\frac{\pi^2 kt}{b^2} + 4(1 + \varepsilon_o)\sigma \bar{T}^3} \tag{64}$$

In Table 5, we have listed the ratio of conductive to radiative "smoothing factors" for a typical Voyager configuration. The average external emittances were assumed to be 0.12 and 0.86 corresponding to cases where all louvers are closed and open, respectively. The material was chosen to be magnesium (ZK 60A T5, k = 1.2 w/cm-K at 20C), and other typical dimensions are listed below.

r - 60 in.

b - 52 in.

t - 0.3 in.

$\bar{T}$ - 273 K (32F)

Table 5

Relative Effects of Radiation and Conduction in Determining Temperature Gradients

	Ratio of radiative to conductive smoothing factor	
	$\varepsilon_o = 0.12$	$\varepsilon_o = .86$
Azimuthal gradients	13.1	21.7
Axial gradients	1.0	1.7

Table 5 shows that radiative effects dominate the azimuthal distribution, however, conductive effects are as important as radiative effects in determining the axial temperature gradients in bays that are highly shielded or have closed louvers.

From this simple analysis, it may be concluded that the frame members, which only contribute to smoothing the azimuthal gradients, need not be exactly scaled for conductive effects. The conductive paths in shear webs and longerons should be modeled because the axial gradients will be influenced by their conductance.

In the following table are listed several typical prototype materials and candidate materials for 1/2 and 1/5 scale models designed in accordance with the temperature preservation technique where all dimensions and conductivities are scaled.

Table 6

Typical Materials Selection for 1/2 and 1/5 Scale Models

Prototype	1/2 Scale Model	1/5 Scale Model
6061 T6 Al. (1.55)*	AZ31 B Mag. (0.77)	Cupro-Nickel 30% (.29)
2024 T6 Al. (1.47)	Al. Bronze Alloy 9C(.71)	410 S.S. (.27)
ZK 60 A Mag. (1.21)	SAE 1020 Steel (.63)	Monel (.26)
AZ 31 B Mag. (0.77)	Copper Alloy Type CDA 757 (.39)	301 S.S. (.157)
Beryllium-Sintered (1.74)	Phosphor Bronze Type 544 (.87)	Cast iron 60-45-10 (.35)

* Numbers in parentheses are conductivities in w/cm-K.

From this table it can be seen that model materials with approximately scaled conductivities (within $\pm$ 10%) can be found. It is to be noted that many others can be found should the material selection be influenced by cost, delivery, or fabrication.

If it is desired to use techniques where temperatures are not preserved in model and prototype, two choices exist. If materials are preserved and all dimensions are exactly scaled because three-dimensional heat flow effects are important within conductive members, the temperature ratios for the 1/2 and 1/5th scale models will be

$$1/2 \text{ scale } - \frac{T_m}{T_p} = 1.26, \quad 1/5 \text{ scale } \frac{T_m}{T_p} = 1.71$$

From experience in analyzing the behavior of Mariner IV, we believe that three-dimensional heat flow effects in conductive members are, in general, unimportant and, therefore, we suggest that Equation (23b) in Section II be used to design the structure.

$$\frac{(k\delta)_m}{(k\delta)_p} = R^2 \left(\frac{T_m}{T_p}\right)^3 \tag{23a}$$

where δ - thickness of members

R - scaling ratio - L_m/L_p

The use of this "two-dimensional" approach requires that a temperature ratio be selected. The conductive paths are scaled by use of Equation (23a) and the internal powers are selected by use of the other equations presented in Table 2, viz. (24b, 25b, 26b). The temperature ratio chosen should be based on the availability of louver actuating springs as described

in Section III. Note that the use of the "two-dimensional" technique allows the use of identical materials with geometrically distorted plate thickness, or, at the other extreme, scaled thicknesses with different conductivities. Here the choice of sizes and conductivities will depend on the details of the prototype.

Electronics Modules

An internal view of an electronics bay (Mariner TCM) illustrating the packaging of electronics modules (sub-chassis) is shown in Figure 22. Typically, the bays may contain 10 to 20 modules which are bolted to the shear web and longerons. First, it is important to determine the need for scaling the heat flow paths in the bolted joints. Modules with low internal dissipation will not operate at temperatures much higher than the average internal temperature, even if they are de-coupled conductively from the shear web. To determine the magnitude of the maximum temperature difference between a module and shear web (which is the heat sink), we assume that the module is completely de-coupled conductively and that the average temperature of the interior of the spacecraft and surrounding modules is T_o. If the temperature rise of the module is not large, the temperature difference between the module and interior is given by

$$\Delta T = \frac{P}{4A\varepsilon\sigma T_o^3}$$

where P - power dissipation (watts)

ε - emittance of the module

A - surface area of the module (cm^2)

Some typical temperature differences have been tabulated in Table 7 for a 6 x 6 x 2 inch module having emittances of 0.04 or 0.85 corresponding to a gold-plated (for RF shielding) or black anodized finish. The average interior temperature of the spacecraft is assumed to be 273K (32F).

Table 7

Temperature Difference of Electronic Modules
(No conductive coupling to shear web)

	Temperature Difference (K)	
Power--watts	$\varepsilon = 0.04$	$\varepsilon = 0.85$
0.125	8.8	0.4
0.25	17.5	0.8
0.50	35.0	1.7
1.0	-	3.3
5.0	-	16.5

This tabulation shows that the thermal behavior of the bolted joints used to support modules having a high emittance and power dissipations less than 1 watt need not be modeled. The maximum error in temperature will be of the order of 3.3K (6F). The heat flow through bolted joints of modules having a low emittance or very high power dissipation is critical. For reference, 59 of approximately 75 modules within the Mariner IV spacecraft had power dissipations of less than one watt. Of these, only three were gold plated to have a low emittance. Thus, we conclude that in most electronic modules, the local temperatures will be determined by radiative effects and scaling of the modules or bolted joints will not be important. The temperatures of modules with a high power dissipation

per unit area such as amplifiers, power supplies, inverters, or those with low surface emittance will be dependent on scaling the heat flow characteristics of bolted joints.

Because the power dissipated per unit area within most modules is small, the conductive paths within a given module need not be exactly scaled. Again, for high power dissipations it will be necessary to model the conductive paths within the module. No particular difficulties should be encountered at 1/2 or 1/5 scale in either case.

It is assumed in this discussion that the power dissipated in the actual electronics modules of the prototype will be simulated by use of heaters in the models. This technique has been used successfully by JPL in tests of Temperature Control Models where the actual electronics are not available, and in tests of the 0.43 scale thermal model of Mariner IV.

In some electronics packaging configurations, the spatial distribution of power dissipation within a given bay is non-uniform. In such cases, for accurate modeling, the power should be dissipated in individual modules. However, for preliminary tests it may be useful to substitute one heating element having a uniform power dissipation per unit area for the individual modules. Figure 23 illustrates one method used in the 0.43 scale thermal model of Mariner IV to simulate the spatial distribution of power by use of individually heated modules. Figure 24 shows another method of simulating the entire power dissipation by use of a single heater element attached to the shear web. Results of

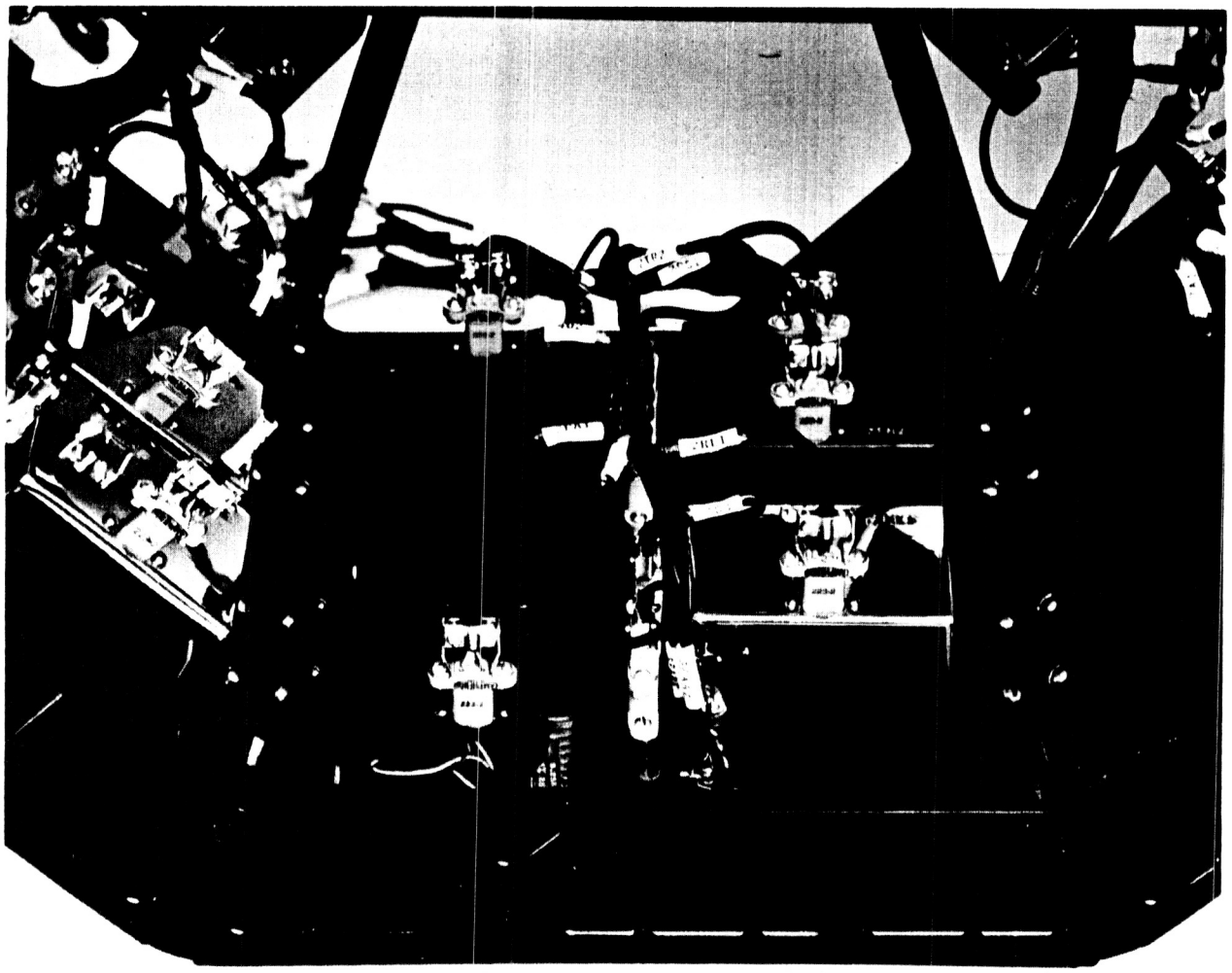

FIGURE 23 BAY 6 CONFIGURATION - TEST 3

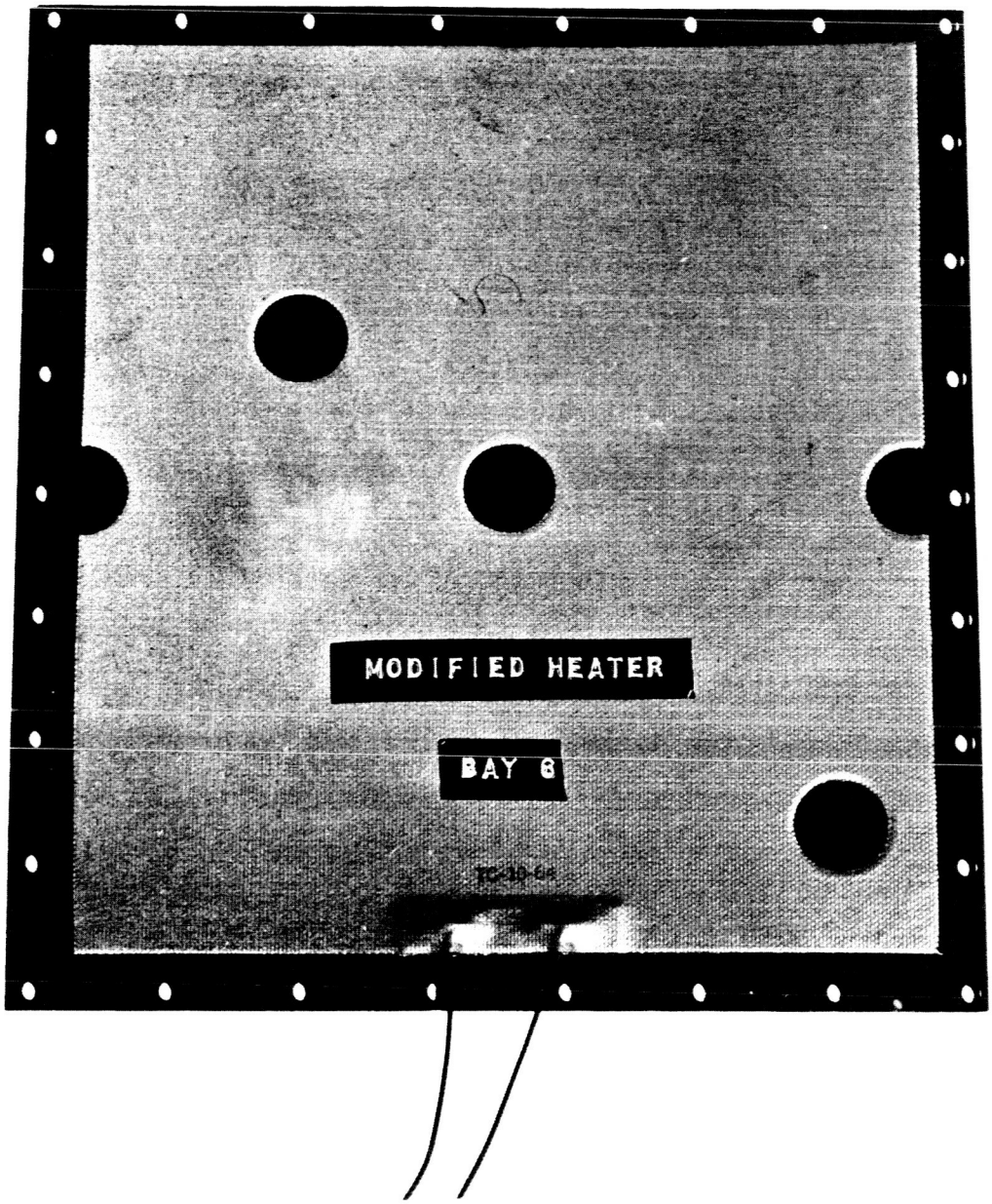

FIGURE 24 MODIFIED BAY 6 CONFIGURATION - TEST 4

tests* comparing the two configurations show that the errors introduced by uniformly distributing the power are less than 5F. This technique is attractive for preliminary modeling tests. Furthermore, if the sizes of the Voyager electronic modules are similar to those used in Mariner IV, the technique of replacing the individually heated modules by a single heater may be the only practical method of simulating the internal power dissipation for a 1/5th scale model.

The power dissipation in each module is related to the corresponding prototype dissipation by the equation (c.f. Eqs. (24a, b))

$$\frac{q_m}{q_p} = R^2 \frac{T_m^4}{T_p^4}$$

where q - power dissipation - watts

R - scale ratio L_m/L_p

and m, p, refer to model and prototype.

If temperatures are preserved the power dissipations scale as the square of the scaling ratio. For models designed to have different temperatures than the prototype, the ratio of absolute temperatures would be selected a priori. (The selection of a convenient temperature scaling ratio would be most likely based on a consideration of the practical problems associated with scaling the behavior of temperature control louvers.)

* "Thermal Scale Modeling of the Mariner IV Spacecraft," Final Report to JPL, Contract 950789, A.D. Little, Inc., Cambridge, Mass., 20 August 1965.

Temperature Control Louvers

A general discussion of problems relating to modeling of temperature control louvers has been presented in Section III. The importance of these findings with respect to modeling Voyager temperature control louvers at 1/2 and 1/5 scale will be summarized in the following paragraphs.

If the Voyager louver assemblies are equal in size or smaller than the louvers used on Mariner IV (approximately 1.62 ft^2, 15" x 15", in area), 1/5 scale models do not appear practical. One-half scale models with individually actuated blades could be successfully fabricated. Based on previous experience, the smallest louver assembly which could be conveniently fabricated is limited to about a 6" x 6" size assuming that individually actuated blades are used and that thermal similitude must be retained in model and prototype. Thus, a prototype Voyager assembly would have to be about 30" x 30" to be modeled at 1/5 scale.

Modeling of louver assemblies when temperatures in model and prototype differ introduce other limitations. If analyses of the Voyager spacecraft bus show that three-dimensional heat flow paths are significant, the maximum temperatures of 1/2 and 1/5 scale models of a prototype operating at 300K (80F) will be 378K (220F) and 514K (463F). A one-half scale model of a louver assembly designed by this technique appears practical, however, the high temperature level in a 1/5 scale model would introduce problems in the manufacture of the bi-metal elements used for actuation, and in the fabrication of blades, etc., where typically, cements are used for assembly of components.

For these reasons, the design of scaled temperature control louvers will be the dominant factor in determining the scaling ratio and temperature level of models of a typical Voyager spacecraft. Until further information is developed on the details of the Voyager prototype, it will be assumed that actively controlled louvers cannot be modeled at 1/5 scale. The alternative is to replace the variable-emittance louver assemblies on the model by equivalent areas of fixed emittance corresponding to the emittance of the prototype louvers in either the closed or open positions. Some useful information on the maximum range of average internal temperatures could be obtained by tests with such a configuration.

Solar Array and Supports

The modeling of the solar array and supports for the Voyager as shown in Figure 16 at either 1/2 or 1/5 scale will be straightforward. With the spacecraft sun-oriented about the roll axis, the solar panel array will be uniformly illuminated and the temperature gradients in the solar panels will generally be small. (The magnitude of the gradients will depend on the intensity of solar illumination and the spacecraft temperature. The temperature gradients will typically be larger at Mars solar intensity because of the greater influence of radiation from the spacecraft.) Therefore, the conductive paths within the solar panel array need not be exactly scaled. Since the temperatures are strongly influenced by radiative effects, it is important to reproduce the emittances and solar absorptances in the model. Actual flight-type solar cells need not be used in the model. It is merely necessary to reproduce their emittance and absorptance (obtained from test measurements) with a painted surface. This procedure was successfully used in the 0.43 scale model of Mariner IV.

It is important to note that the influence of errors in modeling the solar panel temperatures on the internal temperatures and temperatures of scientific instruments on Mariner IV was small.

Perhaps, the only problem area in modeling the solar panels involves the simulation of the heat flow between the inboard edge of the panel and the spacecraft itself and the simulation of the heat flow between the panels and the support arms which are shown in Figure 16 attached to the skin panels. The heat flow in the support arms will be one-

dimensional and the conduction paths can be modeled at 1/2 or 1/5 scale by making emittances equal in model and prototype and selecting the thickness of the tubular elements in accordance with Equations (23a) and (23b) as listed in Table 2.

It is important to note that the diameter of the solar panels may not have to be scaled in the model since the radiation to the spacecraft from the outboard edges of the solar panels is small. Also, if the diameter of the solar simulation beam is limited, it may be convenient to simulate the absorbed solar flux on the panels by use of heaters. (This requires that the solar absorptance of the solar cells be known.) These techniques were successfully used in modeling the Mariner IV solar panels at approximately 1/2 scale. In that case, the simulated solar beam was not large enough to cover the entire solar panel and auxiliary heaters were used to simulate the absorbed flux.

Rocket Engines and Propellants

In discussing the modeling of the rocket engines, it will be assumed that the model will only be used to predict temperatures before firing. Figure 16 shows the installation of four bi-propellant thrust vector control engines and the large solid propellant retro-propulsion engine. The exhaust nozzles of these engines are sunlit and their temperatures will be mainly determined by radiation effects since typically the nozzles are thin in cross section and made of high-temperature alloys of fairly low conductivity. These factors tend to make errors in modeling conductive paths small. Since the heat flow in the nozzles will be two-dimensional, distorted thicknesses can be conveniently used in designing

the conductive paths in the 1/2 or 1/5 scale model. Care should be taken to make the emittances and solar absorptances identical in model and prototype. A typical scale model of a propulsion engine--the mid-course guidance motor of Mariner IV--is shown in Figure 20. In this case the temperatures of the nozzle were difficult to model because the motor was shaded from sunlight and highly shielded from the spacecraft. Modeling of the nozzles on the Voyager is expected to be less difficult because of the orientation with respect to the Sun.

The temperature gradients and heat flow patterns in the retro-propulsion engine and bi-propellant tankage can be modeled using substitute materials. Table 8 lists some substitute materials for both a 1/5 scale model and a model designed in accordance with the materials preservation technique. Solids have been chosen since they will simulate the absence of convective effects in the space environment. The materials listed in Table 8 are only typical selections, many other materials with the proper conductivities can be found. The selection will depend on the ease of fabrication, cost and availability.

In designing scale models of typical propulsion systems, including propellant lines, structural supports, wiring, etc., it is difficult to determine how precisely each element must be scaled. Previous experience with modeling the Mariner IV has shown that it is easier to model conductive and radiative paths than analyze the thermal behavior of each component to determine whether or not it can be omitted, mocked-up, or must be scaled.

Table 8

Typical Materials for Scaling Propellants

	Thermal Conductivity (w/cmK)
Prototype	
Fuel (Aerozene 50)	.151
Oxidizer (N_2O_4)	.072
Solid Propellant[1]	.0059
1/5-Scale Model[2] - $\frac{k_m}{k_p} = 1/5$	
Fuel (conductive epoxy-aluminum)	.02-.05
Oxidizer (cast epoxy - no filler)	0.015
Solid propellant (epoxy foam)	>.001
Materials Preservation Model	
Fuel (Paraffin wax)[3]	.142
Oxidizer (Sylgard potting compound)[4]	.061
Solid Propellant (molded phenolics)	.006

1. Typical Minuteman solid propellant.

2. Many epoxies with and without conductive fillers of aluminum or silver can be used for 1/2 and 1/5 scale models--Emerson & Cuming, Inc., Canton, Massachusetts--typical vendor.

3. Temperature limitation of approximately 150F.

4. Dow-Corning Corporation, Midland, Michigan.

Thermal Modeling of the Spacecraft Bus and Entry Capsule

There are two possible approaches to modeling the spacecraft bus with entry capsule and sterilization canister attached to the lower portion of the bus as shown in Figure 16. The choice of either approach depends upon the nature of the thermal problem. For example, the details of the temperature distributions in the payload of the entry capsule may not be critical during the cruise from Earth to Mars provided that the average temperatures remain within suitable "storage" limits. The primary reason for conducting a thermal test would be to verify the adequacy of the insulation applied to the entry capsule to reduce the heat loss to outer space and thereby minimize the heater power requirements. In this case, the details of the internal configuration of the payload could be made extremely simple. Only those components which influence the heat leak through the insulated capsule would need to be modeled. They would include the sterilization canister and adapter ring, the insulation applied to the canister and any supports, penetrations, or umbilical connections to the exterior surface of the sterilization canister.

The other approach is to fabricate a detailed thermal model of the payload within the capsule as well as the sterilization canister, adapter and insulation. The thermal model of the payload could then be used in simulating conditions after the capsule had been separated from the bus, and the canister and insulation separated from the payload.

In the following paragraphs, we will first consider the modeling of the sterilization canister and insulation system since the

characteristics of the insulation will be most important in determining the internal temperatures during the 234 day cruise period. The full-scale sterilization canister is assumed to be made of aluminum approximately 0.125 inches thick. It is also assumed that the outer surface of the prototype may be highly polished to have a low emittance and thus decrease the heat loss. Because of the importance of keeping emittances equal in model and prototype when radiative effects are important, we recommend that identical materials be used in model and prototype whenever possible. One-half scale models designed with either the temperature preservation or temperature scaling technique would have canister thicknesses greater than .030 inches if identical materials were used in model and prototype (c.f. Eqs. 23a and b, Table 2). However, if identical materials were used in a 1/5 scale model, the wall thicknesses would be 5 mils. This thin section would lead to fabrication difficulties, and, therefore, we recommend that a sheet material of lower conductivity be used in a 1/5 scale model. The outer surface could be coated with vacuum-deposited aluminum to have the same emittance as the prototype. Stainless steel stock would be an appropriate choice because of availability.

The modeling of multi-layer insulations has previously been discussed in Section III of this report. A consideration of the scaling laws showed that the heat fluxes could best be scaled by retaining the same number of layers of insulation and the emittances in model and prototype if temperatures were preserved in model and prototype. This leads to geometric distortions in the insulation thickness since it is necessary to also preserve the packing density (number of layers per inch)

in model and prototype. This is not regarded as a serious problem at even 1/5 scale because the over-all dimensions of the prototype will be large with respect to the insulation thickness.

With models designed to have internal temperatures different than the prototype, precise modeling of heat fluxes will not be possible unless the heat flow is completely dominated by radiation. In this case, retaining the same number of layers and the emittances will properly scale the heat flow. If conductive effects influence the heat flow, it is not possible to correctly scale the heat flux unless the ratio of conductive to radiative transport is known for the particular insulation used on the prototype. Tests of the prototype insulation would be required to determine a suitable scheme for modeling insulations in this case.

Thermal Modeling of the Entry Capsule Without Sterilization Canister

Modeling of the internal components of the payload can be accomplished by use of the same techniques proposed for the spacecraft bus. If temperature control louvers are used on the electronic compartments the feasibility of using 1/5 scale models is questionable because of the small size.

There are several possible configurations which may be used in thermal tests of the entry capsule. One in which the entry heat shield is attached and another in which the heat shield has been separated from the capsule payload. In the first case, it will be necessary to model the radiative characteristics of the surfaces of the heat shield since the capsule may be Sun-oriented. The importance of modeling the conductive

paths in the entry heat shield will depend on the thickness and conductivity of the material. If the heat shield has a conductivity of 6×10^{-4} watts/cmK (10^{-5} Btu/sec ft R), is approximately 1/4 inch thick, and is "black", the temperature drop across the heat shield would be approximately 9K (16F) for an interior temperature maintained at 300K (80F) and the outer surface of the shield illuminated by sunlight. If the shield were facing away from the Sun, the temperature drop would be of the order of 30K (54F). Because these differences are rather large, it is recommended that the conductive paths in the heat shield be scaled. Either geometric distortions or the substitution of materials with different thermal conductivities could be used. (Many choices are available in the required range of conductivities, e.g., epoxy foams.)

The transmissive properties of the window in the heat shield (used for TV camera viewing) must also be considered if the heat shield is Sun-oriented. The transmittances for sunlight should be made identical in model and prototype. Since the window will probably be made of glass or fused silica, of low thermal conductivity, some problems will be introduced in attempting to retain the same materials for optical purposes and scale the conductive paths. One suitable approach would be to use distorted geometry (thickness of the window) to scale the conductive paths in accordance with Equations (23a and b) of Table 2.

When the heat shield is removed, particular attention must be paid to modeling the geometry and surface optical properties of the TV camera and penetrometer, and the conductive paths to payload electronics compartments. Since details of this entire configuration are not available,

it is difficult to determine the exact nature of problems, if any, that might exist in modeling the capsule payload. However, we would not expect the problems to be different than those which were successfully solved in the design of the thermal model of Mariner IV.

V. Scaled-up Appendages

It has been suggested that thermal modeling techniques could be effectively used to predict temperatures of small prototype components having low internal power dissipations by use of increased-scale models. We have considered this possibility, taking as examples, small appendages on Mariner IV with low power dissipations. A typical example is the magnetometer which has a full-scale power dissipation of approximately 1 watt and is approximately 9" long and 3" in diameter. The thermal design of this instrument required that the unit be radiatively isolated, to a degree, from sunlight and conductively isolated from the spacecraft bus. The range of magnetometer temperatures was set by the internal power dissipation. Low emittance surfaces were used to minimize the internal power requirements.

In Section III of this report, we discussed the importance of emittance control in isolated appendages of this type. It was shown that the percentage error in temperature arising from a given percentage error in emittance was equal to the temperature error arising from the same percentage error in internal power.

Accurate simulation of internal power dissipations in even the milliwatt range can be made in tests. However, if a prototype unit is scaled-up, there exists the distinct possibility that the emittances in model and prototype could not be made identical. These errors in reproducing the surface optical properties would, in general, outweigh the errors introduced in simulating a low internal power in a full-scale prototype. Furthermore, if a portion of the instrument or appendage was

covered with a multi-layer insulation, a scaled-up model would require that the thermal behavior of the insulation be appropriately modeled. Previous discussions have shown that modeling of insulations is not easily accomplished.

Similar arguments against scaling-up appendages can be made for other typical cases such as the high-gain antenna feed used on Mariner IV which had an effective power dissipation of approximately 1/2 watt. In this case, the temperatures of the high-gain feed were extremely sensitive to uncertainties in the solar absorptance and emittance.

For these reasons, the use of scaled-up configurations will not be a particularly attractive technique unless the configurations used on the Voyager spacecraft are considerably smaller in size than those used on Mariner IV and have considerably less internal power dissipation.

VI. Recommendation of Test Techniques

The entire subject of simulation of the thermal environment of outer space in ground testing has received considerable attention in the literature. Errors associated with imperfect solar simulation, gas conduction within vacuum chambers, etc., have been adequately defined. Wainwright, et al. (1964), and others have presented a discussion of the effects of finite chamber wall temperature on the equilibrium temperature of objects tested in a simulation facility.

Most of the simulation chambers used in testing have walls cooled to near liquid nitrogen temperature (77K) and a few facilities exist with walls cooled to between 4 and 20K. The walls are treated to have a high absorptance for incident radiation and are generally designed to be considerably larger than the test objects. These design criteria reduce the temperature errors introduced by ground-testing spacecraft (whose average temperature may be near room temperature) to a negligible value.

For a chamber with walls having a high absorptance for radiation and a test object small with respect to the chamber dimensions, the error in equilibrium temperature is related to the wall temperature by the following equation

$$\frac{\Delta T}{T_o} \approx \frac{1}{4} \frac{T_w^4}{T_o^4}$$

where T_o - temperature of the test object

T_w - wall temperature of simulation chamber

The temperature errors for various wall temperatures and test object temperatures are presented below,

	T_o = 300K	T_o = 200K	T_o = 100K
T_w = 77K	0.32	1.1	8.8
T_w = 20K	-	-	0.04

From this tabulation it may be seen that the temperature errors are only significant when the test object has a low temperature.

In the special case of the Voyager capsule which is shielded from direct sunlight and will be insulated to have a low heat leak, the exterior temperature of the outermost layer of insulation will be extremely low, and it is of interest to compute the error in heat flow through a typical multi-layer insulation blanket. We will consider that the insulation blanket is maintained at a constant temperature T_o on one side, corresponding to say the interior of the Voyager capsule and that the external surface of the insulation radiates to a "black" sink representing the chamber wall. The temperature of the sink will be varied to illustrate the effects of wall temperature on the heat flow. An arrangement of the MLI is shown in the diagram. If the heat

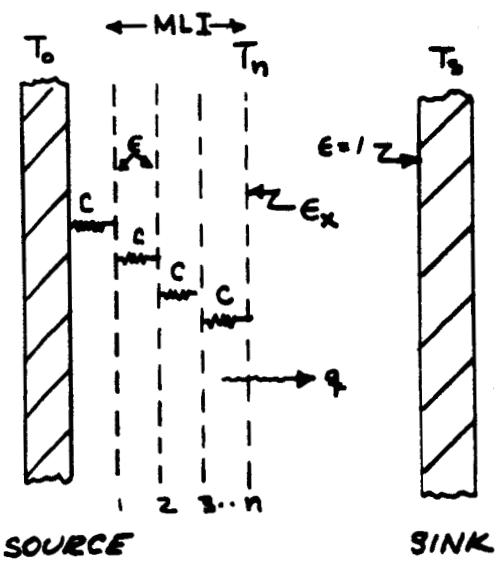

flow through the insulation is dominated by radiative effects, i.e., C = 0, the heat flow per unit area is given by

$$q = \frac{\sigma T_o^4 - \sigma T_n^4}{n\mu} \qquad \text{(VI-1)}$$

Further,

$$q = \varepsilon_x (\sigma T_n^4 - \sigma T_s^4) \qquad \text{(VI-2)}$$

so that

$$q = \frac{\sigma T_o^4 - \sigma T_s^4}{n\mu + \frac{1}{\varepsilon_x}} \qquad \text{(VI-3)}$$

where

- C - thermal conductance between shields (watts/cm^{2}K)
- ε - emittance of radiation shields
- ε_x - emittance of exterior surface of outer shield
- n - number of radiation shields
- q - heat flow per unit area (watts/cm^2)
- q_m - maximum q corresponding to $T_s = 0$
- T_n - temperature of outer (n^{th}) shield (K)
- T_o - source temperature (K)
- T_s - sink temperature (K)
- μ - radiation shielding factor between two adjacent shields = $\frac{2-\varepsilon}{\varepsilon}$

If the sink temperature, T_s, were zero, the corresponding heat flux is a maximum, given by

$$q_m = \frac{\sigma T_o^4}{n\mu + \frac{1}{\varepsilon_x}} \qquad \text{(VI-4)}$$

The fractional decrement in heat flux due to a sink temperature greater than zero is given by

$$\frac{q_m - q}{q_m} = \frac{T_s^4}{T_o^4} \qquad \text{(VI-5)}$$

This quantity represents an error in simulation since black space has an effective temperature approaching 0. Equation (VI-5) is plotted in Figure 25 for T_o = 300K. A heat sink at LN_2 temperature (77.4K) would introduce an error in heat flux of only about 0.45%.

When heat is transferred between adjacent foils of MLI by conduction as well as radiation, Equation (VI-1) must be modified to include the additional flux. It becomes

$$q = \frac{1}{n}\left[\frac{\sigma T_o^4 - \sigma T_n^4}{\mu} + C\,(T_o - T_n)\right] \qquad \text{(VI-6)}$$

Combining this with Equation (VI-2) to eliminate q, we get

$$\sigma T_n^4\left(\varepsilon_x + \frac{1}{n\mu}\right) + \frac{C}{n}T_n - \left(\varepsilon_x \sigma T_s^4 - \frac{\sigma T_o^4}{n\mu} - \frac{C}{n}T_o\right) = 0 \qquad \text{(VI-7)}$$

which can be used to determine T_n and, hence, q, for given sink temperature and properties (i.e., n, μ, C and ε_x).

Equations (VI-6) and (VI-7) were used to determine the effect of conduction through MLI on the error in heat flux caused by a heat sink at LN_2

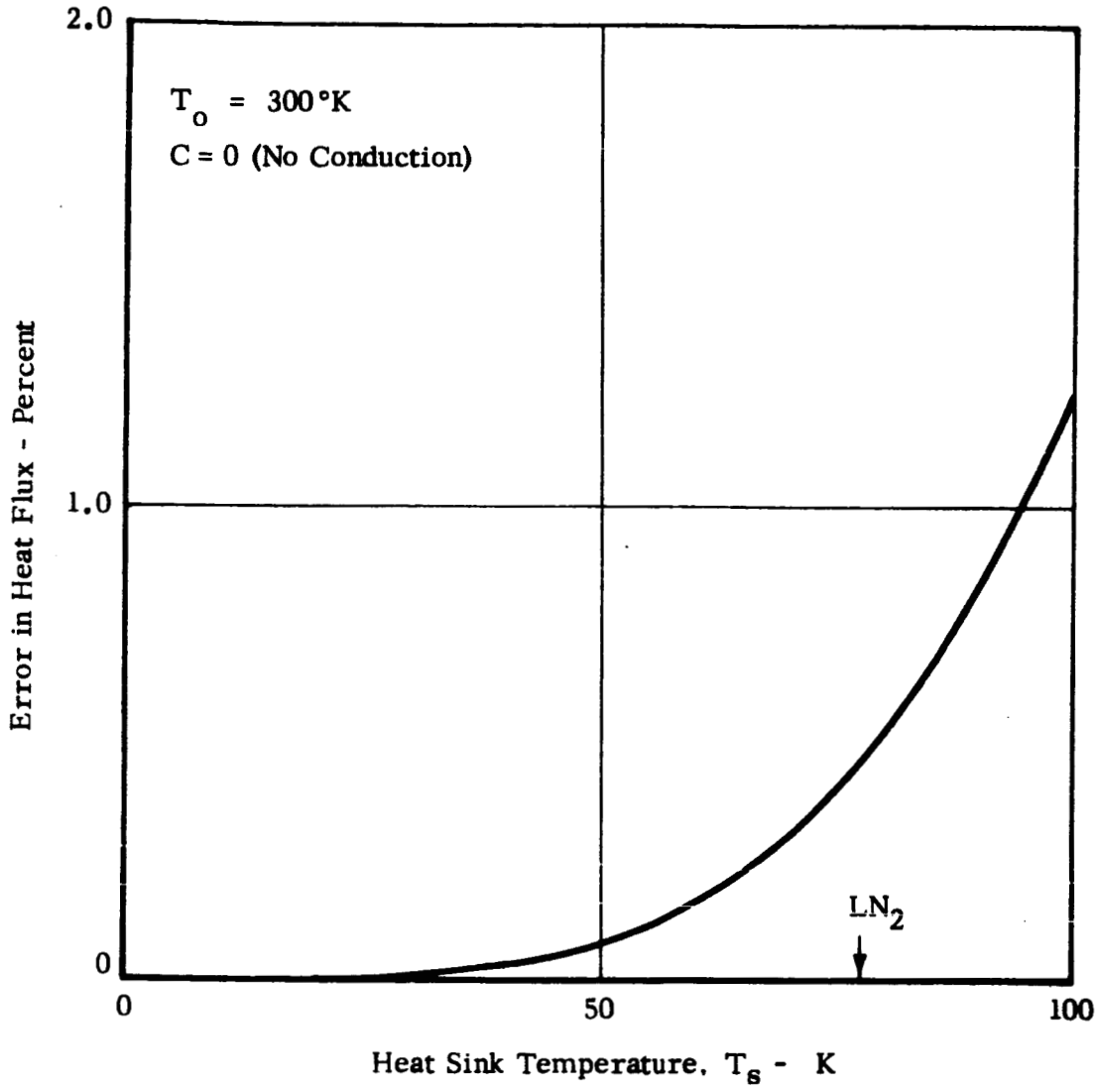

FIGURE 25 EFFECT OF SINK TEMPERATURE ON HEAT FLUX THROUGH MULTILAYER INSULATION WITH NO CONDUCTION

temperature, rather than 0. A typical case was considered in which

$$T_o = 300K$$

$$n = 10$$

$$\epsilon = 0.02, \text{ therefore, } \mu = 99$$

C was varied from 0 to 3×10^{-6} w/cm^2-K, a range which should encompass values that will be realized with carefully applied MLI.

Equation (VI-7) cannot be solved explicitly, so we resorted to computer calculations using Newton's method of successive approximations. The results are shown in Figure 26. A typical value for the inter-foil conductance of MLI is indicated. It was calculated from measurements made with a tank calorimeter that had been carefully insulated with MLI.* The MLI consisted of five mylar shields aluminized on both sides and separated by a lightweight glass fabric. The tank contained LN_2 while the exterior of the MLI was exposed to a radiation source at room temperature. Figure 26 shows that high ϵ_x produces the greatest error. At high values of the conductance, the error in heat flux is of the order of 5% with a chamber wall temperature of 77K. The heat flux through this insulation is approximately 10^{-4} watts/cm^2 (0.32 Btu/hr-ft^2). For a Voyager capsule area of approximately 4.7×10^5 cm^2 (500 ft^2) the heat leak through the bulk insulation, excluding penetrations, seams, etc., would be of the order of 50 watts. The error in modeling the heat flux would be of the order of 3 watts. Therefore, we would conclude that the

* Advanced Studies of Multi-Layer Insulation Systems, Second Quarterly Progress Report, June 1 to August 31, 1965, ADL Report No. 67180-00-02. Prepared for NASA Lewis Research Center, Contract NAS 3-6283.

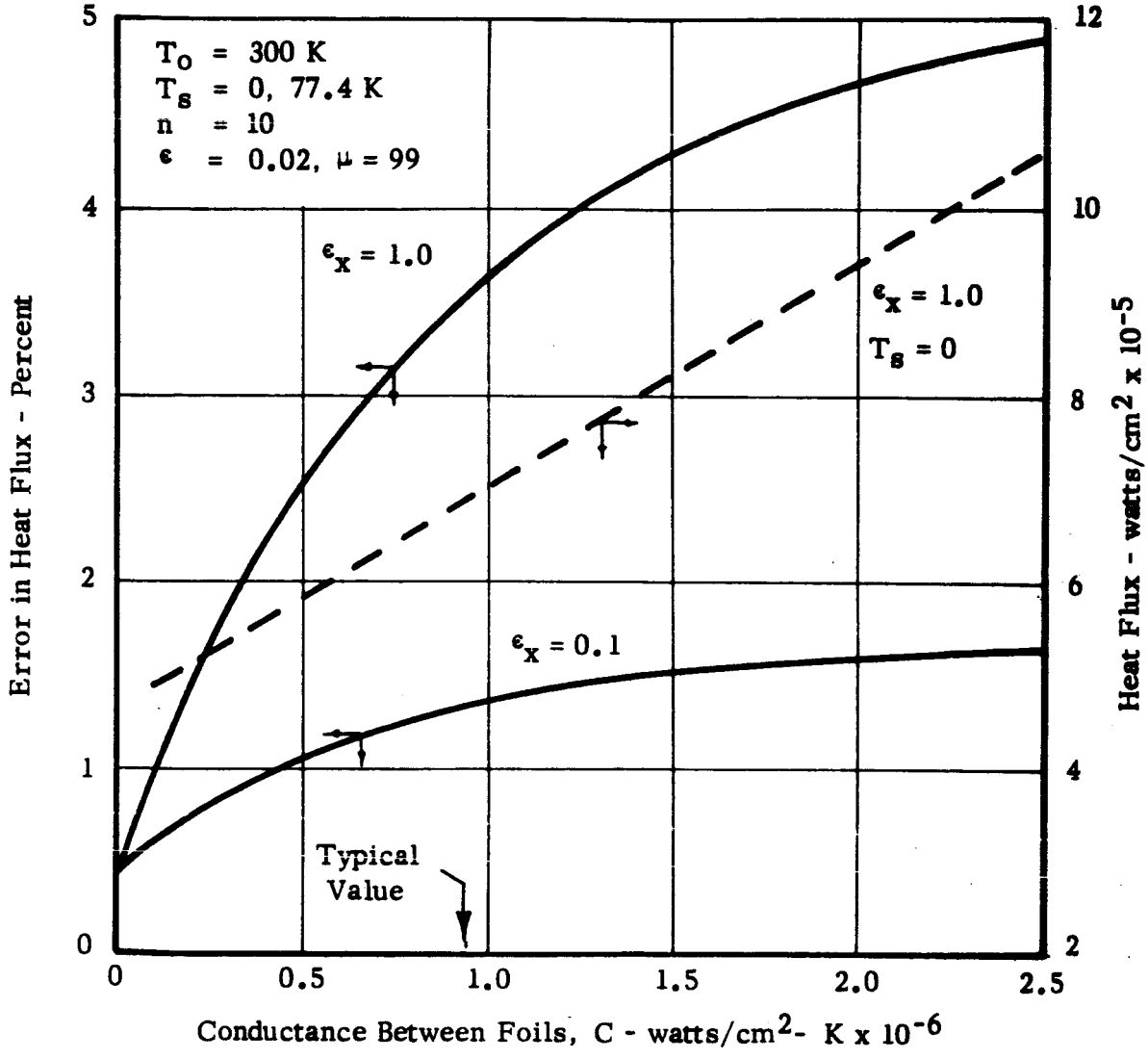

FIGURE 26 EFFECT OF CONDUCTION ON HEAT FLUX THROUGH MULTILAYER INSULATION

errors produces by using a conventional test chamber with walls cooled to near liquid nitrogen temperature would be negligible.

The heat flow through supports and feedthroughs associated with an insulation system and through certain types of insulation, such as evacuated glass fiber, will generally be dominated by solid conduction.

For this case, the heat flux per unit area is obtainable from Equations (VI-2) and (VI-6) from the previous section, by letting μ approach infinity, so that only conductive heat transfer between the source and the skin remains, and by redefining an effective conductance, C_E, so that Equation (VI-6) becomes

$$q = C_E (T_o - T_n) \qquad \text{(VI-6a)}$$

and equation (VI-2) remains

$$q = \epsilon_x (\sigma T_s^4 - \sigma T_n^4) \qquad \text{(VI-2)}$$

Note that T_n has been retained as a symbol for the skin temperature.

Equations (VI-6a) and (VI-2) have been solved for T_n and q for sink temperatures of 0 and 77.4K and the percentage decrease in heat flux calculated, for $\epsilon_x = 0.1$ and 1.0 and a range of effective conductances. The results are plotted in Figure 27. The solid curves show the heat flux decrements and the dashed curves the skin temperatures for the various conditions. As an example of how C_E relates to other system parameters, a value for C_E of 5×10^{-6} watts/cm^2-°K produces a skin temperature in space of about 67°K for $\epsilon_x = 1.0$ or 113°K for $\epsilon_x = 0.1$. The heat fluxes per unit area for these two cases are 9.34×10^{-5} and 1.16×10^{-4} watts/cm^2, and for an external area of 5×10^5 cm^2 (approximately 500 ft^2),

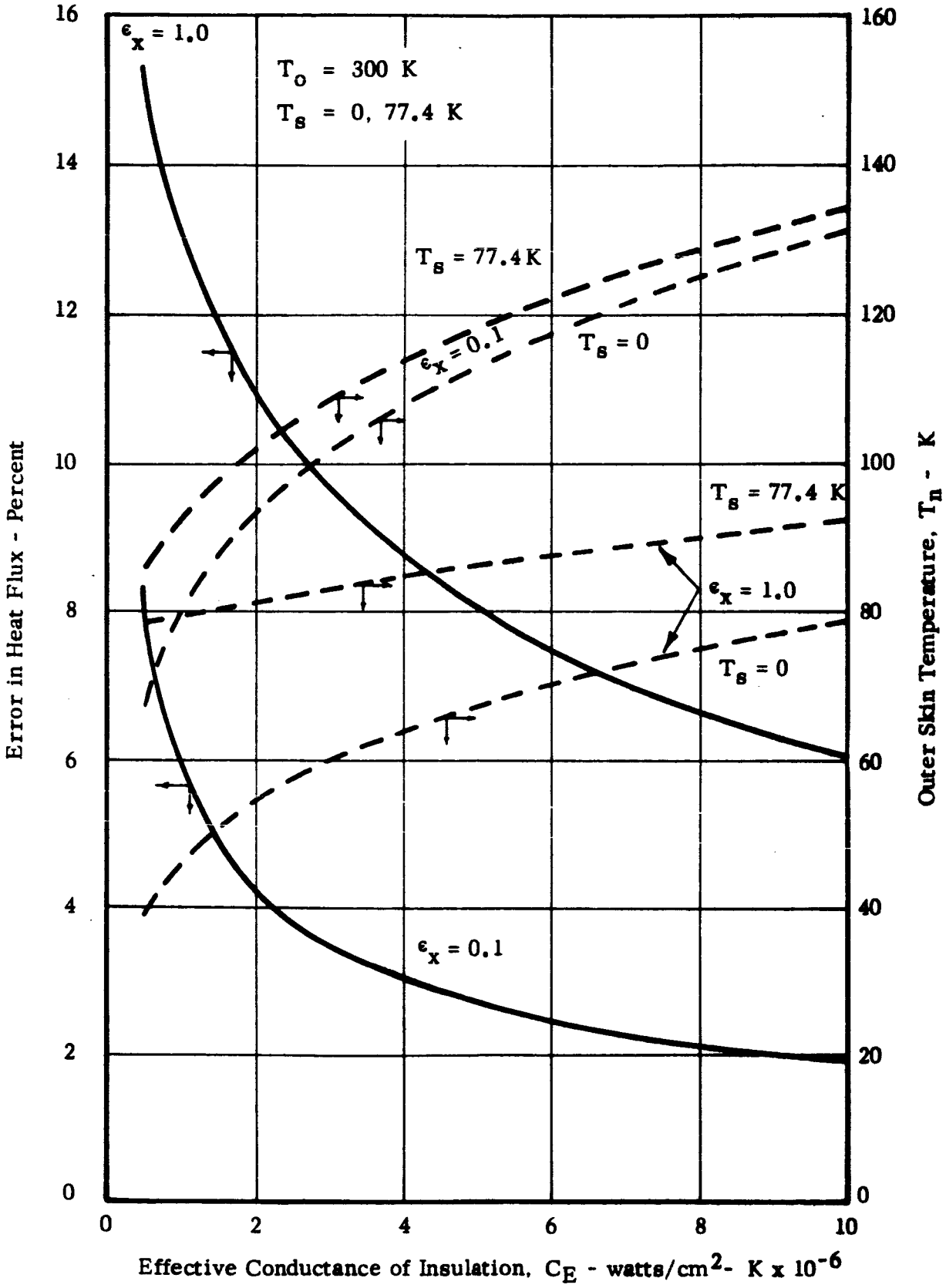

FIGURE 27 EFFECT OF SINK AT 77.4 K ON HEAT FLUX THROUGH CONDUCTION DOMINATED INSULATION SYSTEM

the power dissipations are 46.7 and 58 watts, respectively.

For those portions of the insulation system where radiation is unimportant and the conductance is reasonably high, we again see that the error introduced by use of walls cooled to 77K will be small.

Annotated Bibliography

The following bibliography contains a number of references on thermal scale modeling that have been presented in the open literature. Abstracts of each reference are presented. The bibliography is restricted to the subject of thermal modeling of spacecraft, and therefore does not contain a large number of related references on thermal similitude as applied to heat transfer problems in general. Contractors' reports on thermal modeling studies sponsored government agencies have been excluded from the bibliography because of their limited distribution.

Adkins, D. L., "Scaling of Transient Temperature Distributions of Simple Bodies in a Space Chamber," AIAA Thermophysics Specialist Conference, AIAA Paper No. 65-660, September (1965).

Thermal scaling of bodies with cycled internal heat sources was investigated in a cold high vacuum environment. Modeling relations were derived and tests carried out on two configurations. The first array of bodies consisted of a flat plate, sphere and cylinder arranged in a close network but not in physical contact with each other. The second system consisted of two spheres connected by a cylindrical rod. Material and characteristic temperatures were preserved between the prototype and model. The experimental transient temperature distributions in the models were in agreement with the scaling relations.

Beller, W., "Goddard Seeks Scaling Laws to Cut Cost of Environmental Testing," Missiles and Rockets, pp. 34, 35, July (1964).

This article briefly mentions the need for thermal scale modeling to reduce testing costs. The possibility is raised for using scaling techniques in predicting magnetic torques in satellites.

Birkebak, R. C., Cremers, C. J., LeFebvre, E. H., "Thermal Modeling Applied to Animal Systems," ASME Paper No. 65-WA/HT-8, November (1965).

Predictions of the heat loss from animal systems under the influence of environmental air temperature using thermal modeling techniques are found to agree with available experimental results. To perform the necessary experiments on heat loss, over a variety of environmental conditions for all species of interest, would be a formidable task. The thermal modeling approach circumvents these difficulties by the use of basic heat-transfer equations and properties and is suggested and examplified as an alternative.

Chao, B. T., Wedekind, G. L., "Similarity Criteria for Thermal Modeling of Spacecraft," Journal of Spacecraft and Rockets, Vol. 2, No. 2, pp. 146-152, March-April (1965).

General scaling criteria for thermal modeling of spacecraft are deduced from governing equations of the temperature field for both two- and three-dimensional cases. Surfaces are assumed to be opaque and nondiffuse; variations of bulk thermal properties with temperature are considered. Two techniques, namely, temperature preservation and material preservation, are examined in detail. Difficulties of perfect modeling are pointed out and possible compromises are suggested. For two-dimensional problems, a significant advantage may be obtained by employing models of distorted thickness. Control of apparent thermal conductivity of materials by slitting offers interesting possibilities for both steady and nonsteady simulation.

Clark, L. G., "Temperature Balance of Manned Space Stations," NASA TN D-1504, pp. 21-31, August (1962).

Temperature control of a manned space station to maintain a shirtsleeve environment is a requisite for optimum working conditions and comfortable living. The thermal behavior of a given space station can be solved either by computation or by model test; both methods are discussed.

Model scaling theory and techniques for the experimental thermal analysis of two space-station configurations, one an inflatable torus (30-foot diameter) and the other a rigid modular self-erecting hexagon (150-foot diameter), are presented.

Characteristic experimental and calculated average wall temperature histories are presented for the torus station, whereas calculated inner and outer wall temperature histories for two wall designs of the hexagonal station are also presented. Space radiator rejection rates are also included.

Clark, L. G., Laband, K. A., "Orbital Station Temperature Control," Astronautics, Vol. 7, No. 9, pp. 40-43, September (1962).

A setup for the experimental determination of the thermal behavior of scaled space-station models is described. The thermal similitude relations derived by Katzoff are presented. Instrumentation techniques for determining thermal behavior of spacecraft are discussed.

Folkman, N. R., Baldwin, F. L., Wainwright, J. B., "Tests on a Thermally Scaled Model Space Station in a Simulated Solar Environment," AIAA Paper No. 65-658, AIAA Thermophysics Specialist Conference, September (1965).

The physical size of space vehicles often makes full scale testing impractical; therefore, the development of thermal scaling techniques, as applied to models, offers an attractive solution when testing is required. The results of a test of a thermally scaled model space station subject to both steady state and cyclical transient solar environments, along with the scaling criteria, testing methods, and an analytical approach to verification of results are presented. The scaling criteria were determined from four dimensionless parameters which were matched between model and prototype in addition to preserving the geometry of both model and simulated radiation sources. The model was tested in a 5-foot diameter by 6-foot high space simulation chamber using a 40-inch diameter collimated solar radiation source. Earth emitted radiation was simulated for one test with an array of incandescent line sources. Solar transients were obtained by installing a water cooled shutter in the optical system of the solar simulator to provide an on-off step function. Three dimensional heat transfer analyses were performed on the prototype and model. Analytical results for the model were correlated with test results to obtain evaluation of scaling parameters for the transient and steady-state environments.

Fowle, A. A., Gabron, F., Vickers, J. M. F., "Thermal Scale Modeling of Spacecraft: An Experimental Investigation," Journal of Spacecraft and Rockets, Vol. 3, No. 4, April (1966).

Experiments made in an exploratory development of the technique of thermal modeling for the testing of spacecraft are reported. Comparisons of equilibrium temperature measurements of a prototype and three scaled thermal models of a simulated spacecraft made within a "cold-wall" vacuum chamber form the basis of the investigation. A one-half and a one-fifth scale model of the prototype were built and tested to examine the applicability of a set of thermal modeling laws which specifies different materials of construction to achieve identical temperatures at homologous locations in model and prototype. A third model, also one-half scale, was built and tested to examine the application of another set of thermal modeling laws which allows the use of identical materials but predicts different temperature fields in model and prototype. The experimental results proved that either half-scale thermal model could be used to predict the temperatures of the prototype configuration with an accuracy of approximately one percent

(3°C) of the absolute temperature level of the prototype. The experimental results obtained from the one-fifth scale thermal model indicated that the prototype temperatures could be predicted to within three percent (10°C) of the prototype temperature level.

Gabron, F., Johnson, R. W., Vickers, J. M. F., "Thermal Scale Modeling of a Modified Prototype of the Mariner Mars 64 Spacecraft," AIAA Second Annual Meeting, AIAA Paper No. 65-386, July (1965).

An experimental investigation dealing with the first known attempt to predict the temperatures within an actual spacecraft by use of thermal scale modeling techniques is described. The prototype, used as a basis for comparison, was a modified version of the Mariner Mars 64 spacecraft. A one-half scale thermal model of the prototype was designed to provide temperature preservation at homologous locations in model and prototype. Three separate thermal tests of the prototype spacecraft were completed in a vacuum chamber with liquid nitrogen cooled walls. Solar simulation was not used in these tests. Three independent tests of the thermal model were completed under conditions of thermal similitude. Measurements of the equilibrium temperatures at forty-six homologous locations in model and prototype are reported. Experimental results, obtained in independent tests of the model and prototype, showed that more than 67 percent of the temperatures corresponded within 5F, and 85 percent corresponded within 10F. The test results are interpreted with respect to future applications of thermal modeling techniques, and plans for extending the investigation of thermal scale modeling techniques to include tests in a simulated solar environment are presented.

Gabron, F., Johnson, R. W., Vickers, J. M. F., Lucas, J. W., "Thermal Scale Modeling of the Mariner IV Spacecraft," Third Aerospace Sciences Meeting, AIAA Paper No. 66-23, January (1966).

A half-scale thermal model of the Mariner IV spacecraft was fabricated and was tested in a simulated solar environment. The over-all objective of the experimental program was to determine the feasibility of predicting equilibrium temperatures in a complex flight spacecraft from environmental simulation tests of a small-scale thermal model. The basis for determining the feasibility of the technique was a comparison of scale-model temperatures, measured in solar simulation tests, with temperature data obtained during the recent Mariner IV flight to Mars. Thermal tests of the model were conducted in the 10- x 6-foot diameter NASA Lewis Research Center Space Simulator which is equipped

with liquid nitrogen cooled walls and a carbon arc light source. Twenty temperature measurements were made at homologous locations in the half-scale model and the Mariner IV spacecraft; these measurements were made for three simulated solar intensities corresponding to the 98th, 180th, and 234th days of the Mariner IV flight. For the three tests, 48 percent of the model temperature measurements corresponded within 10F of the Mariner IV temperatures and 85 percent were within 25F. These results show that equilibrium temperature predictions made by use of small-scale thermal models tested in environmental chambers can be successfully applied to the development of large, complex spacecraft.

Hrycak, P., Unger, B. A., "General Criteria for Solar Simulation and Model Testing," Institute of Environmental Sciences, 1964 Proceedings, April (1964).

In the paper, quantitative criteria of successful solar simulation as applied to full-scale and reduced-model testing are discussed. These criteria are related to over-all energy matching, spectral matching, collimation, uniformity, and reproducibility of the solar simulator.

Also, techniques for measuring the criteria are presented; in particular the analysis of a black ball radiometer is given.

From the governing differential equation, an analysis of parameters to be considered in reduced-model testing is made. It is shown that in such testing the similarities of the external geometries are of particular importance.

Jones, B. P., "Thermal Similitude Studies," Journal of Spacecraft and Rockets, Vol. 1, No. 4, pp. 364-369, July-August (1964).

One of the initial objectives of work in thermal similitude is to determine modeling laws and techniques which will find application in thermal scaling of spacecraft and in research problems. Modeling laws for space vehicles are derived from the differential equations used in practice for thermal analysis. The necessary and sufficient conditions for complete thermal similarity between model and prototype take the form of 28 ratios that must remain constant. However, all of these ratios are not independent but contain independent sets of six ratios. An example of thermal scaling is given in which one independent set is used. The general results compare favorably with those of some investigators who used other methods. The purposes of full-scale thermal testing are discussed, and the usefulness of thermal scale modeling as a substitute for full-scale testing is

questioned. It is suggested that the principles of similarity and scale modeling may find the most fruitful application in special research problems.

Jones, B. P., Harrison, J. K., "A Set of Experiments in Thermal Similitude," NASA Technical Memorandum TM X-53346, October (1965).

The analysis and results for two sets of experiments in thermal scale modeling are presented. The prototype and model consist of a plate, cylinder, and sphere exchanging thermal energy by radiation only. They were located relative to one another in an unsymmetrical arrangement.

The experimental results generally confirm the modeling rules, with some exceptions in the details, due largely to an a priori assumption made regarding the volume partitioning of the objects to be modeled.

Katz, A. J., "Thermal Testing," Space/Aeronautics, Part II, pp. 30-34, October (1962).

The dimensionless groups pertaining to thermal scale modeling of spacecraft are presented. A brief discussion of materials and temperature preservation scaling techniques is also presented.

Katzoff, S., "Similitude in Thermal Models of Spacecraft," NASA TN D-1631, April (1963).

Scaling criteria for the design and testing of thermal models of spacecraft are discussed. Four dimensionless similitude parameters are derived concerning radiation, internal heat generation, thermal conductivities of materials, and heat capacities of materials. Difficulties in achieving accurate simulation are pointed out and methods of effecting compromises without seriously affecting the validity of the data are suggested. The most difficult problems appear to be the accurate scaling of thermal conductivity and heat capacity. For manned spacecraft, some additional discussion is given of similitude criteria for the convective heat transfer.

O'Sullivan, W. J., Jr., "Theory of Aircraft Structural Models Subject to Aerodynamic Heating and External Loads," NASA Technical Note 4115, September (1957).

The problem of investigating the simultaneous effects of transient aerodynamic heating and external loads on aircraft structures for the purpose of determining the ability of the structure to withstand flight to supersonic speeds is

studied. By dimensional analyses it is shown that:

(a) A structural model geometrically similar to the aircraft and constructed of the same materials as the aircraft will be thermally similar to the aircraft with respect to the flow of heat through the structure.

(b) The thermal stresses and deformations of the structural model will be similar to those of the aircraft when the structural model is constructed at the same temperature as the aircraft.

(c) The stresses and deformations of the structural model due to external loads will be similar to those of the aircraft.

(d) By aerodynamic means the structural model can automatically be subjected to heating and cooling that correctly simulate the aerodynamic heating of the aircraft, except with respect to angular velocities and angular accelerations, without requiring determination of the heat flux at each point on the surface and its variation with time.

(e) The similitude of aerodynamic forces, moments, and pressures acting on the aerodynamically heated structural model to those acting on the aircraft is determined for the case of zero angular velocity and zero angular acceleration, so that the structural model may be subjected to the external loads required for simultaneous simulation of stresses and deformations due to external loads.

Rolling, R. E., "Results of Transient Thermal Modeling in a Simulated Space Environment," AIAA Thermophysics Specialist Conference, AIAA Paper No. 65-659, September (1965).

An experimental thermal similitude program is described and results presented for measurements on full-scale, half-scale, and quarter-scale thermal models. Steady state and transient observations are presented in terms of full-scale behavior. Model design, test conditions, and test results are described and necessary departures from rigorous compliance with the scaling criteria discussed.

Shanklin, R. V., "Thermal Similitude Study of Parallel Plates Connected by a Conducting and Radiating Path," M.Sc. Thesis, University of Tennessee, Space Institute, Arnold Engineering Development Center, Tennessee, June (1965).

Similarity ratios for thermal scale modeling are derived and the ratios were used to design a model thermally similar to a prototype. The materials and surface properties of model and prototype were made identical. The temperature-

time history of the model was compared to the temperature-time history of the prototype for tests conducted in a thermal-vacuum chamber without solar simulation.

Shih, C., "Thermal Similitude of Manned Spacecrafts," AIAA Third Aerospace Sciences Meeting, AIAA Paper No. 66-22, January (1966).

A general treatise is given on the criteria for thermal similitude of a manned spacecraft in a laboratory space chamber. The criteria were derived from a general heat propagation equation covering the effects of radiation, convection, and conduction. Thus, the correct inter-relation between the various modes is maintained. Discussions of practical application of such criteria are made, including some sound methods suggested by others in the past. Where exact thermal modeling is infeasible due to material thermal property restrictions, reasonable violation of some non-critical similitude may be made in order to satisfy the important criteria. A criterion of the allowable distortion in terms of percent of deviation from the theoretically exact similitude must be set for each particular case. Sometimes more than one model must be used. Two types of manned spacecraft are considered: the gravitationless type and the type with artificial gravity of some magnitude. Some methods for thermal modeling the effect of zero gravity or difference of gravity on Earth and in space are discussed. The mechanism of thermal contact conductance is examined to determine the procedure to be used in thermal modeling of mechanical joints.

Tsien, H. S., "Similarity Laws for Stressing Heated Wings," Journal of the Aeronautical Sciences, Vol. 20, No. 1, pp. 1-11, January (1953).

It will be shown that the differential equations for a heated plate with large temperature gradient and for a similar plate at constant temperature can be made the same by a proper modification of the thickness and the loading for the isothermal plate. This fact leads to the result that the stresses in the heated plate can be calculated from measured strains on the unheated plate by a series of relations, called the "similarity laws." The application of this analog theory to solid wings under aerodynamic heating is discussed in detail. The loading on the unheated analog wing is, however, complicated and involves the novel concept of feedback and "body force" loadings. The problem of stressing a heated box-wing structure can be solved by the same analog method and is briefly discussed.

Vickers, J. M. F., "A Study of Thermal Scale Modeling Techniques," Jet Propulsion Laboratory, Technical Memorandum No. 33-153, September (1963). (Also published in "Proceedings of Symposium on Aeroelastic and Dynamic Modeling Technology," RTD-TDR-63-4197, Part I, pp. 97-126, March (1964).)

The techniques which may be evolved from the basic laws of thermal scale modeling for spacecraft are described. All but two of these techniques can be rejected at once, since they require conditions which are very difficult to fulfill in practice. A comparison is drawn between the two remaining techniques, the technique of preserving temperature from prototype to model and of preserving materials from prototype to model. It is found that, for steady-state conditions, the technique of preserving temperature has inherent advantages over that of preserving materials, but that when transient conditions are to be modeled much of this advantage is lost.

Vickers, J. M. F., "Thermal Scale Modeling," Astronautics and Aeronautics, pp. 34-39, May (1965).

This paper contains a comprehensive review of what has been done and what work is in progress in the field.

Wainwright, J. B., Kelly, L. R., Wallace, D. A., Keesee, T. H., "Modeling Criteria and Testing Techniques for the Simulation of Space Environments," Technical Report No. AFFDL-TR-64-164, Air Force Systems Command, Wright-Patterson Air Force Base, October (1964).

The report covers an investigation of the possibility of using scale modeling to simulate environmental stresses on a space vehicle. General scaling laws were derived for simulating solar and planetary radiation, reaction jets impinging on a vehicle surface and mechanical vibration. Distortions in the simulated environment such as those produced by imperfect radiation sources, residual test chamber gas and the near presence of chamber walls were evaluated relative to induced measurement errors. Thermal simulation and mechanical vibration experiments are described which were designed to demonstrate the utility of the derived techniques.